Proceedings of the 2st[h] International Ship and Offshore Structures Congress (ISSC 2022) – Xiaozhi (Christina) Wang and Neil Pegg (Eds.)

COMMITTEE V4
OFFSHORE RENEWABLE ENERGY

COMMITTEE MANDATE

Concern for load analysis and structural design of offshore renewable energy devices. Attention shall be given to the interaction between the load and structural response of fixed and floating installations taking due consideration of the stochastic and extreme nature of the ocean environment. Aspects related to design, prototype testing, certification, marine operations, levelized cost of energy and life cycle management shall be considered.

AUTHORS/COMMITTEE MEMBERS

Chairman: A. Kolios, *United Kingdom*
K-H. Kim, *South Korea*
C-H. Cheng, *Taiwan*
E. Oguz, *Turkey*
P. Morato, *Belgium*
F. Ralph, *Canada*
C. Fang, *China*
C. Ji, *China*
M. Le Boulluec, *France*
T. Choisnet, *France*
L. Greco, *Italy*
T. Utsunomiya, *Japan*
K. Rezanejad, *Portugal*
C. Rawson, *USA*
J-M. Rodrigues, *Norway*

KEYWORDS

Offshore wind turbine, floating wind turbine, wave energy converter, tidal turbine, ocean current turbine, design , integrated dynamic analysis, model test, hybrid testing method, field measurement, marine operations

CONTENTS

1. INTRODUCTION

This is the sixth time that ISSC has included the Specialist Committee V.4 Offshore Renewable Energy, which started in 2006. Two members of the committee for this term (2018-2022) were involved in the work for the previous term (2016-2018), which formulates a good base for the cooperative work in the last three years.

The mandate of the committee was discussed at the beginning of the work and it was slightly modified to include extreme environmental and interaction of structures to the seabed, reliability-based design, safety and integrate design, topics which have been central to the discussion for developing offshore renewable energy, and hence should be discussed in the committee report. Another variation of this committees report, has been the consideration of floating wind developments in a separate chapter as deployments are currently moving further offshore and in deeper waters, as well as the explicit references to hybrid solutions.

Offshore wind energy still dominates offshore renewable energy technologies with extensive installed capacity and ambitious targets which constitute this technology as a key contributor towards the ambitious 2050 net zero targets. For these targets to be achieved through it is imperative to innovate and further develop not only wind energy but also other offshore, marine and hybrid energy technologies, harvesting as much as possible the energy potential. Challenges related to wind energy include, among others, the upscaling at both a unit as well as a farm level, development of foundations relevant to deep waters, serial production of floating foundations and effective mooring systems, and investigation of support systems to inform end-of-life scenarios including service life extension, repowering or decommissioning. Marine renewables on the other hand, still need to overcome challenges related to structural response in extreme phenomena and reliability of mechanical components which sharply escalate the levelized cost of energy.

Within this report we have considered peer reviewed academic articles, selected conference proceedings and some reference industry reports. Overall, more than 500 sources have been reviewed and 350 have eventually qualified to be included in this state of the art review. The time span of the review includes contributions from August 2017 to August 2021. The term of this committee has been extended due to the COVID-19 pandemic.

The report has been organized into 9 subsections. Following this short introduction, a session on bottom fixed wind turbines is included, following the structure of the previous committee's report, with the addition of design provisions for extreme phenomena which are particularly relevant in South-East Asia and a subsection on advanced structural analysis. Next, a dedicated section on floating wind turbines is included, following a similar structure, with the addition of moorings and dynamic cables which is relevant to this class of foundations. Next three sub-sections follow, presenting developments on wave energy converters, tidal and ocean current turbines and other offshore renewable energy technologies and hybrid solutions. Following this, a subsection on life-cycle cost and operational management of offshore renewable energy is presented, identifying key cost elements that attract attention for research and development. Section 8, summarizes the efforts the committee members to investigate a benchmarking study on the comparison of the existing design guidelines with respect to design of mooring systems. Finally, the last section of the report lists some conclusions which stem out of the review and key challenges that research should try to address in the next few years.

2. BOTTOM-FIXED OFFSHORE WIND TURBINES

2.1 Recent industry development

The wind energy sector was limited to onshore wind turbines prior to 1990s, after which offshore wind turbines were introduced as a more efficient way of harvesting wind energy. Europe has pioneered revolutionary innovations in offshore wind where majority of the installed OWFs are located. China, Japan and the US are countries that make large investments in offshore and a great part is reserved for offshore in their renewable energy policies. Monopile foundations are the most preferred foundations in Europe with its ease of application, relatively low production cost and proven heritage in the offshore oil and gas industry. This section reviews the recent industrial developments of offshore wind turbines between the years 2017-2022.

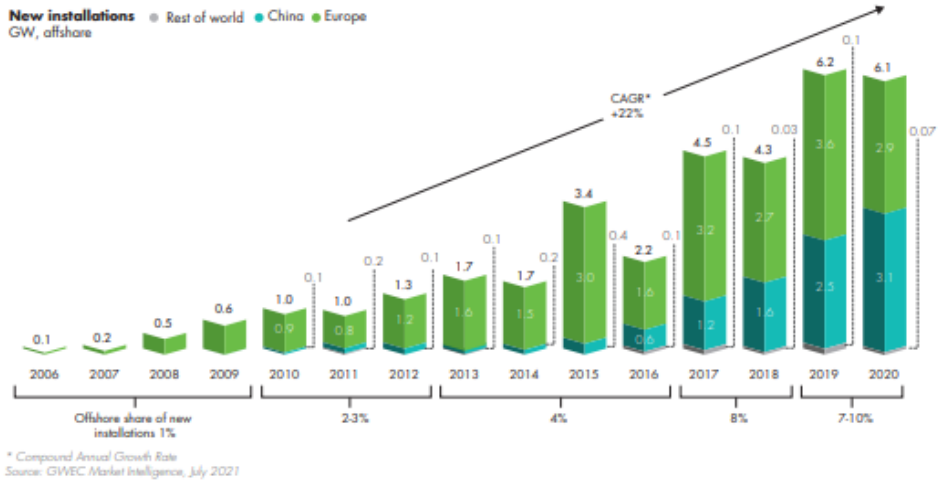

Figure 1: New installation in China, Europe, and Rest of the World (Lee and Zhao, 2021)

Figure 1 shows installed offshore wind capacities around the World. Despite the Covid pandemic, 2020 became the second-best year in the offshore wind industry based on installed capacity. The total new installation of China exceeded 3 GW. The total installed capacity in Europe is 2.9 GW; the leading country became the Netherlands in Europe with 1.5 GW new installation (Lee and Zhao, 2021). Also, in Figure 2, recently installed onshore and offshore wind turbines in Europe, including both offshore and onshore, are shown for 2020 (Komusanac et al., 2021).

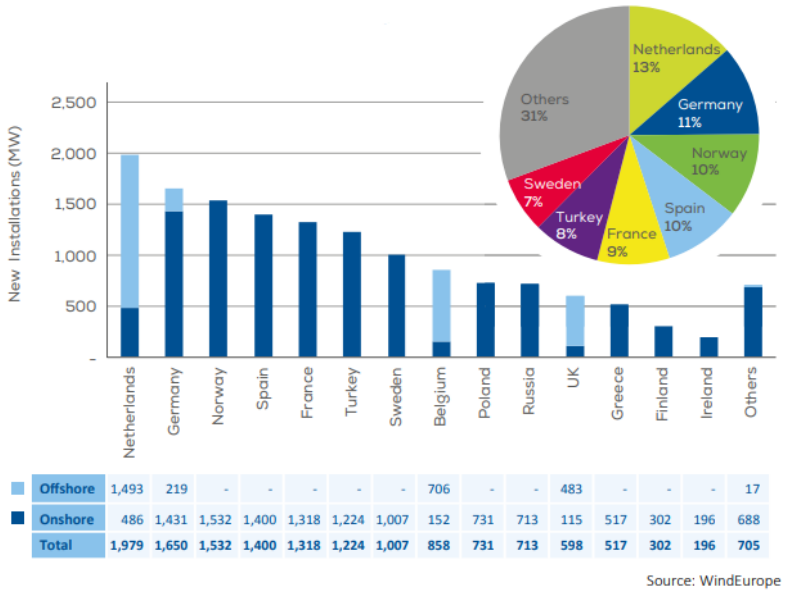

Figure 2: New onshore and offshore wind installations in Europe in 2020 (Komusanac et al., 2021)

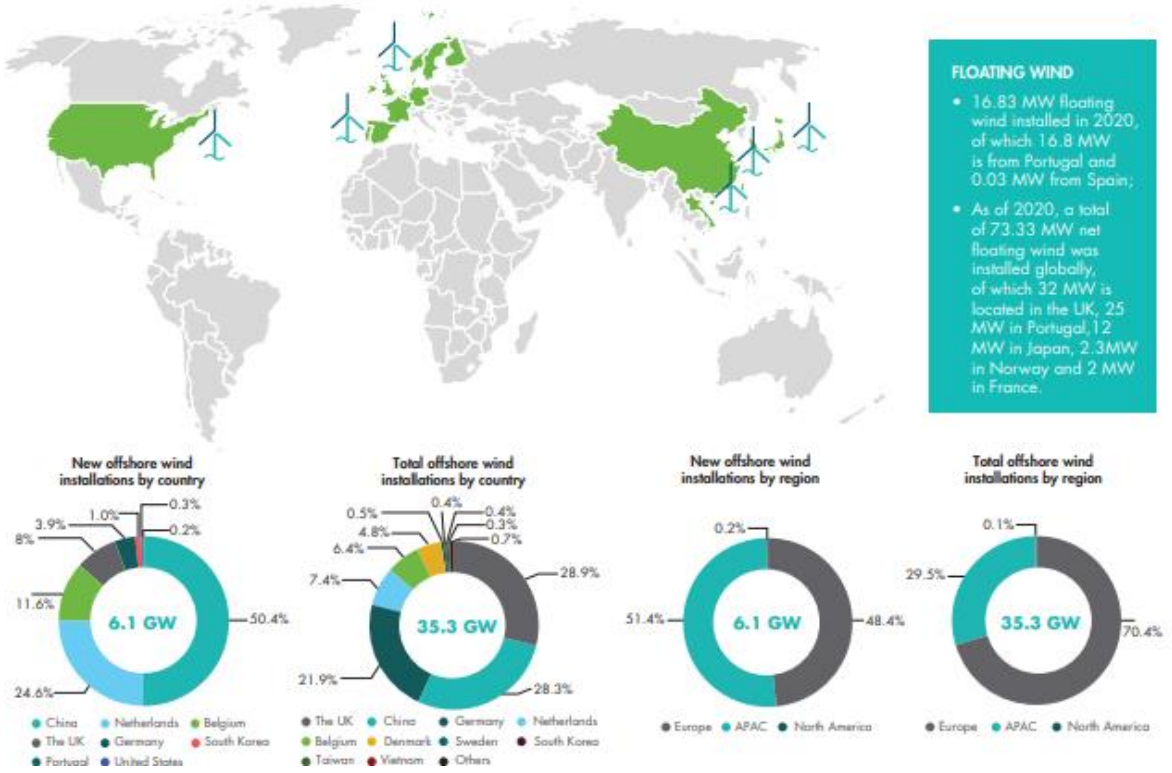

Figure 3:Offshore wind turbine installations around the World (Lee and Zhao, 2021)

The distribution of new offshore wind turbine installations to countries is presented in Figure 3. As stated, the total new installation capacity had reached 6.1 GW in 2020. The cumulative total installation of offshore wind capacity around the World is 35.3 GW (Lee and Zhao, 2021).

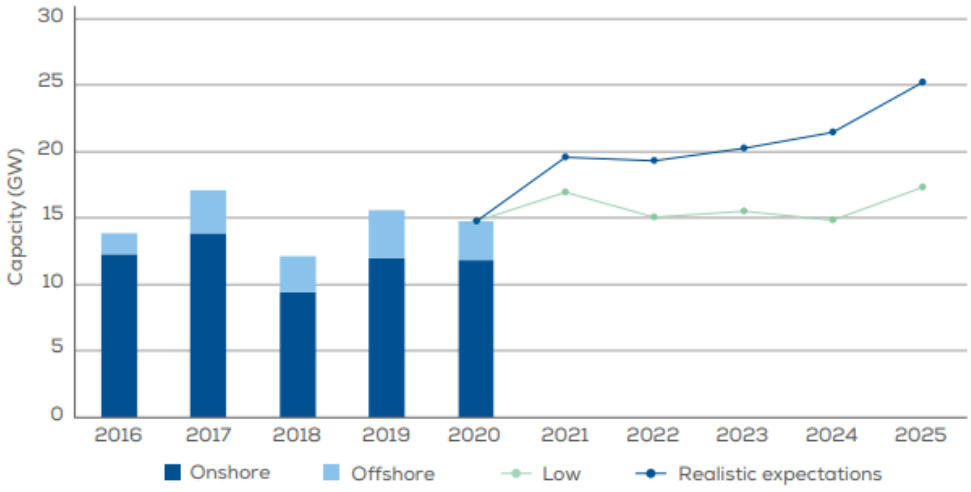

Figure 4: New installations in Europe – WindEurope's scenarios

For Europe, installed wind turbine capacities, both for offshore and onshore, between 2016 and 2020 are shown in Figure 4. WindEurope predictions are also shown as low expectations and realistic expectations for coming years.

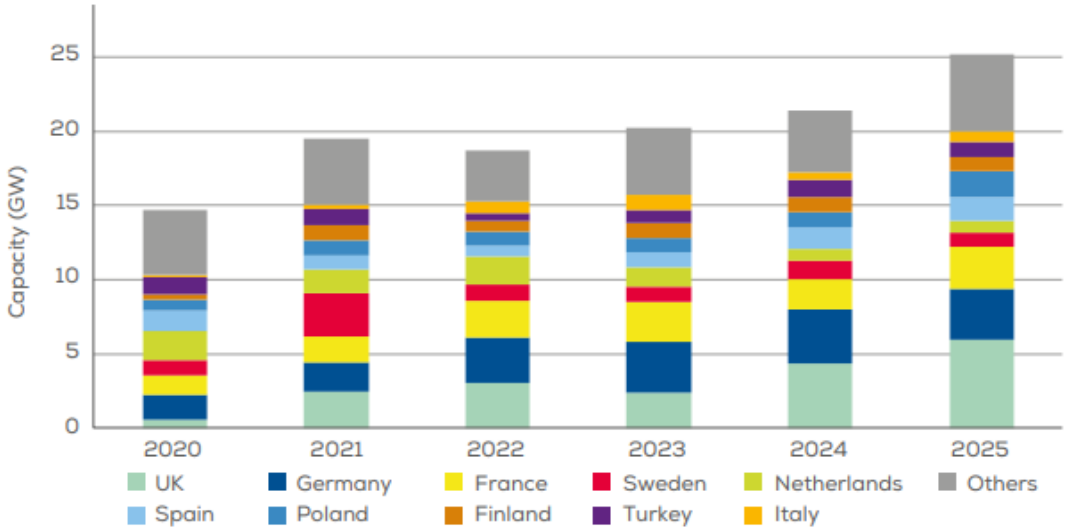

Figure 5: New installations per country – WindEurope's Realistic Expectations Scenario

Besides Figure 4, new installation expectations for European countries are presented in Figure 5. Note that these expectations include both offshore and onshore wind technology.

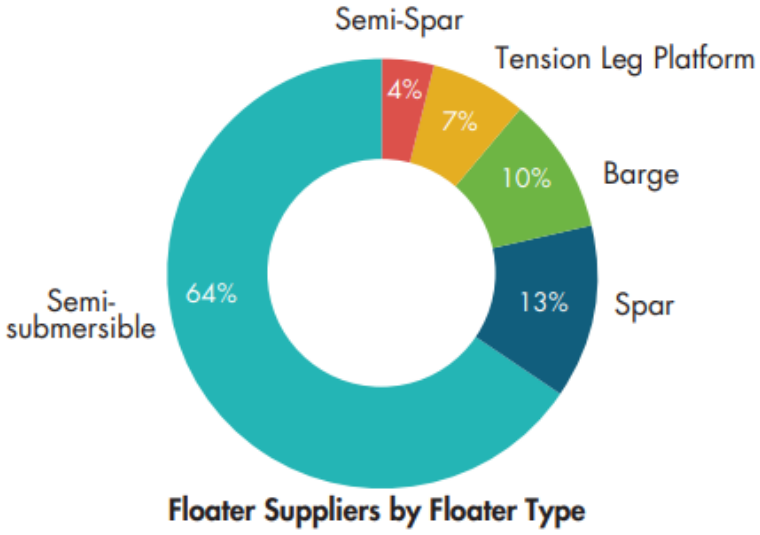

Figure 6: Share of floater type in global floating offshore wind projects at various development stages, excluding decommissioned ones (Lee and Zhao, 2021)

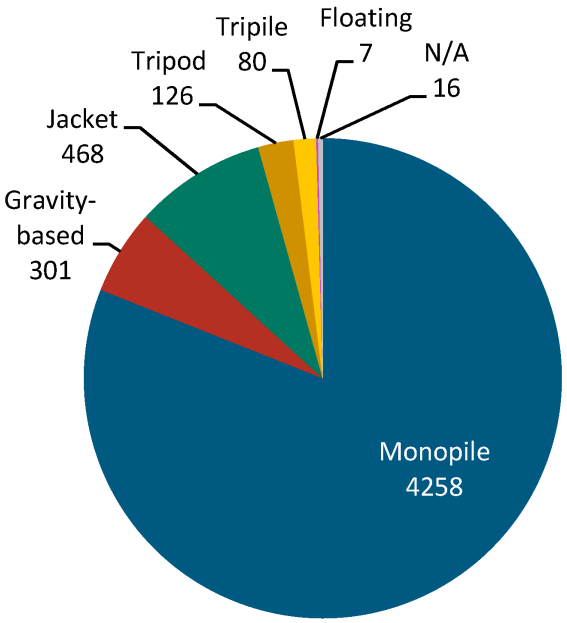

Figure 7: Share and numbers of fixed-bottom type in global floating offshore wind projects (Mathern et al., 2021)

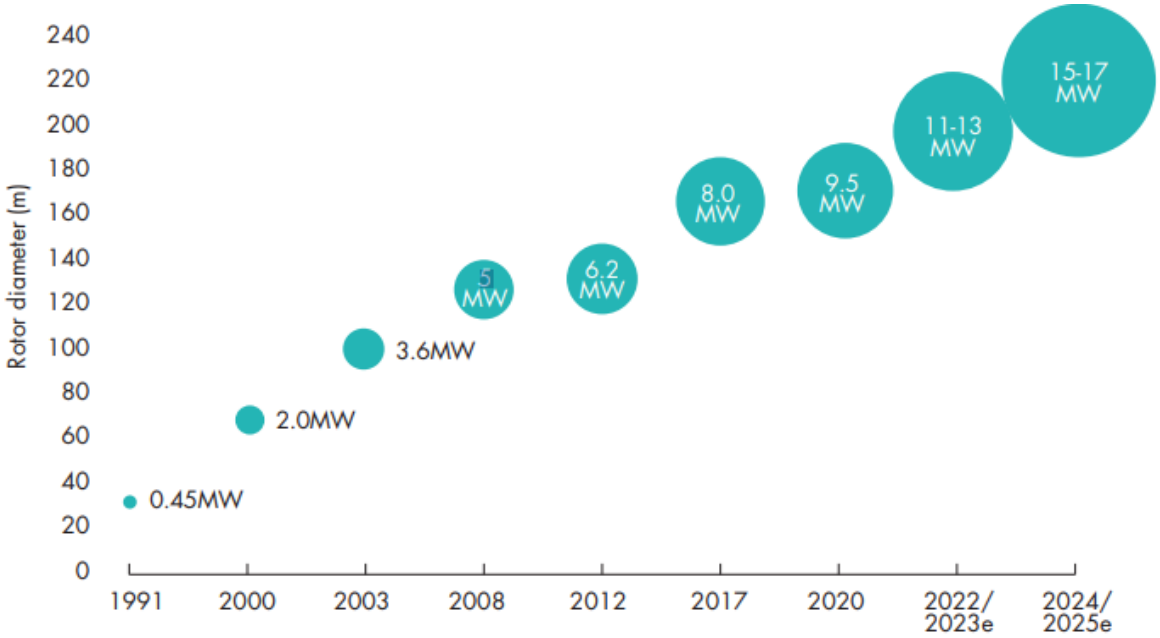

Figure 8: Rotor size and power rating continue to increase (based on commercial offshore wind turbine installation) (Lee and Zhao, 2021)

The World's first offshore wind farm was installed in 1991 at Vindeby (Denmark), the nominal capacity of this wind farm was 450 kW. After that, the size of offshore wind turbines has started to grow. In 2000, 1.5 MW capacity was passed, in 2005 2.5 MW, and in 2020, 6 MW sizes have been passed. It already reached 8.3 MW in 2020, and most probably, it will be surpassed 12 MW in 2025. Figure 8 shows the increase in the turbine size year by year and capacity predictions for 2022 to 2025 (Lee and Zhao, 2021).

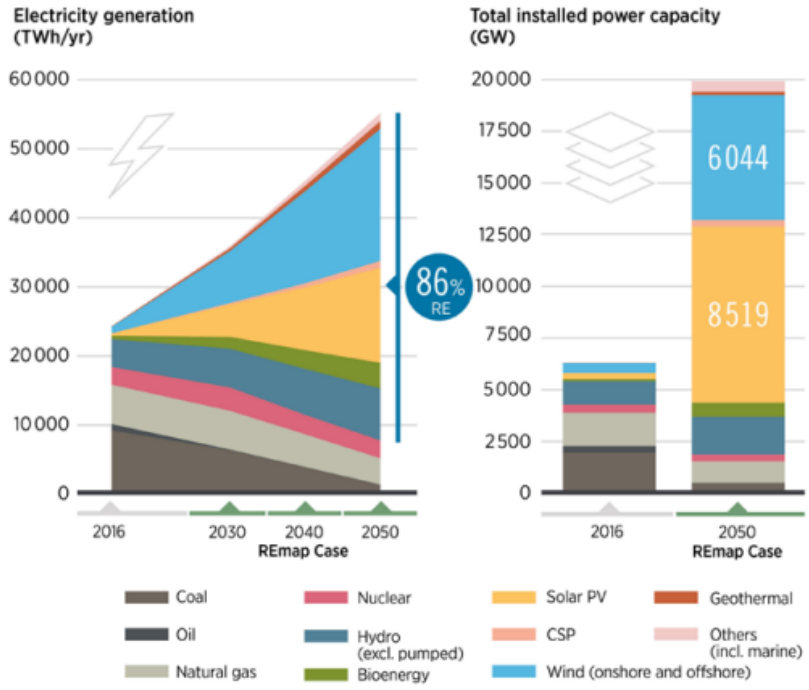

Figure 9: Wind would be the largest generating source, supplying more than one-third of total electricity generation needs by 2050 (International Renewable Energy Agency (IRENA), 2019)

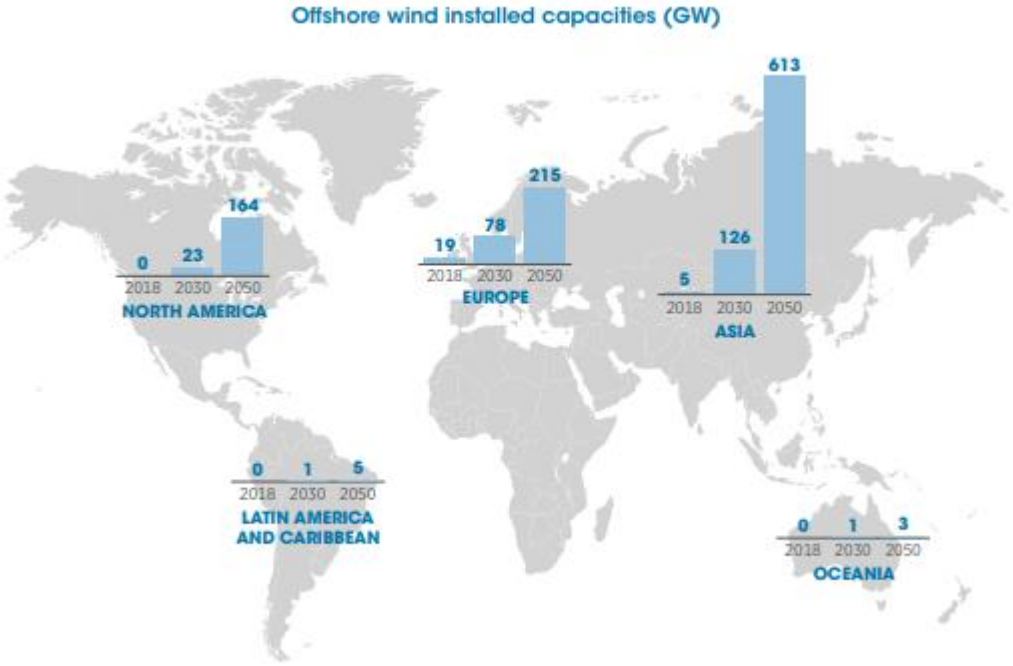

Figure 10: Offshore installed capacities (by 2018) and predictions for future (International Renewable Energy Agency (IRENA), 2019)

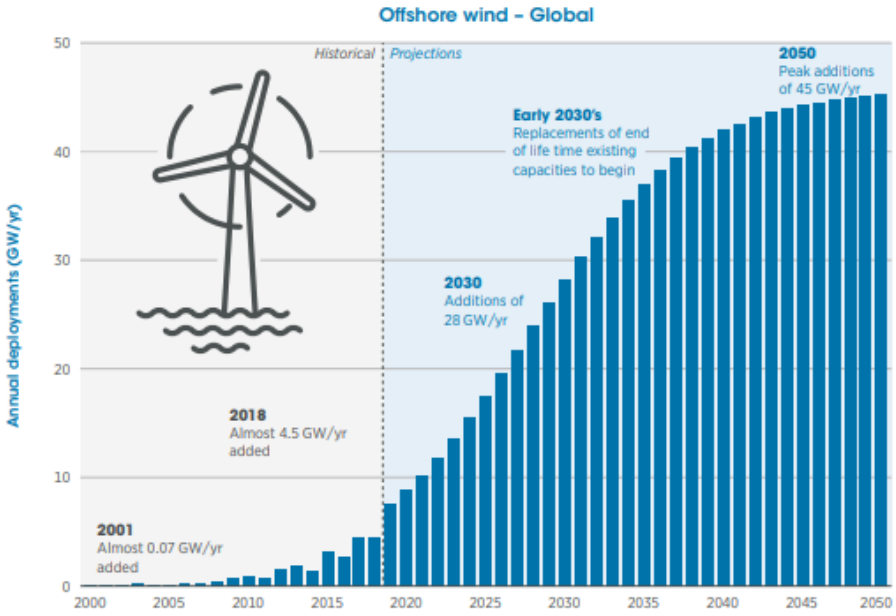

Figure 11: Annual offshore wind capacity additions would need to scale up more than six-fold to 28 GW in 2030 and almost ten-fold to 45 GW in 2050 from 4.5 GW added in 2018 (International Renewable Energy Agency (IRENA), 2019)

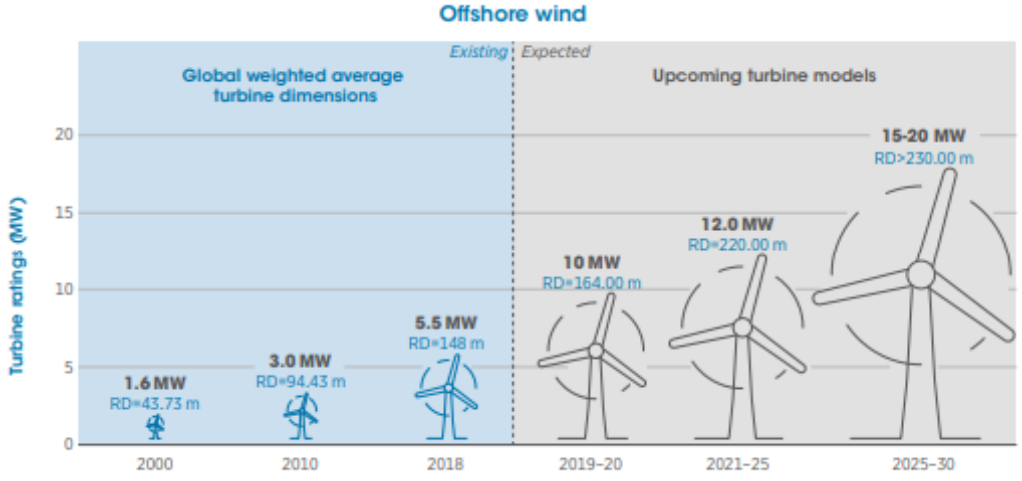

Figure 12: The average size of offshore wind turbines grew by a factor of 3.4 in less than two decades and is expected to grow to output capacity of 15–20 MW by 2030 (International Renewable Energy Agency (IRENA), 2019).

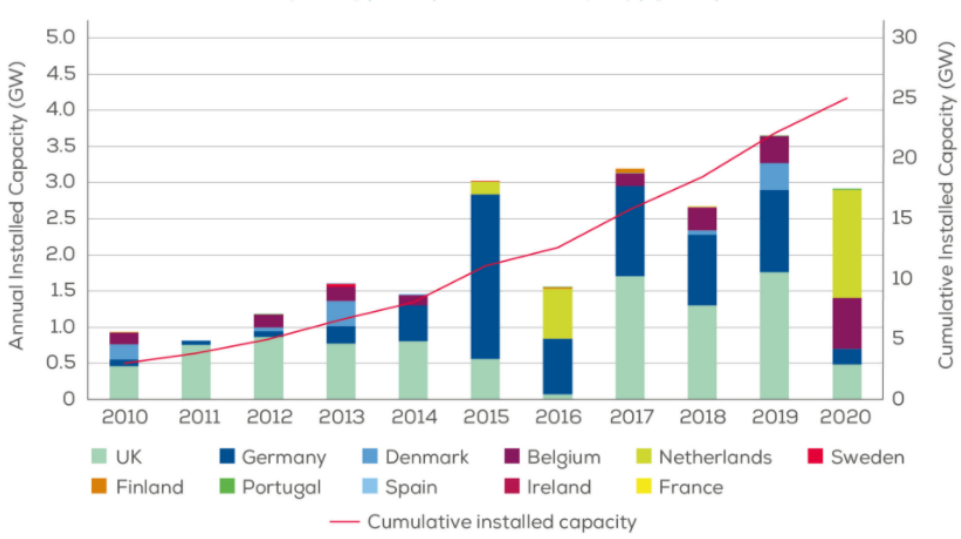

Figure 13: Annual offshore wind installations by country (left axis) and cumulative capacity (right axis) (WindEurope, 2021)

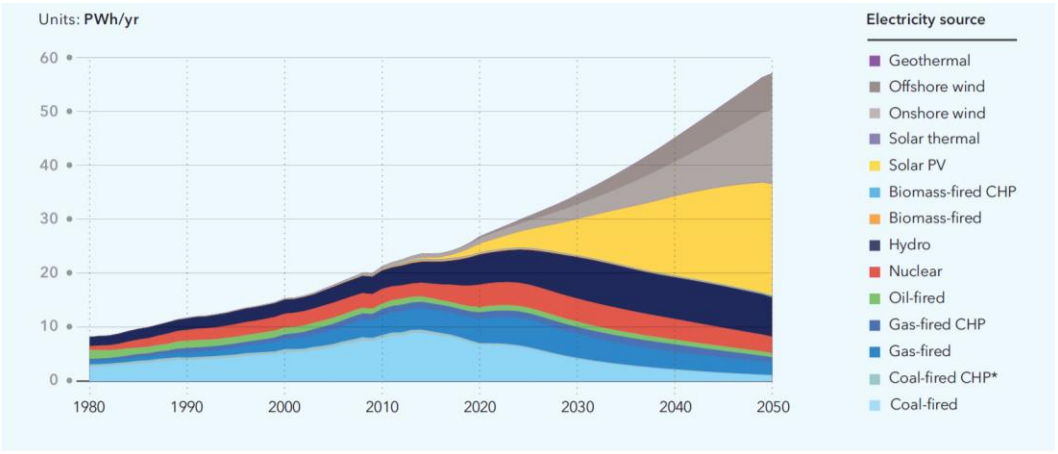

Figure 14: World electricity generations and expectations by sources (Det Norske Veritas (DNV), 2017)

2.2 Numerical modelling and analysis

2.2.1 Numerical tools – state-of-the-art and validation

Bottom fixed offshore wind turbines (BFOWT) represent a mature technology, as it is demonstrated by the large number of worldwide installations. Anyhow, cost reduction and Operation & Maintenance (O&M) optimization are still fundamental issues for the design, construction and deployment of such systems. These aspects must be tackled into a multidisciplinary context involving the interaction among rotary-wing aerodynamics, tower/blades structural dynamics, soil-pile interaction phenomena and control strategies.

Within this scenario, recent research has focused mainly on the validation of existing comprehensive numerical codes for loads and response analysis of BFOWT, on the development of novel soil-pile interaction models and on the definition of efficient numerical methods to be adopted for fatigue analysis and optimization purposes.

From a general standpoint, comprehensive numerical predictions with good levels of accuracy and low computational burden are of great interest for those involved in the preliminary design of offshore wind turbines. Recent results from the IEA Task 29 Phase IV on Detailed Aerodynamics of Wind Turbines (Schepers et al, 2021) highlight the limitations of Blade Element Momentum Theory (BEMT), widely used by the industry, in predicting blade aeroloads under off-design (unsteady) flow conditions, specifically when the operating conditions are characterized by significant yaw errors or wind shear. Nevertheless, with the aim

of helping the conceptual design of the new generation FOWT, a comprehensive and fast understanding of the system dynamics is still crucial to save costs in later design phases. This requires low- and medium-fidelity models that are currently still used and enhanced. Among the different examples of such approaches, the widely used FAST comprehensive aeroelastic engineering simulation tool, developed by the U.S. Department of Energy, National Renewable Energy Laboratory (NREL), is used in (Guntur et al, 2017) for an in-depth validation and code-to-code verification. In detail, a set of 1141 test cases, for which experimental data from a Siemens 2.3 MW machine are available and are in accordance with the International Electrotechnical Commission 61400-13 guidelines, are simulated using FAST as well as the Siemens in-house aeroelastic code, BHawC. Modelling enhancements within the latest version of FAST are represented by the capability of simulating all the elastic deformations (extension, shear, bending, and torsion) and the coupling effects between all six DOFs for both isotropic and composite slender structures. A detailed analysis using statistics including the means and the standard deviations along with the power spectral densities of turbine parameters (e.g. rotor speed, electrical power), selected loads (e.g. blade-root bending moments, main-shaft bending moments, tower-top torsional moment, tower-bottom bending moments) and blade tip deformations (in and out of the rotor plane) is presented. Results indicate good agreement among the predictions using FAST-BD (latest version), FAST-ED (previous release), BHawC, and experimental measurements. The main outcomes are reported in Tables 1 and 2, where the analysed quantities of interest (QOI) are listed and results are ranked (the lower the rank, the better the agreement with the measured data). It is anyhow acknowledged that further work on the analysis of experimental uncertainties (inflow wind, shear, TI, measurements errors) and the analysis in yaw and under wind speed variations (also extreme conditions) must be addressed.

QOI (time domain)	FAST (BD)	FAST (ED)	BHawC
Elec. power	–	–	–
Rotor speed	2	2	1
Rotor thrust	1	3	1
Blade in-plane tip deflection	1	3	2
Blade out-of-plane tip deflection	1	3	2
Blade-root in-plane bending moment	–	–	–
Blade-root out-of-rotor-plane bending moment	2	3	1
Main-shaft bending moment – yaw	1	3	1
Main-shaft bending moment – tilt	1	2	3
Tower-bottom side–side bending moment	–	–	–
Tower-top torsion moment	1	3	1

Table 1 - The tools FAST (BD), FAST (ED), and BHawC ranked according to how well their results compare to the experimental measurements in the mean and standard deviation for each QOI. No value indicates that no discernible difference could be seen among the different tools for that QOI. From (Guntur et al, 2017).

QOI (freq. domain)	FAST (BD)	FAST (ED)	BHawC
Elec. power	2	3	1
Rotor speed	2	3	1
Rotor thrust	2	2	1
Blade-root in-plane bending moment	1	3	1
Blade-root out-of-rotor-plane bending moment	–	–	–
Blade in-plane tip deflection	1	3	1
Blade out-of-plane tip deflection	–	–	–
Main-shaft bending moment – yaw	2	2	1
Main-shaft bending moment – tilt	2	2	1
Tower-bottom side–side bending moment	2	3	1
Tower-top torsion moment	2	2	1

Table 2 - The tools FAST (BD), FAST (ED), and BHawC ranked according to how well their PSD results compare to the experimental measurements for each QOI. No value indicates that no discernible difference could be seen among the different tools for that QOI. From (Guntur et al, 2017).

Further examples of comprehensive code-to-code and code-to-experiment validations are proposed also in (Sorum et al, 2017). Specifically, FAST outcomes are compared to SIMA (SINTEF Ocean) and vpOne (Virtual Prototyping) tools sharing BEMT aerodynamics with different implementations whilst the hydrodynamic loads modelling in FAST does not take into account diffraction effects nor hydrodynamic stretching. Soil modelling in SIMA and vpOne use distributed nonlinear springs whereas in FAST an equivalent cantilever beam approach is adopted. Blades, tower and monopile structural modelling is based on a non-linear finite element method in SIMA and vpOne, whilst FAST uses a modal approach for blades/tower and a FEM code for the monopile. The analysis performed on the DTU 10 MW reference wind turbine on a monopile foundation under several load cases (see Table 3) shows that for the deterministic load cases (steady state and stepped wind) all models predict a similar response. Differently, the stochastic load cases with turbulent wind conditions and the combined effect of wind and waves (see Figure 15) reveal major discrepancies between the models. Considering fatigue calculations, 14% difference in damage equivalent bending moment at mudline is shown demonstrating that fatigue utilization is very sensitive to codes capabilities (see Figure 16).

Another important example of state-of-art codes validation is proposed in (Popko et al, 2019) addressing the Phase III of the OC5 project where the measurements recorded on a Senvion 5M wind turbine supported by the OWEC Quattropod from the Alpha Ventus offshore wind farm are used considering different operating conditions (idling below the cut-in wind speed, rotor-nacelle assembly rotation maneuver below the cut-in wind speed, power production below and above the rated wind speed, shutdown). Although large measurement uncertainties related to the open-ocean environment created additional challenges when setting up the validation load cases and in spite of the need for a thorough quality check of sensor measurements, the reported results are satisfactory and show that the numerical models can reasonably mimic the full-scale system when they are carefully tuned.

Table 3. Load Cases

Load Case	Simulation type	Wind	Waves	Turbine operational	Tower top
1	Decay test	None	None	No	Free
2	Steady state	Constant uniform	None	Yes	Free
3	Stepped wind	Stepped, uniform	None	Yes	Fixed
4	Turbulent wind	Stochastic, w/shear	None	Yes	Free
5	Irregular waves	None	Irregular	No	Free
6	Combined wind and waves	Stochastic, w/shear	Irregular	Yes	Free

Table 3 - Load cases. From (Sorum et al, 2017).

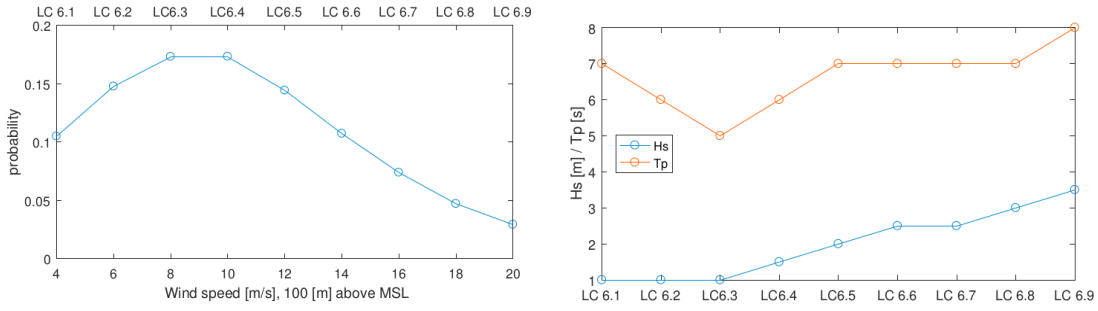

Figure 15: Wind speed with probability of occurrence (left) and corresponding wave parameters. From (Sorum et al, 2017).

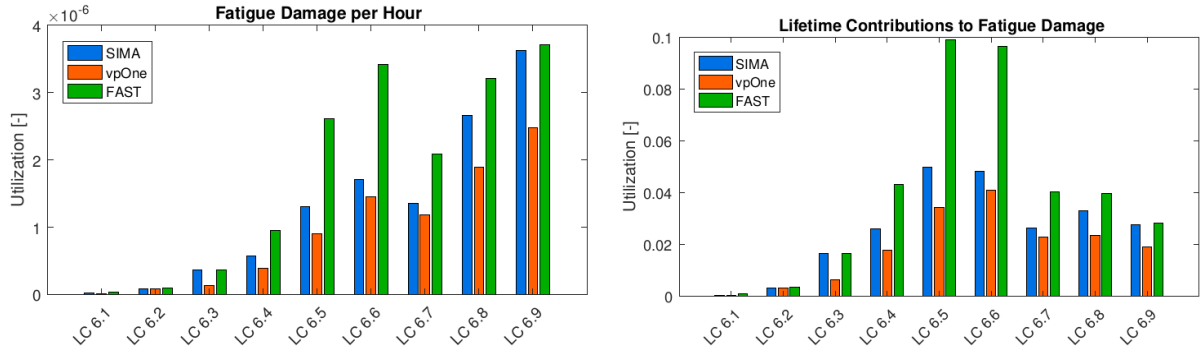

Figure 16: Utilization in one hour (left) and over 30 years (right). From (Sorum et al, 2017).

The availability of well validated and comprehensive tools forms the basis for the conceptual design and preliminary verification of new technological improvements for the next generation of BFOWT. As an example, (Thakur et al, 2017) proposes the implementation of controllable trailing-edge flaps on an offshore wind turbine for load reduction. In detail, the NREL 5 MW turbine is used and different bottom fixed support structures (monopile, tripod and jacket) and water depths are analyzed by using FAST with coupled stochastic aerodynamic-hydrodynamic analysis for obtaining the responses. The flap is controlled using a PID controller with the feedback of flapwise blade root bending moment. A significant impact of the flap on mean blade loads and deflections for all cases is observed with a reduction of out-of-plane shear force, flapwise moment at blade root and flapwise deflection (see Tables 4 and 5) whereas the PSD of tower base loads for rated wind speed for jacket structure is shown in Fig. 3.

Monopile (case1)	11.4m/s	18m/s	25m/s
Out-of-plane shear force	16.1	10.8	8.65
Flapwise moment	19	17.2	8.1
Flapwise deflection	27.7	23.7	16.8
Tripod (case2)	11.4m/s	18m/s	25m/s
Out-of-plane shear force	17.1	10.8	8.7
Flapwise moment	19.3	13.5	9.7
Flapwise deflection	28.4	28.5	15.7
Jacket (case3)	11.4m/s	18m/s	25m/s
Out-of-plane shear force	17.2	12.5	9.6
Flapwise moment	20	19	9.7
Flapwise deflection	22	24	16

Table 4 - Percentage blade mean load reduction. From (Thakur et al, 2017).

Monopile (case1)	11.4m/s	18m/s	25m/s
Tower base fore-aft shear force	-10.1	-8.6	-8.1
Tower base fore-aft moment	-5.8	-4.7	-2.6
Nacelle shear force	-9.9	-9.7	-9.8
Nacelle moment	-6.7	-6.1	-6.5
Tripod (case2)	11.4m/s	18m/s	25m/s
Tower base fore-aft shear force	-9.4	-8.2	-7.9
Tower base fore-aft moment	-4.9	-4.3	-2.2
Nacelle shear force	-9.1	-8.8	-8.9
Nacelle moment	-6.5	-6.1	-6.3
Jacket (case3)	11.4m/s	18m/s	25m/s
Tower base fore-aft shear force	-8.1	-7.9	-7.5
Tower base fore-aft moment	-4.1	-3.4	-1.9
Nacelle shear force	-8.9	-8.7	-8.8
Nacelle moment	-6.3	-5.8	-6

Table 5 - Percentage change in tower and nacelle mean loads. From (Thakur et al, 2017).

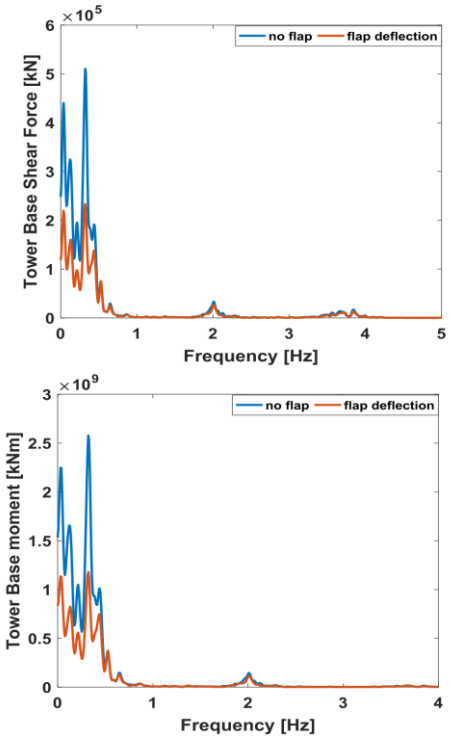

Figure 17: Spectral plots for tower base loads for wind turbine model supported on jacket substructure at 11.4m/s wind speed. From (Thakur et al, 2017).

Another example of the application of the available integrated tools to the analysis of specific BFOWT issues is proposed in (Liu et al, 2017) with the aim of better understanding the role of aerodynamic damping in the interaction of wind and wave with the structure in order to quantitatively evaluate the effects of aerodynamic damping on the lifetime fatigue load on offshore horizontal axis wind turbines towers. The aerodynamic loads are estimated using the Blade Element-Momentum theory, including the effects of dynamic inflow and dynamic stall whilst wave dynamics is estimated assuming 'random sea state' described by the JONSWAP spectrum, with wave loads calculated using Morison's equation and water kinematics modelled using linear wave theory. The foundation and pile in water are considered rigid (no hydrodynamic damping is included). Two aerodynamic damping models are proposed: (1) a model based on the analysis of rotor aerodynamics including the tower-top motion and including a correction factor to account for rotor speed variations due to changes in wind speed; and (2) a model based on Salzmann and van der Tempel's method to calculate the aerodynamic damping as the increase in the thrust per unit increase in the wind speed. The models are incorporated into a transient load analysis and the load analysis of a 5 MW offshore wind turbine is carried out. Following the proposed approach, it is observed that the aerodynamic damping can greatly affect the structural response and fatigue life of an offshore wind turbine in operation, playing a key role in restraining tower vibrations. Moreover, as the directions of wind and sea waves are usually parallel, aerodynamic damping induced by the rotor aerodynamics can significantly reduce tower vibrations caused by hydrodynamic forces, thus the fatigue load on the tower is much higher if only the effect of the waves is considered instead of the joint action of wind and sea waves (see Table 6). Finally, this analysis suggests that calculation of aerodynamic damping under different wind speeds for a specific design is required.

	Wind and wave			Wind only			Wave only
	No AD	AD Method A	AD Method B	No AD	AD Method A	AD Method B	
FDEL of M_y (kN m)	118647	20173	18249	71030	14374	13124	58330

Table 6 - Fatigue Damage Equivalent Load (FDEL) of tower base bending moment My. From (Liu et al, 2017)

Many research studies related to novel numerical modelling tools for BFOWTs have been recently focused on the topic of soil-pile interaction. Optimising the geotechnical design of these structures, through modern analysis techniques such as 3D Finite Element Modelling (FEM), has played a key role in helping to reduce costs. In (Murphy et al, 2018), a methodology for accurately modelling monopile behaviour using Cone Penetration Test (CPT) data to calibrate the non-linear stress dependent Hardening Soil (HS) model is proposed. The monopile field tests are modelled using the commercially available Plaxis 3D software and considering a full three-dimensional mesh with the pile positioned at the centre, thus ignoring the axisymmetric nature of the problem (see Figure 18). The lateral boundary is set at forty pile diameters and the depth is twice the embedded pile length. The soil elements are modelled as ten-node tetrahedral elements whilst the pile wall is modelled as an 18 sided cylindrical plate using six-node plate elements.

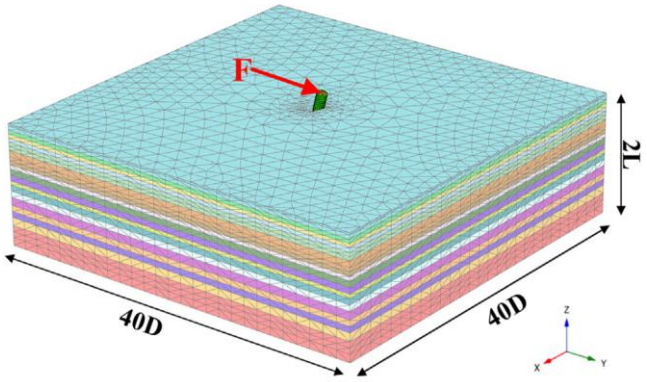

Figure 18: Sketch of the FEM mesh used for pile analysis. From (Murphy et al, 2018).

In parallel to the numerical analysis, a devoted experimental campaign on prototype scale piles embedded in an over-consolidated dense sand deposit is performed to validate the proposed FE model. Figure 5 shows the comparison of the Plaxis model outputs with the field tests demonstrating the excellent agreement between the FEM displacements and the measured ground line displacements for all piles. An analysis of the pile resistance components is presented showing that, for the considered pile geometries, ~75–90% of the restoring moment from the soil acting on the pile comes from the distributed lateral load. Moreover, as the L/D ratio of the piles reduces, the second order resistance components make a larger contribution to the ultimate moment resistance of the foundation and the additional soil reaction components when combined can account for 10–25% of the moment resisted by the pile depending on the L/D ratio. Ignoring these effects may result in an overly conservative pile design for low slenderness monopiles (L/D < 6).

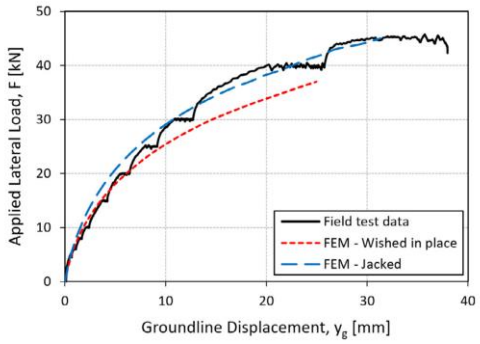

Figure 19: Comparison of field tests results and modelled pile behaviour. From (Murphy et al, 2018).

The paper demonstrates how the soil-pile reaction response curves can be extracted from the FE model. Nevertheless, for the geotechnical design of an individual monopile, a number of limit states must be considered. Moreover, for each individual turbine, a significant number of load cases must be analysed, including time domain analyses for the dynamic response during operation. Hence, when considering the optimisation of an entire offshore wind farm, relying solely on 3D FEM is too computationally expensive for running all the necessary design iterations and therefore simpler Winkler beam type models are still required (Burd et al, 2017). A novel way of reducing the number of simulated environmental states (load cases) while maintaining an acceptable accuracy is proposed in (Stieng et al, 2019) where from one full fatigue analysis of a base design (i.e. the OC3 monopile with the NREL 5MW turbine), the distribution of fatigue damage per load case is used to estimate the lifetime fatigue damage of a range of modified designs. Using importance sampling and a specially adapted two-stage filtering procedure, pseudo-optimal sets of load cases are obtained to estimate the fatigue damage. The methodology is tested for several with the conclusion that sampling less than 1% of all load cases can give damage estimates with median errors of less than 2%. Even for the most severe cases, using 3% of the environmental states yields a maximum error of 10%.

Two different foundations modelling techniques, referred to as the *simplified apparent fixity method* and the *improved apparent fixity method* are proposed in (Loken et al, 2019) and coupled with the aero-hydro-servo-elastic simulation tool FAST to perform sensitivity analyses of different monopiles and suction caisson foundations dimensions as well as fatigue analyses for the considered foundation models. FAST simulations for the fixed-base model, the simplified AF model, and the improved AF model of the 5MW NREL turbine are documented. The operating conditions refer to a full-field turbulent wind field (generated by TurbSim, using the Kaimal spectral model with a mean wind velocity U of 12 m/s and turbulence intensity TI = 14 %). The hydrodynamic loads are generated by HydroDyn with an irregular JONSWAP wave spectrum, including consideration of second-order sum-frequency hydrodynamic effects. The considered significant wave height Hs is 6 m and spectral wave period Tp is 10 seconds. A time window of the mudline moment in the fore-aft direction for the three foundation models is shown in Figure 20 demonstrating the relevance of small adjustments in the implementation of the foundation model. The sensitivity analyses performed in this paper, although obtained for a certain set of soil, foundation and structural parameters, show that neglecting the effect of the foundation in the BFOWT model (i.e. the fixed base default model in FAST) provides inaccurate and underestimated results for the structural dynamic response and fatigue damage. A significant reduction in fatigue life of 22% is observed for the flexible foundation model compared with the fixed base model. Moreover, the method chosen for modelling the turbine foundation is important to obtain a correct representation of the structural dynamic response.

The motion of a mono-pile foundation as a result of cyclic loads caused by wind and wave, and the effect of upper structures such as offshore wind turbines (known as pile rocking) is addressed in (Zhang et al, 2018), where a three-dimensional integrated numerical model, combining the effect of wave loads with the seabed and mono-pile, is adopted to investigate wave-structure-seabed interaction (WSSI) considering the pile rocking effect. The proposed model is based on user-defined PDE (Partial Differential Equation) method, which is a novel and flexible way to study the rocking-induced response. The wave sub-model with mono-pile is governed by Volume Averaged Reynolds-Averaged Navier-Stokes Equations (VARANS) equations in the framework of FLOW-3D, a commercial CFD solver for free-surface problems. The seabed sub-model is treated as an isotropic medium governed by Biot's QS model and the mono-pile is solved based on the elastic theory implemented in COMSOL Multiphysics. In addition, the pile rocking motion is simulated by cyclic displacements applied on the head of the monopile. Results indicate that local pressure enlargement occurs near the mudline and the rate of pore pressure decrease in depth is slowed down due to pile rocking, leading to a relatively high pore pressure in the upper soil range. The analysis shows that, due to the interaction between seabed and monopile in the pile rocking process, the value of bending

moment depends mainly on the horizontal displacement of the monopile and maximum bending moment usually appears at the position just below the mudline surface because of the seabed counter-force (see Figure 21). Furthermore, the pile rocking effect has a significant influence on the liquefaction distribution and enlarges the liquefaction zone in the vicinity of mono-pile foundation. Finally, a sensitivity analysis shows that monopile parameters have a great influence on its interaction with the seabed. Parametric studies of the pile rocking displacement and the pile diameter on pore pressure response indicate that larger rocking displacements and pile diameter lead to larger local increase of pore water pressure (see Figure 22).

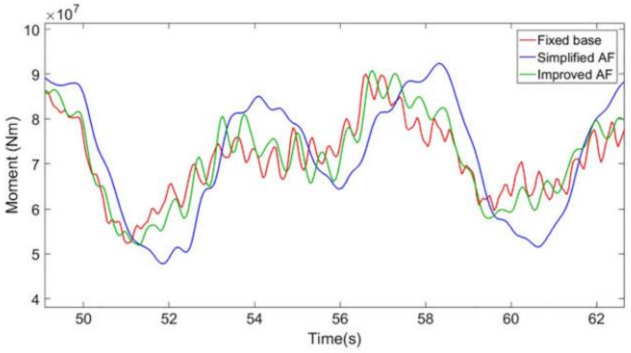

Figure 20: Mudline moment oscillations for the three foundation models. From (Loken et al, 2019).

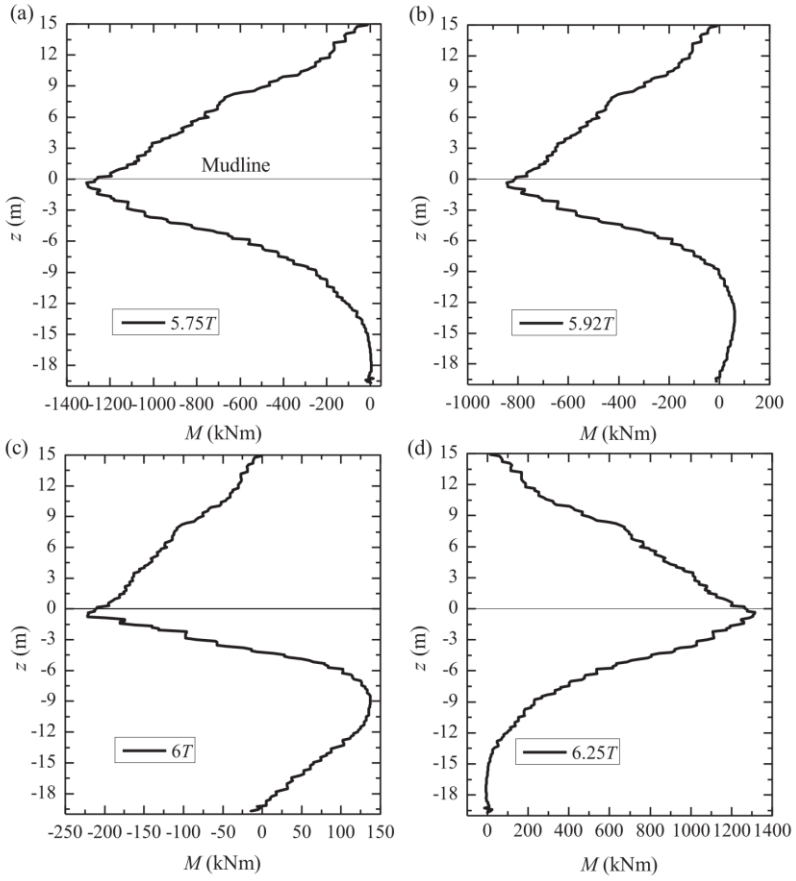

Figure 21: Distribution of bending moment of the mono pile at different times of the rocking pile model. (a) pile at position xp=10 mm, (b) pile at position xp=5 mm, (c) pile at position xp=0 mm, (d) pile at position of xp=10 mm. From (Zhang et al, 2018).

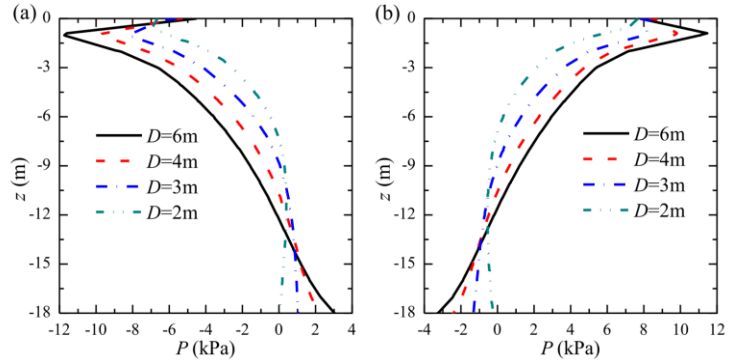

Figure 22: Effect of the pile diameter on pore water pressure vertical distribution. (a) t/T=5.75, (b) t/ T=6.17 (T=wave period). From (Zhang et al, 2018).

2.2.2 Load and response analysis of bottom-fixed wind turbines

Altough deployment of offshore bottom-fixed turbines are practiced worldwide very well, there is still a need for further research and development to increase their efficiency (Kumar et al., 2016). Due to state-of-the-art technological developments, nowadays, energy investors aim to minimise risk associated of accidents in the harsh weather conditions. It is also critical to carry out load and response analysis of bottom-fixed wind turbines.

Sorum et al. (2017) investigated DTU's 10 MW turbine on a monopile system for a number of deterministic and stochastic load cases using open source codes SIMA, vpOne and FAST. They found the damage equivalent bending moment at mudline changes between 1.60 and 1.87 kNm in the final fatigue analysis. They indicated the reason of variation (0.17-0.37) estimated utilization is due to small differences in the predicted tower top displacement which leads to unequal aerodynamic damping, and discrepancies in the controller dynamics.

Since aerodynamic loads are the main dominating loads on fixed-bottom offshore wind turbines, there are some studies which aimed to decrease loads on turbine components. For example, Thakur and Saha (2017) investigated load reduction by using controllable trailing-edge flaps on an offshore wind turbine using three fixed bottom foundations (namely monopile, tripod, jacket) for various water depths. Their findings indicated that all fixed-bottom wind turbines having trailing edge flaps reveal a load reduction in blade, tower and nacelle compared to standard turbines. This leads a decrease in maximum load range on the wind turbine units.

Structural health monitoring (SHM) systems are known as the solutions providing an early warning of damage to reduce operation and maintenance costs. For this purpose, Vidal et al (2020) introduced a methodology in order to detect the structural damage in jacket-type foundation and observations are taken for four different locations of the jacket wind turbine in a laboratory environment. While the majority of the studies in this area use measurable input excitation and vibration response signals, they assumed that wind is not measurable and can be taken as the only available excitation. They modelled wind Their findings also emphasised the significant importance of modelling environmental and operational conditions in a laboratory for long term monitoring.

Ju et al. (2020) used the Powell's method to find coupled dynamic equation of an OWT and TMDs. Also, they tried to determine the minimised objective funtion of fatigue damage.

2.2.3 Design provisions for extreme phenomena (earthquakes, tsunamis, typhoons)

Risk of damage causing by extreme phenomena (earthquakes, tsunamis, typhoons) is an important factor in the development of the offshore wind energy industry. Design provisions are intrinsically linked to local unique meteorological and ocean (met-ocean) conditions. IEC 61400 series of standards specify essential design requirements to ensure the structural integrity of wind turbines. Its purpose is to provide an appropriate level of protection against dam-

age from all hazards during the planned lifetime. IEC 61400-1 applies to wind turbines of all sizes. IEC 61400-3-1 provides additional requirements to offshore wind turbine installations. These standards is intended to be used together with the appropriate IEC and ISO standards. The new editions (IEC 61400-1:2019, IEC 61400-3-1:2019) includes the significant technical changes with respect to the previous edition,such as: extension of wind turbine classes to allow for tropical cyclones and high turbulence,adding two informative annexes concerning tropical cyclones,etc. Additional standards and guidelines from the American Petroleum Institute (API), International Organization for Standards (ISO), and class societies such as Germanischer Lloyd (GL), Det Norske Veritas (DNV), and the American Bureau of Shipping (ABS) are also considered essential to address key aspects of offshore wind turbine project. Based on experience as certification body in the wind industry, class societies standards and guides fill gaps and provide clarity and additional guidance. The requirements of class societies standards and guides focus on reaching the intended safety level in an economic way and have in general been aligned with requirements of other international standards, in particular with the IEC 61400 series of standards.

Tropical cyclone (Typhoon)

An offshore wind turbine shall be designed to safely withstand the wind conditions and marine conditions adopted as the basis of design. The wind regime and marine conditions for load and safety considerations are divided into the normal conditions which occur frequently during normal operation, and the extreme conditions which are defined as N-year return period. Combining marginal N-year events directly will in general produce load effects of longer return period than N years. The more environmental parameters that are combined in this way, the more conservative the design potentially becomes. Thus for offshore wind turbine design, the assessment of joint environmental conditions by specifying associated conditions instead of direct combinations of marginal conditions of equal return period is appropriate. To determine joint environmental conditions for design, the approach of environmental contours is introduced in IEC61400-3-1:2019. The joint environmental conditions to be designed for are then defined as those among all conditions on the environmental contour that cause the most extreme response.

The application of the method of environmental contours generally requires information defining the long-term joint probability distribution of wind and marine conditions. In practice not all environmental conditions are typically measured simultaneously. Environmental contours are instead developed for subsets of parameters, e.g. wave heights and water level, wave height and wave period , etc. The met-ocean conditions associated with tropical storms may exhibit greater variability (a larger coefficient of variation [COV) of the extreme values) than those associated with extratropical storms . This potentially requires changes to design rules , i. e. characteristic values (e.g. return periods) or safety factors, to maintain the same safety level as implied by the design rules contained within this document for extra-tropical conditions. Annex J of IEC61400-1:2019 describles a Monte Carlo Simulation (MCS) method for the prediction of tropical cyclone induced extreme wind speeds. The guidance is provided by IEC61400-3-1:2019 on assessment of extrem wave condition during tropical cyclone condition and at least 30 years of data are required in each case. The robustness level criteria used to verify the globe structure integrity of the substructure and foundation in tropical cyclone regions is also recommended in IEC61400-3-1:2019.

Germanischer Lloyd iseued Technical Note Certification of Wind Turbines for Tropical Cyclone Conditions in 2013 (GL-TN-TC, 2013). This Technical Note is supplemented with more information concerning tropical cyclone conditions of onshore sites, especially in the vicinity of oceans where tropical cyclones may occur. The definitions and requirements stated can be applied for offshore wind conditions, in conjunction with type and project certification of offshore wind turbines and their components as described in GL Guideline for the Certifi-

cation of Offshore Wind Turbines(2012). The definition of marine requirements in tropical storm conditions is site specific and has to be considered on case by case basis.

ABS published the revision of the Guide for Building and Classing Bottom-Founded Offshore Wind Turbine Installations in October, 2015 and updated in March, 2018. In this Guide, the Frøya wind model for tropical cyclone is adapted and validated by tropical cyclone wind data collected on the platforms in the Gulf of Mexico in the past 20 years. The formulation of the wind speed profile, wind speed standard deviation, turbulence intensity and gust factors presented in Guide is found to provide reasonably good representations of the easurements of tropical cyclone wind in the Gulf of Mexico. In absence of site data, the formulation in Guide may be used to model tropical cyclone conditions over the open ocean (ABS (2015)).

Earthquake

The earthquake resistance requirements are only design driving in a few regions of world. For locations where the seismic load cases are critical, the engineering integrity shall be demonstrated for the wind turbine site conditions. The evaluation of load shall take into account the combination of seismic loading with other significant, frequently ocurring operational loads. The seismic load shall depend on accederation and response spectrum requirements as defined in local Codes. Assessments of earthquake loading are described in IEC 61400-1:2019, in which it is defined that the ground acceleration shall be evaluated for 475 year return period. DnVGL-ST-0437 introduces the analysis of the dynamic response detailly. The follwoing recognized procedures and methods are suggested:

— response spectrum analysis

— time history analysis.

A three-dimensional model of the structure should be used for the analysis. When applying the seismic response spectrum, it shall be ensured, that the recurrence period is the same as that the chosen analysis method is based on. When the response spectrum analysis is applied for the combination of the modal maxima, the use of the complete quadratic combination (CQC) method as described in EN 1998 is recommended. When time domain simulations are used, the ground acceleration at the surface of the seabed shall be derived from the seismic response spectrum taking into account the soil properties. A sufficient number of stochastic acceleration time series of sufficient duration shall be taken into account.

Tsunami

Generally, a tsunami is generated by the uplift of the sea floor caused by earthquakes. The very long periods of Tsunami wave can result in substantial loads on moored floating structure (such as FOWT). So consideration should be given to the exposure of site to the possible directions of Tsunami wave approach and the associated currents from possible earthquake sources. The numerical model of tsunami is described in the IEC61400-3-2:2019.

2.2.4 Advanced structural analysis (Reliability based design/analysis, structural reliability)

Reliability analysis of offshore wind turbines is challenging since it involves time-consuming computational simulations. In (Morato et al, 2019) this paper, a kriging model is therefore used to efficiently estimate the response of the system, thus facilitating the computational demand in the reliability analysis. First, Latin Hypercube Sampling (LHS) technique is used to choose the Design of Experiments (DoE) from the random input variables (geometry, material, environmental parameters). Fully coupled simulations are performed on Matlab interface which links FAST v8 for aero-hydro-servo-elastic simulation and Abaqus for structural finite element analysis. In particular, the tower top resultant loads and mudline bending moment computed in FAST v8 are applied to the finite element model in Abaqus where a time-domain structural analysis is performed. Material and geometry nonlinearities are also introduced in the structural analysis. Consequently, the kriging models are fitted using the DoE and the desired structural

responses (i.e., von Mises stress, tower base bending moment, etc). The sensitivity of the kriging models is studied on the number of sample sets, stochasticity of waves, wind turbulence and the number of random seeds in the simulations. The developed kriging models are further applied to estimate the structural response in different load cases in the reliability analysis. Several limit state functions (LSF) are used to estimate the structural reliability, namely, Von Mises stress reaching yield, simplified tower buckling model, plastic yielding, blade – tower clearance, pile top displacement and pile top rotation.

In (Shittu et al, 2020), structural reliability analyses are performed using two different reliability approaches. The first approach uses the commercial tool (ANSYS DesignXplorer©) for the probabilistic finite element analysis (FEA). The second approach is the non-intrusive stochastic formulation, developed by the authors. In the first approach, a stochastic parametric finite element model is built by defining random distribution to the input parameters. The developed finite element model is employed in performing a series of FEA simulations on the offshore wind turbine support structure through the DoE module packaged in the DesignXplorer© facility in ANSYS. The standard response surface of DesignXplorer©, full second-order polynomials with manual refinements, is also used to map the response domain to the input parameters. The six-sigma analysis of DesignXplorer© which is based on Latin Hypercube Sampling (LHS) is used in the probabilistic assessment. In the second approach, the FEA simulation results are imported to MATLAB to develop a response surface model. A multivariate regression is used to approximate the response of the system and link output variables to the global inputs (wind and wave). The probability of failure and the reliability index is then calculated through first order reliability method (FORM) or Monte Carlo Simulations (MCS).

The framework presented in (Mai et al, 2019) the paper addresses how the oceanographic (wind, wave, etc) data can be utilized to predict the remaining fatigue life in a structural reliability context. In particular, the remaining fatigue life is described in terms of the cumulative failure probability which is obtained by evaluating the limit state function formulated based on Miner's rule. Strain data and oceanographic data are employed in the proposed methodology in which the former is used to derive stress-range distribution parameters and the latter is to update the probability distributions of the environmental conditions. Firstly, the formulation of the joint distribution function of the wind speed, significant wave height and wave period is presented. The short-term fatigue damage in each bin of oceanographic data is computed from the strain data. The Weibull distribution is used to describe the stress ranges in each bin, and its parameters are regressed such that the damage from the strain data is equal to the damage generated from the Weibull distribution. The fatigue limit state function is then formulated based on Miner's rule considering the probability of oceanographic data and its associated damage (generated through Weibull distribution parameters). The remaining fatigue life is modelled as the time to reach a target cumulative failure probability with respect to the formulated limit state function. The joint distribution of the wind speed, significant wave height and wave period can be updated when more oceanographic data is gathered on-site and subsequently, the failure probability and the remaining fatigue life can also be reassessed.

(Hlaing et al, 2021)This paper explores the influence of fracture mechanics models and failure functions on inspection and maintenance planning. Two different fracture mechanics (FM) models are employed to estimate the crack propagation. Whereas the one-dimensional FM model can be solved through an analytical equation, the two-dimensional FM model demands more computation to perform coupled numerical integrations. The conventional through-thickness failure criterion and a failure assessment diagram are used to evaluate the failure/survival of the fatigue component. In a through-thickness criterion, the failure happens

when the crack penetrates the thickness of the structural member. In a failure assessment diagram criterion, the through-thickness cracks may grow further, and failure is expected when the interaction of the crack-driving parameter and the load ratio exceeds a resistance threshold. Since the design of offshore wind turbines are based on the SN curves, the failure probabilities of FM models are calibrated to the SN model. The inspection and maintenance planning is then performed based on a pre-posterior decision analysis. Heuristic decision rules have been applied to identify the optimal maintenance policies (optimal interval and optimal annual failure threshold). For redundant structures with high fracture toughness, the failure assessment diagram is preferred since the occurrence of a failure event is significantly delayed compared to the through-thickness criterion.

(Yeter et al, 2019) quantifies the effect of the uncertainty in soil properties on the dynamic behavior of monopile wind turbines. A logistic sigmoid function allows to model different soil profiles, i.e., to reach the dense sand or hard rock layer in < 5m or >>25 m. Two possible scenarios of pile penetration are considered:

1. The pile structure is driven into the soil until it reaches a very dense soil, i.e., the natural frequency is affected by the mass of the pile.
2. The pile length is constant for any soil condition, i.e., the natural frequency is affected by the flexibility of the pile.

The dynamic characteristic, i.e., the first fore-to-aft natural frequency of the monopile offshore wind turbine is analyzed based on the Finite Element Method (FEM) employing the commercial software ANSYS. The uncertainties to physical variability of the soil, statistical uncertainties, and the model uncertainties are considered in the FEM analysis. The Monte Carlo simulation technique is employed to assess the probabilistic nature of the structural natural frequency of the monopile OWT support structure. The Probabilistic Design System (PSD) tool provided by ANSYS is used to perform the Monte Carlo simulations. The first natural frequency follows a Weibull distribution and its associated uncertainty is within the allowable range designated for the offshore wind turbine support structures. The uncertainty in the first natural frequency is the most contributed by the soil profile, and moderately by the elastic modulus of soil. Random variables associated with the modelling uncertainties have rather less influence on the first natural frequency.

2.3 Physical testing

2.3.1 Lab testing

As (Bhattacharya et al., 2021) correctly state, bottom fixed offshore wind turbines are complex dynamic systems involving wind–wave–foundation–structure interaction, where the control system in the RNA adds further interaction. The same authors list some established methodologies for testing the main critical components:

- Wind tunnel testing can model the aerodynamics and aeroelasticity interaction, and the performance of the blades.
- Wave tanks can be used to model hydrodynamic issues, including tsunami loads.
- Geotechnical centrifuge testing can model soil–structure interactions with correct stress–strain behaviours.
- A shaking table at 1 g or in a geotechnical centrifuge can model the seismic performance, including dynamic soil–structure interaction.

The selected references in this sub-chapter also fall within such a division. One hopes these will give a sense of what has be published in the period 2018-2021 in this specific field. It should also deliver an, arguable, suggestion of the current state-of-the-art in lab testing of bottom fixed offshore wind turbines.

Tests focusing on foundations, or on geotechnical aspects related to the foundations, seem to have been a very hot topic in the past 4 years. Bhattacharya et al (2021) provided an overview of the complexities and the common serviceability limit state performance requirements for offshore wind turbines and discuss the use of physical modelling for verification and validation of innovative design concepts, considering possible angles to de-risk the project. Examples of applications in scaled model tests are provided.

Good examples of tests focusing on foundations and where centrifuge tests are carried out are (Wang et al., 2018), who tested static and cyclic load conditions for a hybrid monopile foundation, (X. Wang et al., 2020), who performed shake table tests to the hybrid monopile foundation to investigate the seismic response, and (Jeong et al., 2020), who applied one-way and two-way cyclic loads to a suction bucket. Also, with the focus of seismic response, it is worth mentioning the work by (Chen et al., 2020) who performed (non-centrifuge) tests in air of grouted connections. These were subject to constant axial and cyclic lateral loads to study the hysteretic behaviour of grouted connections in offshore wind turbine support structures.

Also focusing on foundations but under a different approach, (Al-Hammadi and Simons, 2019) performed experiments in a flume tank to study the local scour mechanism. Cycle loads and non-loaded stages were alternated to mimic the effect of occurring storms. Another interesting study is that by (Lian et al., 2021) who studied the long-term performance of the wide-shallow bucket foundation model (WSBF) for offshore wind turbine in saturated sand by performing a 1-g cyclic experiment. Of particular interest is the modelling of an artificial neural network to obtain the relationship between loading conditions and the long-term performance of the WSBF model.

In terms of hydrodynamic loads' assessment in tanks, several interesting small scale physical model studies have been performed. (Bachynski et al., 2019) carried out an assessment of the experimental results for the response amplitude operator for regular waves and the 90th percentile seabed bending moment in long-crested irregular waves for a monopile wind turbine in waves tested in an ocean basin. Two models (analytical and numerical) were used for uncertainty propagation, with conclusions suggesting that bias errors in the model properties and in the wave elevation contribute the most to the total uncertainty. (H. Dadmarzi et al., 2019) carried out an experimental validation of hydrodynamic loads on two large diameter monopiles in regular waves at a scale of 1:50 in a medium sized wave tank. The monopiles were modelled as rigid bodies and measurements of the moment and shear force were taken at the base of the model. The first, second, and third harmonics of the total wave loads, where measurements were available, were calculated with different methods exhibiting differing levels of accurate prediction. Third harmonic loads, however, were overpredicted by the calculations, in general. In (Bachynski et al., 2020), experimental observations from a hydrodynamic test campaign with a flexible monopile in the same tank subject to irregular waves were reported.

Assessment of loads from steep and breaking waves from experiments is also a relevant field of study for which three paradigmatic research works are mentioned here. (Banfi et al., 2019) studied loads arising from broken wave impacts on a cylindrical turbine substructure in shallow waters, using a small-scale cylindrical model fitted with load-cells. (S. Wang et al., 2020) performed tests with a jacket structure under steep and breaking waves. Global forces on the structure were measured through force transducers iwo the connection of the model to its support. The authors conclude that their work provides a first step for calibration of a distributed slamming load model, through the characterization of the total external impact force. (Zeng et al., 2021) compared experimental and numerical (URANS) results of breaking waves in a monopile-type offshore wind turbine. Specifically, the wave run-up around the monopile and the nonlinear total horizontal wave force on the monopile were examined. A 1:80 scaled physical model in a wave flume tank was used.

On a less usual approach to testing, (Tödter et al., 2021) resorted to digital imaging correlation (DIC) to measure the deformation of a monopile subject to vortex induced vibration. The objective was to measure the response without influencing model properties and the flow field. Results obtained from the conventional technique using triaxial accelerometers were compared with the ones using DIC.

2.4 Transport, installation, operation and maintenance

2.4.1 Transport and installation

Offshore wind turbines include foundations, towers, nacelles and blades, etc. The foundation has different choices according to the sea environment, water depth and geological conditions. According to the various conditions of different sites, geological and maritime weather conditions are different from the environment. European wind farms are stable in wind conditions and the landforms are mostly flat. Some other regions are threatened by natural disasters such as typhoons and earthquakes. As a result, such special factors must be taken into consideration in the design stage of offshore foundations.

Furthermore, a wind turbine with a larger capacity helps to capture more air volume, which is accompanied by wind turbine technology and manufacturing. The more mature, the stability of the foundation becomes more important. Different types of foundations are applicable to different seabed conditions; depending on the fixed foundation structure, the foundation can be roughly divided into several types including gravity, mono-pile, tripod, jacket and suction bucket as shown in Figure 23.

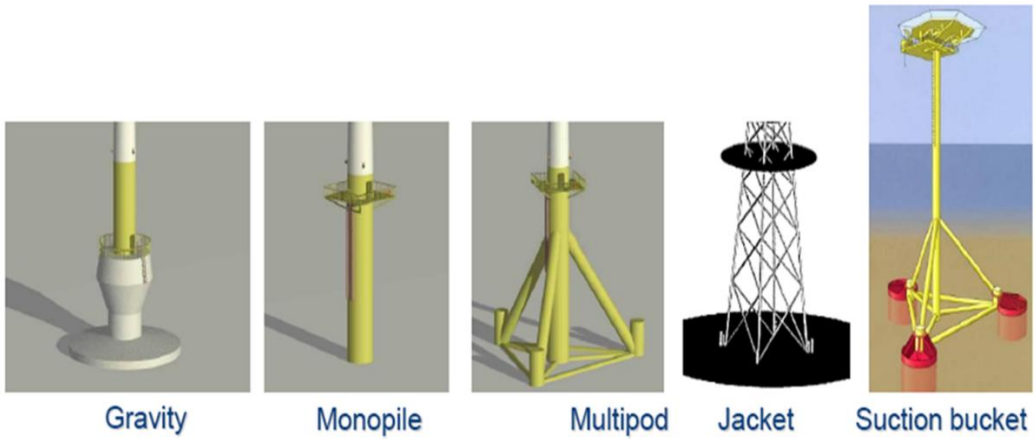

Figure 23: Fixed type foundations

Monopile foundation is suitable for shallow water and sea areas with gravel, sand or clay on the seabed. Small wind farms can use it to shorten the construction time, and large-scale wind farms can be used to reduce development costs, such as The London Array wind farm, the world's second largest wind farm in the UK, or the expanded Kentish Flats wind farm, and the world's largest Walney Extension wind farm use this type.

When in deep waters and less restricted by seabed conditions, jacket foundations should be the first choice. The Steel truss system is very suitable for applications in wind farms with large winds or storms. Those adopting this type include the first commercial-scale Tamra wind farm in South Korea, Block Island, the first commercial wind farm in the United States, and Saint Brieuc, which is about to be operated wind farm in France in 2023. The piling methods include pre-piling and post-piling. Nowadays, for the convenience of schedule, the pre-piling is mostly used for installation.

The same is not limited by the seabed conditions, but in the waters of medium depth, the "tripod foundation" can be selected. It is suitable for use in wind farms with strong ocean currents or

severe weather, but due to the heavy weight, the manufacturing cost is high. Less common internationally, Alpha Ventus, Germany's first offshore demonstration wind farm, is one of the few adopting this technology. If it is shallow water and the geologically hard sea area, there is another option for gravity type foundation. However, concrete is used to lay the seabed in the world, so flat geology is less constructional concerns. Denmark, which was decommissioned in 2017 Vindeby wind farm adopts this type.

The fixed foundation has its applicable water depth range. Exceeding the applicable water depth may increase the cost. Therefore, the technology of floating platform has appeared internationally. The Hywind Scotland wind farm, which has been connected to the UK, is the most famous, and the neighboring country Japan has also invested. The relevant research and the construction of two demonstration projects. As the offshore wind power development phase will move from potential sites to block development, the current forward-looking technologies will be possible.

2.4.2 Operation and maintenance

Recent theoretical and technical advancements have been documented in the literature on offshore wind operation and maintenance aspects. Logically, and due to the inherent autonomous nature of offshore wind operation as well as the potential for cost reduction, the efforts have focused more on the maintenance front. The reader is directed to (Ren, 2021) for a complete and detailed overview. The main challenges associated with maintenance optimization approaches include the need of properly treating the uncertainties involved in the estimation of failure statistics and imperfect observations collected from the offshore wind turbines, i.e. variability of environmental conditions, deterioration mechanisms model uncertainty, potential false alarms raised from remote sensing, and the subjective technician skills. The developments registered are, therefore, twofold, seeking the improvement of weather forecasting and investigating modern and more efficient maintenance optimization approaches.

In terms of offshore wind assets maintenance scheduling, the need for predictive maintenance approaches is repeatedly addressed, predictive maintenance provides more cost-competitive strategies than reactive, calendar-based or condition-based monitoring, yet at the expense of more complex and sophisticated maintenance optimization (Yan, 2021). The emphasis thus is on developing predictive maintenance methods that can provide optimal policies within a reasonable computation time. Newly conceived methods for maintenance optimization and scheduling of offshore wind assets include deterministic optimization of costs via genetic algorithms (Rinaldi et al, 2020) and advanced stochastic optimization methods through an integration of Markov decision processes and deep reinforcement learning (Morato, 2021). Generally, digital twins and machine learning are also increasingly facilitating more modern automated diagnostic and prognostic schemes (Rinaldi, 2021).

As aforementioned, significant attention has been devoted to the development of structural health monitoring techniques (Dong 2018, Lian 2019). SCADA systems and condition-based monitoring schemes, e.g. strain sensors, are widely reported in the literature, registering improvements in accuracy and efficiency detection (Mai et al, 2019). In the future, the emphasis will most likely be on system-level structural health monitoring approaches, sensing at the wind farm level, and examining existing statistical and/or functional correlations among offshore wind components. Further development on feature extraction and identification techniques can also be expected applicable to both data-driven and physics-based models.

2.5 Design standards and guidelines

Text

3. FLOATING OFFSHORE WIND TURBINES

3.1 Recent industry development

The years since the last issue of this report showed rapid progress in the readiness of floating wind turbines. The first commercial wind farm (Hywind Tampen : 11 x 8MW on concrete spars) is currently in the construction phase. Several pilot wind farms (Hywind Scotland : 6x6MW on spars, Kincardine : 5x9.5MW on semi-subs, Windfloat Atlantic : 3x8.4MW on semi-subs) were commissioned. In parallel, 4 pilot wind farm projects are underway in France in the bay of Biscay and the Mediterranean Sea. The Maine floating wind project is also progressing. The first commercial tenders open to floating wind were open in Scotland and France. All these farms use horizontal axis wind turbines with very limited modifications.

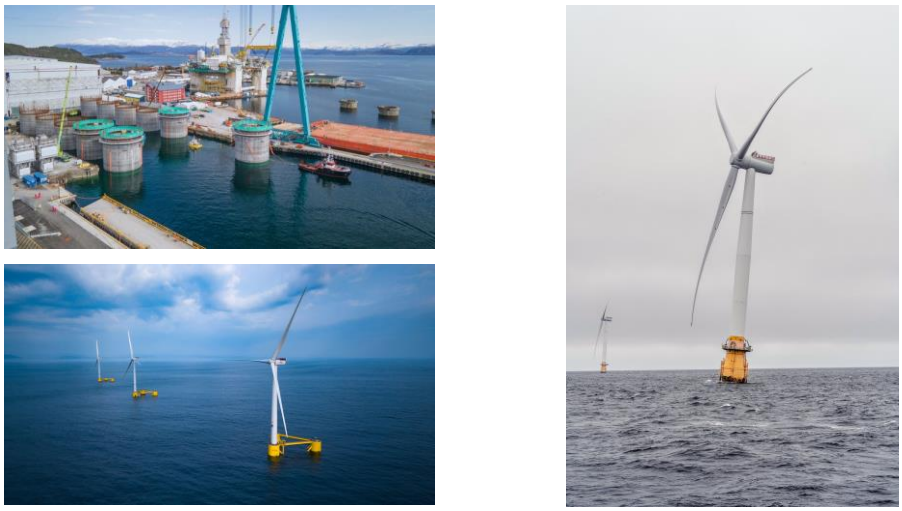

Figure 24: The Hywind Tampen wind farm under construction (top left), the Kincardine farm after completion (bottom left) and the Hywind Scotland farm in operation (right)

In parallel, technology development progresses. Several full scale demonstrators were commissioned : two Damping Pool barges in France and in Japan in 2018 and the TetraSpar in Norway in 2021. Smaller scale prototypes were also commissioned : the Eolink in France and BlueSATH in Spain. Worth noting is that the BlueSATH floater capsized in a storm. Little information is available about this incident, but it is not the first serious stability accident on a floating wind turbine (Sway sinking in 2011, MODEC's Sqwid loss in 2014, JMU's advanced spar uncontrolled tilting in 2016). We will show in this section that simulation models were reported to be on the conservative side, but the occurrence of accidents would push reasonable technology developer to deploy full-scale prototypes before commercial wind farms.

Figure 25: Full scale demonstrators : TetraSpar (left) Damping Pool (Right)

Figure 26: Intermediate-scale demonstrators : BlueSATH (left) Eolink (right)

A number of rules were issued since the last report by the International Electrotechnical Committee and major classification societies (DNV, BV, ABS, LR, NK) have their own set of rules. Insurers are also addressing risks and a recent whitepaper by the World Forum Offshore Wind (WFO) proposes ways to mitigate risks. The main risks anticipated relate to mooring and cable systems. Although unquestionable, the track record of stability incidents should also teach us prudence in this respect. The WFO hence recognizes the merits of redundancy when it comes to mooring systems, although keeping the possibility to design non-redundant mooring systems associated to emergency plans.

Although technology is maturing fast, recent outcomes of the Offshore Code Comparison, Collaboration, Continued, with Correlation project (OC5) Robertson et al. (2017) show that research and technological challenges must be faced when floating offshore wind turbines are considered. A consistent level of safety and prediction of the performance is the result of a comprehensive analysis where tower-blades aeroelasticity is strictly coupled with the floater-waves interaction problem. They are also the result of well-structured global and local verifications. For these reasons, and in view of the costs and complexity of devoted experimental tests, reliable and accurate numerical tools are seen as a complementary way to address floating offshore wind turbines analysis.

This chapter will address the simulation of the hydrodynamic loads, the simulation of aerodynamic loads, testing at sea and in laboratory and aspects for technology and components qualification.

3.2 Numerical tools Integrated and hydrodynamic aspects

One of the aims of integrated design tools, is to help the conceptual design of the new generation FOWT, a comprehensive and fast understanding of the system dynamics is crucial to save costs in later design phases. This requires low- and medium-fidelity models that are currently still used and enhanced. Among the different examples of such approaches, Lemmer et al. (2020) shows a comprehensive flexible multibody model including rotor aeroelasticity and floater hydrodynamics coupled with a quasi-static mooring analysis and blade control system to analyse fatigue and short-term extreme responses of the FOWT. Moreover, Wang et al. (2020) investigates the computational methods for calculating the dynamic responses of a floating wind turbine proposing a new identification method for fitting a state space model to approximate the convolution term in the motion equation of the floating wind turbine have been specified.

The increasing availability of fully integrated numerical tools for the analysis of FOWT has recently produced several applications to the analysis of different specific issues. As an example, Souza et al. (2019) explore the external loads acting on a FOWT, with special attention to nonlinearities which affect its low-frequency global motions. Surge and pitch decay periods variations were observed for FOWTs operating under different incident wind velocities by using SIMA, a software developed by SINTEF OCEAN combining na hydrodynamic module (SIMO) with a FEM-based tool for the analysis of the blades, tower and mooring lines (RIFLEX). It is found that the period variations in surge are mainly linked to the mooring system nonlinearities, whilst for the pitch they are induced by the thrust at the turbine, in

combination with the nacelle motion and height relative to sea water level. This effect is expected to be more relevant for higher towers, and thus more important for turbines of higher capacity. On the other hand, the phenomenon can be attenuated by proper tuning of the FOWT's own pitch natural period, by “placing” the oscillations in a range where the apparent inertia effect is less relevant.

Lemmer et al (2020) carried out a numerical study on semi-submersible wind turbine. Their study consists of two parts including setting up an integrated optimization procedure for semi-submersible FOWTs and introducing a new design indicator considering optimal dynamic behavior of semisubmersibles in future designs. The emphasis was also given to possibility of designing a FOWT platform with minimized effect of the waves on power generation and suitability of carrying a wind turbine.

Within an effective FOWT design process, a very relevant role is played by optimization techniques. The availability of comprehensive low-/mid-fidelity tools is thus the basis for the integrated design optimization of these systems. As an example, in Hegseth et al. (2020) a linearized aero-hydro-servo-elastic floating wind turbine model is presented and used to perform integrated design optimization of the platform, tower, mooring system, and blade-pitch controller for a 10 MW spar floating wind turbine. Optimal design solutions are found using gradient-based optimization with analytic derivatives, considering both fatigue and extreme response constraints, where the objective function is a weighted combination of system cost and power quality. The optimized platform has a relatively small diameter in the wave zone to limit the wave loads on the structure and an hourglass shape far below the waterline. The shape increases the restoring moment and natural frequency in pitch, which leads to improved behaviour in the low-frequency range (see Fig. 8). State-of-the-art nonlinear time-domain analyses show that the proposed linearized model is conservative in general, but reasonably accurate in capturing trends suggesting its suitability for preliminary design calculations.

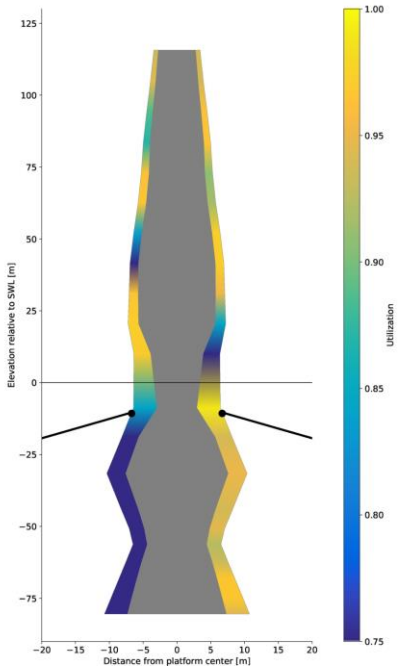

Figure 27:Optimized tower and platform design with fatigue utilization (left) and buckling utilization (right). The wall thickness is scaled by a factor of 40 relative to the diameter for visualization purposes. From Hegesth et al.

Another study on hydrodynamic design of a free-float capable TLP was carried out by Uzunoglu and Soares (2020) utilizing 10 MW wind turbine. In this work, basic principles of hydrodynamic design of a dynamically self-stable hybrid platform (Barge TLP hybrid floater) which has a free-float capability TLP, namely CENTEC-TLP, were presented in detail. They

introduced a dynamically stable design capable of free-floating on a shallow draft which also works well for a TLP. Towing the system without facing into any shore-side depth limits can be possible by using this design. Also, the emphasis was given to total mass where it still be maintained low enough as long as it redistributed accurately.

3.3 Aerodynamic aspects in simulations

From a general standpoint, performance predictions with good levels of accuracy and low computational burden are of great interest for those involved in the preliminary design of on/off-shore wind turbines. Recent results from the IEA Task 29 Phase IV on Detailed Aerodynamics of Wind Turbines in Schepers et al. (2021) highlight the limitations of Blade Element Momentum Theory (BEMT), widely used by the industry, in predicting blade aeroloads under unsteady flow conditions.

A thorough analysis of BEMT limitations for FOWT applications is addressed in Leroy et al. 2019 by the design tool InWave where the lifting-line prescribed vortex wake (PVW) and free vortex wake (FVW) aerodynamics solver CACTUS, developed at the Sandia National Laboratories (USA), are coupled to a multi-body mechanical solver and to the Boundary Element Method (BEM) code Nemoh for platform hydrodynamics (see Fig. 1). This study demonstrates that differences can be observed between BEMT (implemented in the well-known solver FAST), PVW and FVW codes especially at high tip speed ratio (TSR) for which unsteady aerodynamic phenomena and complex wake dynamics occur. In detail, Fig. 2 shows that at rated wind speed (11.4 m/s) under regular waves and constant wind, although the pitch amplitude is similar between the three codes, the PVW and FVW codes predict much greater power coefficient variations and different mean and amplitude variations of the controlled blade pitch. These discrepancies are confirmed under irregular waves (defined by a JONSWAP spectrum with 6 m significant height, 10 s peak period and 3.3 peakness factor) and turbulent wind conditions (based on a Kaimal spectrum with a 8.5% turbulence intensity). Figure 3 shows the PSD for the two wind speeds. At high TSR (Fig. 3, left), a good agreement between the three solvers at wave frequencies (around ω = 0.62 rad/s) is shown, but there are significant differences at low and pitch resonance frequencies responses (respectively around 0.05 and 0.17 rad/s). At low TSR (Fig. 3, right) the three approaches are in good agreement. In particular, both vortex methods results are superimposed. Similar conclusions can be obtained for the other DOFs, the aerodynamic loads and mooring tensions. In misaligned wind and wave conditions, the motion of the rotor is even more complex as more platform DOFs are excited. At high TSR, this induces highly unsteady phenomena in the wake dynamics and in the rotor/wake interactions. Eventually, they strongly impact the rotor aerodynamic loads and thus the motions of the FWT especially at low frequency motions when the wave loads are not dominant.

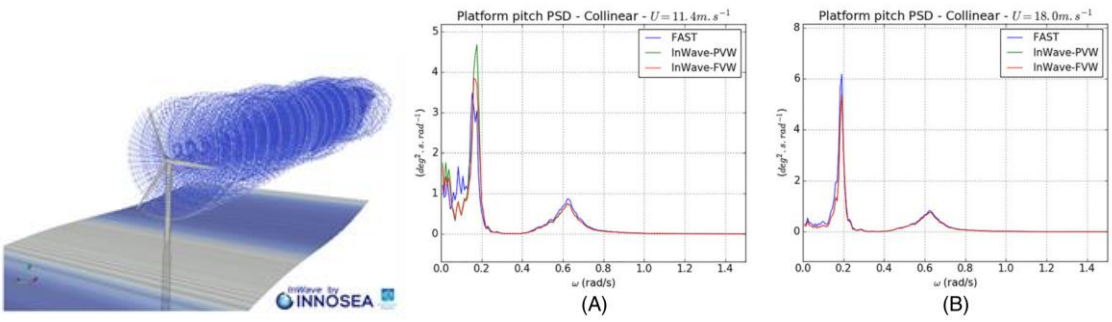

Figure 28: Fig. 1 - Screenshot of a FOWT simulation, Platform pitch power spectral density (PSD) in collinear wind and waves at high tip speed ratio (TSR) (centre) and low TSR (right) from [3].

On the other side of a hierarchy of aerodynamic formulations, Computational Fluid Dynamics (CFD) tools based on Reynolds Averaged Navier-Stokes Equations (RANS) Porcacchia et al.

(2017), Detached Eddy Simulation (DES) [Porcachia et al., Boorsma et al. (2018), Bangga et al. (2017)] or Large Eddy Simulation (LES) [Sedaghatizadeh et al. 2018 Benard et al. (2018)] have shown the capability to yield physically consistent predictions of turbine performance and aerodynamics, thus interest in coupled CFD-CSD (Computational Structural Dynamics) techniques is increasing as well [ANY REFS HERE??]. Nevertheless, the high computational costs of such simulations make their application impractical during the earlier stages of the design, especially in view of massive aeroelastic and aeroservoelastic analyses required to comply with IEC-61400 standard regulations. Indeed, within the vast literature on the subject, to the authors knowledge, the CFD studies of the coupled aerodynamic-hydrodynamic response of a floating offshore wind turbine are typically addressed under the assumptions of rigid bodies for the rotor, tower and platform, whilst the lumped mass approach is used for the mooring lines. An example of such high-fidelity and detailed simulations is reported in [Tran et al. 2018] where the commercial code STAR-CCM+ is used to perform a multi physical simulation including simultaneously the 6-DOF platform motions, the rotating blades, and the constraint effect of catenary lines. The volume of fraction (VOF) method is applied to investigate the complex wave interference effect on the moving platform structure. In addition, a moving overset grid technique to effectively solve the large dynamic behaviors of a FOWT due to the combined wind-wave coupling is considered. The computational mesh used for the calculations is shown in Fig. 4. The analysis of the DeepCwind semisubmersible floating platform with the NREL 5MW wind turbine rotor is compared with outcomes from FAST code implementing unsteady aerodynamics based on the Generalized Dynamic Wake (GDW), the dynamic stall model by Beddoes-Leishman and tower shadow modelling. Even if under uniform wind conditions the calculated blade aerodynamic loads show a good agreement, the combined effect of uniform wind (11 m/s) and regular waves (H=7.14 m, T=14.3 s) yields that the average values of heave and pitch response of the platform are in good agreement whilst the amplitudes show some discrepancies and the percentage differences between the average values of the surge (19%) and the mooring line tensions are relatively large (see Fig. 5). Concerning the aerodynamic loads acting on the rotor, differences in the oscillating amplitude of thrust and power coefficients (33% and 140%, with respect to FAST-FDW, respectively) and on the corresponding average values (1.6 % and 5.6 % with respect to FAST-GDW, respectively) are observed (see Table 1).

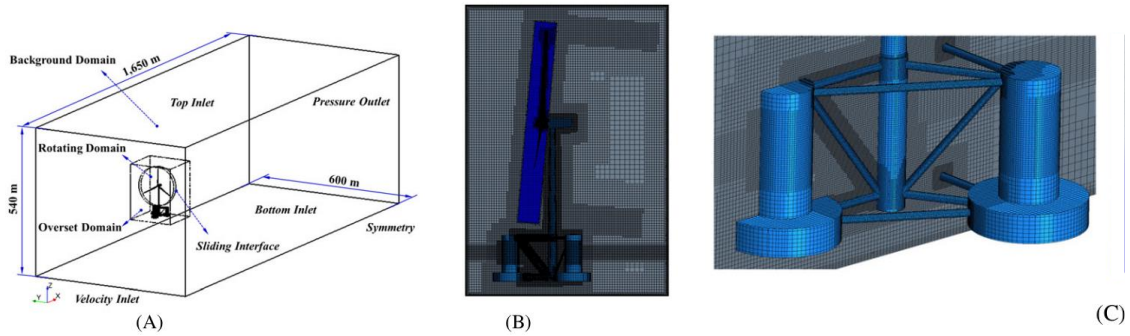

Figure 29: Computational mesh for floating offshore wind turbine model. (A) Computational domain, (B) entire turbine model with overset region, and (C) close view of turbine parts and platform surface mesh. From [11].

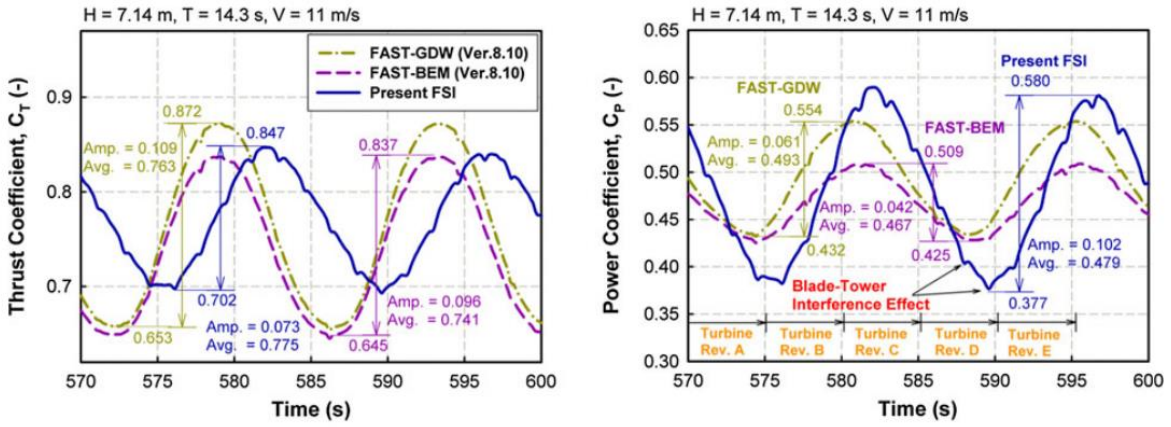

(A) Thrust coefficient (B) Power coefficient

Figure 30: Comparison of aerodynamic performance, platform dynamic responses, and mooring line tension. BEM, blade element momentum; FAST, fatigue, aerodynamic, structure, and turbu-lence; FSI, fluid-structure interaction; GDW, generalized dynamic wake. From [11]

A detailed investigation about the onset of propeller and Vortex Ring State (VRS) conditions for a FOWT is addressed in Kyle et al. (2020), where the effect of surge motion on the thrust is investigated with OpenFOAM, a general purpose widely used software based on the finite volume method and solving the incompressible Reynolds-Averaged Navier-Stokes (RANS) equations. In this work, an overset mesh method is used to create separate individual sub-meshes (for the rotor, tower and background domain) and then merge them into one, with the boundaries between each individual sub-mesh overlapping to act as a bridge between the various sub-domains. The analysis addresses the NREL 5 MW wind turbine undergoing an imposed sinusoidal surge motion of amplitude 9.4 m and period 8.1 s at different wind speeds (rated and below rated). The kinematics conditions are preliminary identified by using the Actuator Line theory to estimate under which wind and surge conditions propeller state or VRS might occur. The analysis shows that the combination of strong waves with low/moderate wind speeds leads to propeller-like conditions: a negative thrust for the entire rotor, through the combination of an inboard region of negative and outboard region of small but still positive thrust, was observed during the expected part of the surging cycle (see Fig. 6). VRS was observed with blade tip-vortex interaction and root vortex recirculation due to the duration with a negative relative rotor velocity being similar to the blade passing period, inhibiting vortex advection downstream (see Fig. 7).

Although very accurate, the CFD methodologies mentioned above require a very high computational resource and can therefore not be developed into a design tool to simulate several load cases for the single rotor and many wind turbines in an array for the different wave and wind conditions experienced by an installation. Indeed, this family of tools is necessary to develop a better understanding of the conditions giving rise to unsteady aerodynamics phenomena like propeller and vortex ring states and their effect on turbine performance and blade loadings.

In order to reduce the computational costs of FOWT simulations, hybrid formulations where low/mid-fidelity rotor aerodynamics models are coupled with high-fidelity tools for the analysis of the floater hydrodynamics have been recently proposed. This kind of approach aims at including also rotor aeroelastic effects within the simulations. An example of such methods, although still applied under rigid body assumption for all FOWT components (except the moorings, which are divided into a number of segments) is presented in Cheng et al. (2019) where an unsteady Actuator Line model for rotor aerodynamics is coupled with the three-dimensional RANSE solver OpenFoam. The application of this solver to the analysis of the NREL 5 MW wind turbine mounted on a semi-submersible platform shows that, in the fully

coupled system, both aerodynamic thrust and power decrease with respect to the bottom fixed condition. The incoming wave frequency is found to be the main driver of rotor unsteady aerodynamic loads whose amplitude increases with the wave height. Differently, little influence of the wave is found on rotor average loads. The analysis of the platform dynamics shows that the effect of turbine aerodynamics as an external load on the supporting platform has a relevant impact on platform surge, heave and pitch DOF average values, while the influence of turbine loads on the fluctuation of platform is negligible.

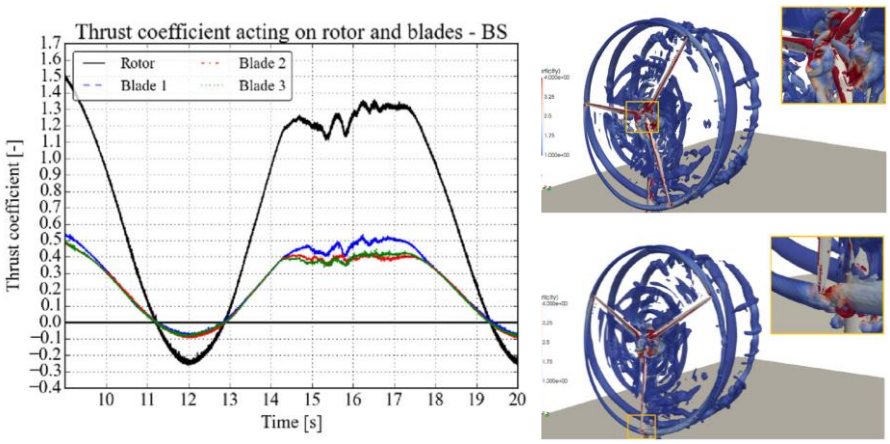

Figure 31: Thrust coefficient acting on the rotor as a whole and each blade individually under below-rated conditions in surge motion. From [12].

A good trade-off among accuracy of simulation, CPU time demand and out-of-the-box functionality is nowadays represented by potential flow methods; in fact, outcomes of the EU AVATAR project and literature works (see, for instance, Boorsma (2018)) demonstrate that three-dimensional (3D) unsteady panel methods based on a Boundary Element Method (BEM) formulation for subsonic inviscid and irrotational flows provide predictions in good agreement with experimental results for a variety of operational and inflow conditions. In this framework, viscous effects can be roughly modelled by invoking the behaviour of an equivalent flat plate whose local Reynolds number matches the blades operating conditions Greco et al. (2021). However, better predictions able to account for flow separation effects, as those occurring in off-design, may be achieved through Integral Boundary Layer (IBL) techniques [Ramos-Garcia (2017), Vaithiyanathasmy et al. (2018) or Reduced Order Models [Calabretta et al. (2016)]. Several literature works demonstrate how potential flows aerodynamic methods, like lifting line or vortex lattice based theories, are widely used in the prediction of turbine performance (see, e.g., Blondel et al. (2017)), especially for onshore installations. Although fast and easy to be coded in numerical algorithms, such modelis are inherently less accurate with respect to BEM-based formulations, whose application, to the author's knowledge, is however limited to few investigations. Among these, Netzband et al. (2018) proposes a wake stabilization method freezing the free-wake after one-third of rotor revolution within the coupled hydro/aerodynamic analysis of a turbine on a floating platform. Furthermore, Nelson et al. (2017) introduces a novel approach to model severe separation phenomena within potential flow methods. Following this family of aerodynamic and hydrodynamic modelling, an investigation of the fluid-structure interaction of a floating wind turbine is presented in Wiegard et al. (2021), where a partitioned approach is used to couple the first-order panel method panMARE for simulating floating offshore wind turbines (FOWTs) in time domain with a detailed finite element model built within the commercial code ANSYS to analyze the global deformations, and the corresponding stresses, on blades, tower and floater.

Finally, the interaction between a floating wind turbine with the atmospheric flow and with other FOWT in a large wind farm is becoming increasingly relevant. In Doubrawa et al. (2019), large-eddy simulations of turbulent velocity fields that are stability-dependent and

contain three-dimensional coherent structures are performed. These flow fields are then used to investigate the suitability of the Kaimal Spectrum Exponential Coherence (KSEC) and Mann stochastic turbulence generation models for the prediction of loads on a realistic spar-system floating offshore wind turbine, and to quantify how the assumption of neutral stratification propagates to short-term load estimates. Using the NREL SOWFA software, it is found that both stochastic turbulence models overpredict fatigue loading in high-wind scenarios (in some cases, by more than 25%) and underpredict it when the wind speed is low (by as much as 20%). Finally, turbine loading is found to be sensitive to atmospheric stability even when the turbulence intensity remains fairly constant. This sensitivity is most pronounced at low wind speeds, when fatigue load estimates on the spar system can differ by 40%. This analysis may suggest that using the Mann model could lead to overly conservative design decisions for spar systems. While this is an important finding, a lifetime fatigue estimate must be carried out to expand these conclusions beyond short-term fatigue estimates. Even in offshore environments where the turbulence intensity does not undergo as much variation as it does over land, atmospheric stratification can still have a noticeable effect on load fluctuations. This result may carry over to design decisions and suggests that neutral stratification assumptions might need to be reconsidered for design load calculations of large offshore rotors.

As an example of the analysis of wake interaction between multiple floating wind turbines, the application of the FAST.Farm model developed by NREL is proposed in Adam et al. (2020). This software is an extension of the widely used aero-hydro-servo-elastic tool OpenFAST (formerly known as FAST) and incorporates instances of OpenFAST together with wake dynamics and ambient wind and array effects modules to capture the wake interaction within a wind farm. A low-resolution wind domain (in space and time) of the entire wind farm is used for resolving wakes, while a high-resolution domain around each wind turbine is used to accurately compute structural loading. With the aim of analyzing wake meandering effect on platform motion and fatigue loads on the FOWT structure, a 10 MW two-turbine case with three different FOWT concepts (semisubmersible, spar, tension leg platform), separated by eight rotor diameters in the wind direction, are analyzed at different wind speeds and turbulence intensity levels (Fig. 10). The main outcomes of the analysis show that for the semi submersible platform at the below-rated wind speed, when wake meandering is most extreme, yaw motion standard deviations for the downstream FOWT are approximately 40% greater in high turbulence and over 100% greater in low turbulence when compared with the upstream turbine. Moreover, the low yaw natural frequency (0.01 Hz) of the semisubmersible is excited by meandering, while quasi-static responses result in approximately 20% increases in yaw motion standard deviations for the spar and TLP. Differences in fatigue loading between the upstream and downstream turbines for the mooring line tension and tower base fore-aft bending moment mostly depend on the velocity deficit and are not directly affected by meandering. However, wake meandering affects fatigue loading related to the tower top yaw moment and the blade root out-of-plane moment. As a general conclusion, fatigue tends to increase for the below- and above-rated wind speed whilst low-frequency resonant responses at a given ambient or waked wind speed are more important drivers for determining fatigue.

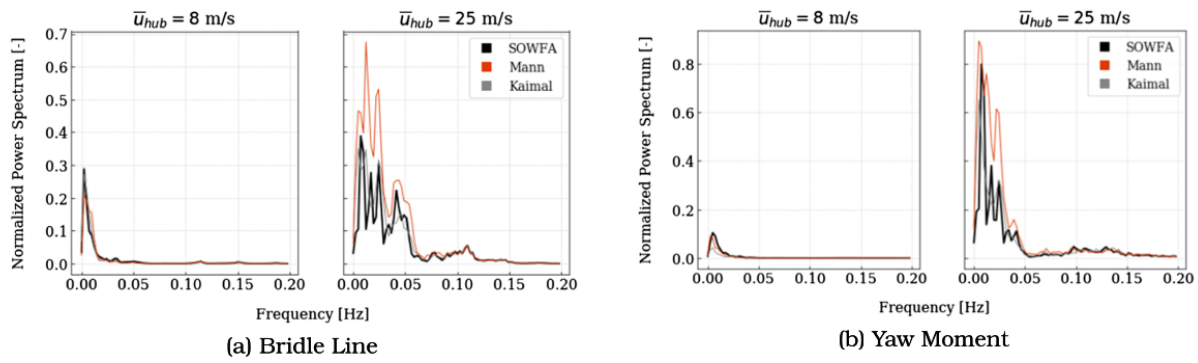

Figure 32: Comparison of turbine response in terms of load spectra for two wind-speed scenarios (be-low and above) and the three flow-simulation methods [SOWFA (black), Mann (red), and KSEC]. Fairlead tension on one of the upstream bridle lines (a), and the tower-base yaw moment (b). The mean magnitude of spectra is not given. From [25].

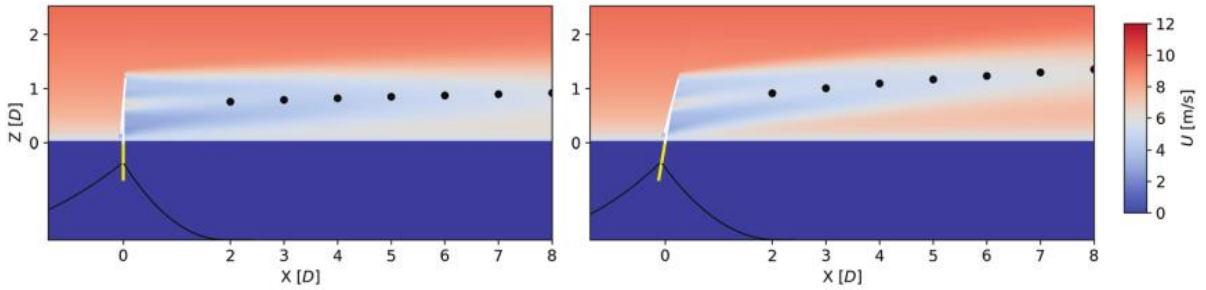

Figure 33: Flow visualization of the wind speed in the XZ -plane for a spar without (left) and with (right) a pitch offset of 10°. The black dots represent the vertical wake center position. From [26].

3.4 Physical testing

3.4.1 Lab testing (also include moorings and dynamic cables)

In general, lab testing of floating offshore wind turbines (FOWT) in the last 4 years has mainly resorted to the application of so-called hybrid testing approaches to work around the different scaling requirements for turbine aerodynamics and floater hydrodynamics. In these approaches, either the hydrodynamic or the aerodynamic related loads are applied to the structure through actuator devices. These loads (or motions) are either pre-computed or resolved in real time by use of numerical software that responds to the tests' physically driven behaviour and governs the loads to be applied at the actuators. Many authors typically identify the implementation of these hybrid approaches as Hardware-In-the-Loop (HIL) or Software-In-the-Loop (SIL) tests. A (less flexible) possible alternative is to redesign the turbine blades in model scale using a steady thrust-matched rotor design to deliver a targeted thrust, as in the experimental analysis of a scaled DTU10MW TLP FOWT with different control strategies by (Madsen et al., 2020).

(Tomasicchio et al., 2018) performed the experimental scaled modelling of the dynamic behaviour of a spar buoy wind turbine subject to waves and wind loads. These tests were performed at the Danish Hydraulic Institute (DHI) through the EU-Hydralab IV Integrated Infrastructure Initiative, so the raw data are public domain. Static wind loads were reproduced by applying the mean thrust force to the nacelle. This was done with a weightless line connected to the nacelle, passing through a pulley and with a suspended mass. In (Hall & Goupee, 2018), a cable-based wind loads hybrid coupling approach was applied to a 1:50 scaled model of the DeepCwind semisubmersible FOWT. The tests considered a 1 DOF wind driven force applied to the model. It included two cables acting longitudinally at the height of the nacelle and connected to actuators (winches) on "land".

Employing fans connected to the model instead of cables to apply wind forces on the models, (Azcona et al., 2019) used a ducted fan installed at the nacelle of a 1:45 FOWT scaled model to apply wind driven loads to the model. Another example is the approach by (Kanner et al., 2019) considering the scaled model tests of of two counter-rotating vertical-axis wind turbines fitted on a floating platform (similar to the WindFloat one). Only tangential forces on the VAWTs are modelled and used to mimic the power production stage of the turbine.

While the abovementioned approaches consider only the thrust force being applied to the model at any given time, (Urbán & Guanche, 2019) presented a new hybrid system which can include other loading aside from thrust and wind turbine torque. It is based on a "multi-fan" serving as a wind force actuator system, which allows the high-fidelity reproduction of a wide range of wind turbine aerodynamics. Another approach, also capable of modelling a wide range of turbine aerodynamics, is the one presented in (Thys et al., 2019). Recent advances to this cable-driven wind force actuation type method are described, including extended testing capabilities and load application up to the 3p frequency and the first tower bending frequency. Tests on a 10-MW semisubmersible FOWT at SINTEF Ocean are reported. In (Thys et al., 2018), procedures are recommended to perform hybrid model tests with a FOWT in a wind tunnel and an ocean basin. The recommendations are an outcome of the European project LIFES50+ project, where hybrid model tests were performed in the wind tunnel at Politecnico di Milano, as well as in the ocean basin at SINTEF Ocean. The model tests in the wind tunnel were performed with a physical wind turbine positioned on top of a 6DOF position-controlled actuator, while the hydrodynamic loads and the motions of the support structure were simulated in real-time.

Focusing on wind tunnel tests, but still under a hybrid testing approach, the work by (Fontanella et al., 2018) on the implementation of a variable-speed variable-pitch control strategy on a wind turbine scale model for hybrid/HIL wind tunnel tests provides a relevant case study for application of HIL system described in (Fontanella et al., 2019). Another case study is the analysis of FOWT dynamics in 2-DOF hybrid HIL wind tunnel experiments by (Bayati et al., 2020).

Dedicated component and performance testing is also an important aspect for floating systems and dedicated rigs can be used for accurate assessments. An example of such is the large-scale physical testing of a hydraulic-based mooring component with non-linear stiffness characteristics (an Intelligent Mooring System –IMS), carried out by (Harrold et al., 2020). The IMS was tested at the University of Exeter's Dynamic Marine Component Test Facility (DMaC). Rigs such as DMaC are tensile test machines that can replicate the motions and forces that mooring lines and subsea cables are subject to through actuators.

Another relevant publication to be mentioned is that by (Robertson et al., 2020), addressing total experimental uncertainty. In their work, systematic uncertainty components in hydrodynamic tests of the OC5-DeepCwind semisubmersible are propagated to response metrics of interest using numerical simulation tools, and combined with the system's random uncertainty. The authors report the uncertainty in the low-frequency response metrics to be most sensitive to the system properties, and also the wave elevation.

3.4.2 Field testing (also include O&M)

The previous version of the report showed that limited field testing data from floating wind turbines prototypes is available. Since then a few articles were issued on a range of concepts : a spar buoy (Utsunomiya et al.), an advanced spar (Wright et al.), a barge with a large moonpool (Choisnet et al.) and a semi-submersible floating foundation (Nakamura et al.)

In Wright et al. (2019) an advanced spar floating substation installed in Japan on the Fukushima wind farm is modelled in Orcaflex and compared to onsite measurements in wave cases up to 6.0m significant wave height, peak periods from 9s to nearly 15s. Simulations are run in

the time domain using Orcaflex as the solver. Hydrodynamic properties were calculated with a panel code and complemented by a drag model, with drag coefficients varying with the Keulegan-Carpenter number. The work is focused on low frequency motions, and show that low frequency motions are a little underestimate both with Newman's approximation of low frequency loads, and a full QTF formulation. Mean loads and motions appeared well captured with both second-order wave load models. Using the new drag formulation allowed to match motions, while the drag coefficient taken from model tests yielded larger motions.

Utsunomiya et al. (2019), showed good agreement between simulated and measured pitch, motions. The models covered a hybrid concrete / steel spar floating wind turbine and included the flexibility of the blades and tower, but also the flexibility and dynamics of the hull and mooring lines. The simulation model uses Adams as the solver and FAST as a pre-processor for the wind turbine modelling. Although the mooring used finite element models, the natural frequencies in surge and sway were said to be affected by installation inaccuracies. Pitch motion and power were discussed showing good agreement in power production and mean pitch. The simulations also showed that pitch motions were slightly over-estimated in comparison to measurements, even though the turbulence intensity was lower in simulations than in onsite records. The data set features significant wave heights of less than 1m and wind speed from 7m/s to 15m/s, which makes these results representative of wind effects.

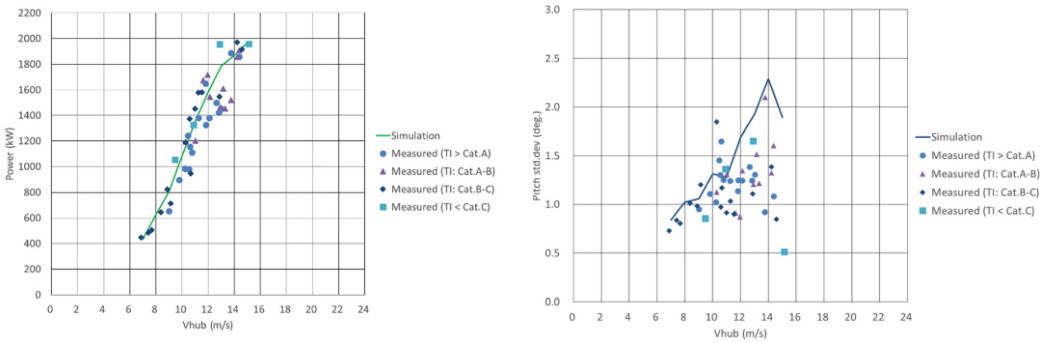

Figure 34: Power curve and standard deviation of motion from Utsunomiya et al.

In Nakamura et al. (2018), a few results from onsite measurements of a 7MW floating wind turbine sitting on 'V'shaped semi-submersible platform. This paper uses the commercial software Bladed which is a blade element momentum software modelling blades, tower, drivetrain and hull as flexible beam elements on which aerodynamic and hydrodynamic loads are distributed. Hydrodynamic loads are applied through Morison's equations, and wave spreading is used. Although the hydrodynamics are rather basic in modelling, tower base fatigue and ultimate loads are well calculated. An original approach is used in the determination of tower base 50-year return period loads, by fitting a probability distribution of records, and extrapolating to the 50-year return period event. This method showed again the conservatism of models. Wave data included significant heights between 2m and 6m significant wave height.

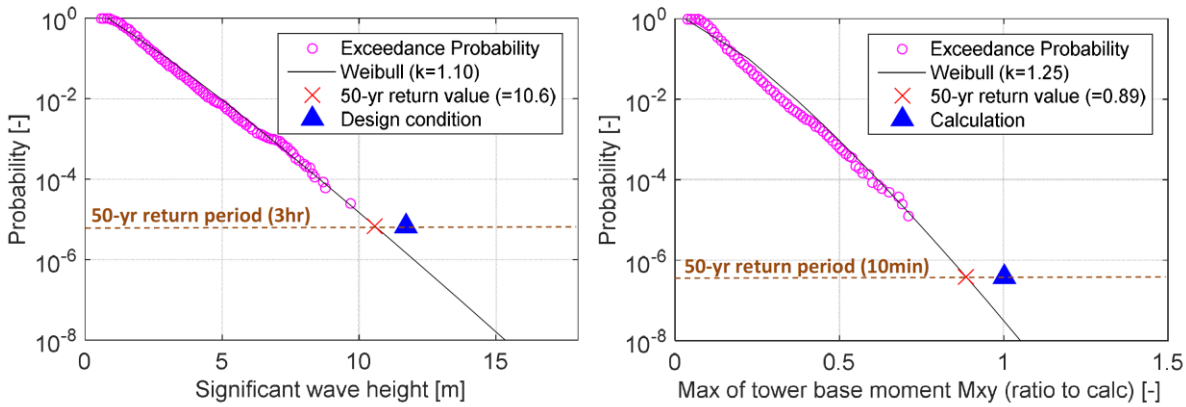

Figure 35: Extrapolation of loads to 50YRP the 7MW semi-submersible FOWT at Fukushima FORWARD project site (Nakamura et al.)

Measurements of half a year of operation including storms are reported for a barge-type FOWT in Choisnet et al. (2020). The results focus on wind turbine components loads: blades, shaft and tower bending. In this dataset, which covers the whole operation range of the wind turbine, no loads reaches more than 50% of the design load, which confirms the adequacy of the floating wind turbine in normal operation. It is also noted that blade, drivetrain and tower top loads are not driven by tower top accelerations, even at accelerations as high as 0.7g. Tower base load is however very much governed by tower top accelerations. In another article (Choisnet et al. (2018) on the same floating wind turbine, measured and simulated motion RAOs are compared, showing the conservatism of the simulation model that uses Orcaflex coupled to FAST and Aqwa as the hydrodynamic loads calculation.

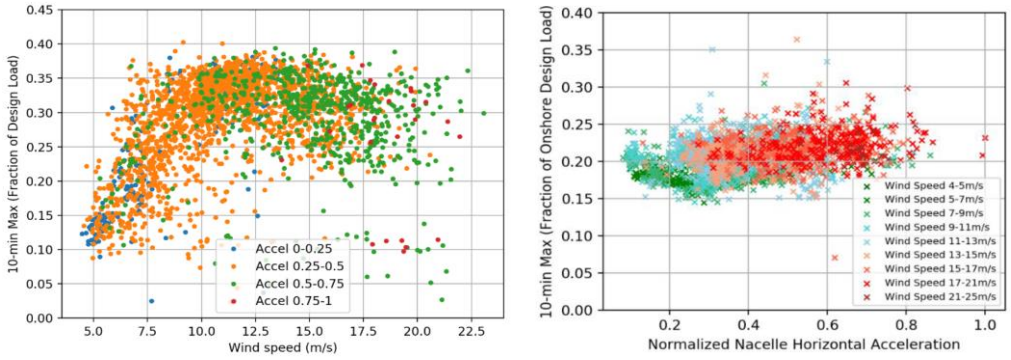

Figure 36: Blade root bending as a portion of design load of Floatgen demonstrator Vs wind speed (left) and RNA acceleration (right) from Choisnet et al.

Ruzzo et al. report an original testing method that uses intermediate scale models (1:30) on an open-sea test site. The main point of these tests, is to limit scale effects that are inherent to model testing, and also to allow to test a broader range of conditions. The test site was selected to feature a combination of directional wind seas to investigate specific response, and broad range frequency spectra for model identification. The tests performed on the intermediate-scale spar buoy were focused on motions and showed that the damping levels in irregular wave conditions, were actually lower than those estimated from wave tank decay tests. This shows again the conservatism of the classical calibration of numerical models by small scale model decay tests. It was noted however that the damping levels were higher on the intermediate scale model on decay tests than in irregular waves. Ruzzo et al. detail in another publication the methods used to perform the spectrum analysis specific to this method.

It appears from these works that loads and motions were all on the safe side when compared to model tests, even at small scale. More work should be undertaken to pinpoint the reasons for this conservatism.

3.4.3 Technology qualification of new components

New technology development and qualification was very active for floating wind turbine concepts, but also controllers, mooring and cable systems.

A wide range of controller functions were addressed during the period of the report. These include power production smoothing but also load reduction, position control and heading control. Research also progressed in the field of physical modelling toward controller design as well as fault detection and condition monitoring, all of which require rigorous physical modelling and understanding.

Madsen et al. [2020] investigated the influence of different control systems on a 10MW floating wind turbine sitting on a Tension Leg Platform. They mainly investigated regular controllers, and performed the comparison by wave-tank tests. Their controller consisted of an open-loop controller before rated, and a closed-loop controller after rated. The difference between controllers lied after rated wind speed. Their three controllers were a constant torque, fixed pitch controller and two variable-pitch controllers. One of the latter, the onshore PI controller is a PI controller with a regular bandwidth. The other variable pitch controller, the offshore controller is also a PI controller, but with slower response obtained by decreasing the gains by factors of 4 to 5 compared to the onshore version. The tests showed that the response in surge and mooring line tension as well as rotor speed was better, i.e. featuring less dynamic loads with the offshore controller. The results also show that all design variables that were measured were affected by the change of the controller, which confirms that model tests, although very useful to investigate specific physical phenomena, cannot be used to derive design loads for Tension Leg Platforms. A combined tests/simulation approach is consequently mandatory to assess a floating wind turbine system.

In an equivalent work for a semi-submersible 8MW floating wind turbine, Fleming *et al.* proposed improvements to the baseline controller of a floating wind turbine to alleviate the effect of the negative damping, or the tendency of turbine controllers to interact with the low-frequency motions of the floating wind turbine. A range of solutions were proposed and compared to the original turbine controller. A common feature of these new controllers, is that they included a tower-resonance avoidance scheme combined with a bandpass wave frequencies response avoidance. Other options were investigated which included the incorporation of platform pitch, nacelle horizontal velocity and a specific loop to switch control loops above rated wind speed. The reduction of tower base fatigue loading proved significant with a larger impact at lower speeds for the nacelle velocity feedback, and a better impact of the platform pitch controller at higher wind speeds. The main drawback of the controller, is that its blade pitching activity was very significantly increased, especially with the nacelle-velocity feedback. It is consequently possible that the tower loads limitation would be at the cost of blades pitching and bearings reinforcement.

Reducing tower base loads can also be done using dampers, passive or active. The work by Park *et al.* for a tension-leg platform compares the efficiency of mass dampers to that of similar equipment for a monopile offshore wind turbine. Simulations with FAST investigated a regular mass-spring damper tuned to the tower first natural frequency. It was considered as a passive damper, but also as a semi-active damper which increases the damping force dynamically in certain conditions. The damper was considered weighing approximately 20tons. The results showed that all dampers and controllers enabled to decrease fatigue loadings by a very significant amount in the side-side direction. Loads in the forward-aft direction could be reduced too with a monopile, but on the floater : fore-aft fatigue loads are mostly caused by wave excitation in this case. Ultimate loads were actually increased with the mass damper on the floating units, whereas is could reduce significantly monopile loads. Another interesting conclusion, is that the trends were not the same at two different water depths, with the dampers more efficient in the shallower (55m) water depth.

Another difficulty in floating wind turbines design, is the possibility for single-point moored wind turbines, to maintain the correct heading. Kanner *et al.* proposed for the case of a two-rotor vertical axis wind turbine to use the differential torque moment that can be generated by two contra-rotating rotors to yaw the floating wind turbine towards wind. The configuration selected comprises two vertical axis wind turbines sitting each on a column of a three-column semi-submersible structure. The third column receives the mooring system. The investigations were made at UC Berkely lab and involved mechanical modelling of turbine loads by mechanical means. Even though the modelling technique proved successful, the controller could not yaw the floater at the right heading for significant wave heights higher than 2m. The controller used the torque of the generators as the main moment to yaw the floating wind turbine. This proves the difficulty of yawing a wind turbine at the right angle when it is moored on a single point mooring system.

This possibility of using the aerodynamic thrust of the wind turbine was also investigated more successfully by Han *et al.* where they used the aerodynamic thrust of horizontal axis wind turbines to adjust the position of floating wind turbines. The main objective of this possibility, is to offset slightly floating turbines relative to one-another and reduce wake losses in downwind turbines. In their research, the authors used a chain-moored 5MW turbine mounted on the OC4 DeepCwind semi-submersible hull. They were able to show that the turbine could be offset several meters in any direction and generate power with a LQI (Linear-quadratic-integrator) controller.

Fault detection in the context of floating wind is of particular interest due to the expected long distance and transit time from shore to the wind farms. In this context, Ghane *et al.* extended automatic probabilistic fault detection methods to the case of floating wind turbines drivetrain. In their case study, they investigated main bearing wear detection capabilities by extending the likelihood test methods to the actual probability distribution of bearings vibration : the t-distribution. Their investigations based on relative accelerations between the bedplate and main bearing of a simulated OC3 5MW spar floating wind turbine allowed to detect the vibrations caused by bearings wear. Wear was modelled by a stiffness change of the bearing, which was showed to be linked to the wear of the rolling elements or raceways. The models used included a SIMO-RIFLEX-Aerodyn aeroelastic code which served as input to a detailed model of the drivetrain done with Simpack. The models could not however model slow increase of the wear, and were only capable of modelling rapid changes. This aspect would need to be investigated to confirm the adequacy of the proposed MLE estimator.

Another approach developed by Cho *et al.* consists in detecting abnormal response of sensors and/or actuators to prevent the escalation of faults. The authors used Fault Detection and Isolation (FDI) in combination to Fault Tolerant Control (FTC) methods applied to the pitch control of a 5MW spar floating wind turbine (the OC3 Hywind model). The FDI consisted in this work to actual measured parameters to real-time simulated parameters. In the errors introduced by the authors, 99% of the faults were detected within 11.5s after the fault. The principles of the Fault Tolerant controls were to include a reconfiguration block and associated PI controller which goal is to replace the faulty signal/input by a synthetised signal. The approach proved effective in reducing loads and motions caused by the faults in single and multiple pitch system faults. The systems are even capable of running the wind turbine within its operating limits in fault condition.

Research on Floating wind turbines is mostly focused on floaters, or vertical axis wind turbines. Gaertner *et al.* showed however, that wind turbine blades can be optimised to improve the overall performance of floating wind turbines. The principles of their work, was to play on the twist and chord of wind turbine blades to yield an optimum turbine blade. They worked on the optimisation of the wind turbine, starting from the NREL 5MW wind turbine, mounted on the OC3 Hywind spar buoy. Their optimisation maximised the energy yield for a severe North Atlantic environment, changing turbine blades chord and twist along the span. They simulated

with FAST the energy yield for the full wave / wind scatter diagrams, and coupled these simulations in an optimisation framework that played on the chord, twist of the blades but also designed automatically the structure of the blades. This work is of much interest because a full structural and performance framework is integrated, but also because the results of the optimisation show that the optimum blade has a slightly lower chord and twist. The same framework was used for an optimised onshore turbine, yielding slightly smaller twist and nearly the same blade chord distribution.

In floating wind farms, another critical aspect is the possibility to export the energy to the shore. Although fixed substations allowing energy transportation from offshore farms to the shore can be deployed in a number of cases, floating substations would unlock more regions and provide an effective alternate to large jackets. Guignier *et al.* proposed designed dynamic 220kV cables for a floating substation. The design case is a severe environment case with the 100-year return period at 13m significant wave height, 41m/s wind speed and 1.5m/s current in 100m water depth. The verifications included ultimate strength and fatigue designs. The cable included three 1200mm², 220kV rated copper conductors. Each conductor is sheathed with longitudinally seemed corrugated copper. The relatively large allowable bending radii in service of 5.3m caused the configuration to be a double lazy-wave. Two different fatigue analysis methods were used : irregular wave and rainflow counting on one hand, regular waves combined with an individual wave scatter diagram on the other hand. The irregular / rainflow method can be considered as a reference and yielded a fatigue life in excess of 300years for the conductors' copper sheathing and in excess of 1300 years for the armour wires which makes these cables suitable for the service life.

3.5 Design standards and guidelines

At the time of editing the 2018 edition of the ISSC renewable energy report, a small number of standards and guidelines were published and some were still in their early version. As a large number of standards have since then been issued, table 1 compares the main verifications specified in these standards. The main differences in these standards will be commented here.

Table 1: Main design criteria in industry standards

Standard	Mooring redundancy	Stability		Structures	
		Damaged stability	Type of criteria	Design format	Materials
IEC	Optional, Increased safety factor	Optional	Quasi-static or dynamic-response-based	LRFD or WSD	Not specified
ABS	Optional, Safety factor increase 20%	Yes in 1YRP	Quasi-static or dynamic-response-based	LRFD	Steel, concrete
BV	Optional, Safety factor increase 20%	Optional	Quasi-static or dynamic-response-based	WSD, LRFD optional	Steel
DNV	Optional, Safety factor increase 15% to 25%	Optional	Quasi-static or dynamic-response-based	LRFD	Steel, concrete
LR	Optional, Safety factor increase 50%	Yes	To IMO MODU or other	LRFD	Steel, concrete
NK	Mandatory, 1YRP check	Yes	Quasi-static	LRFD	Steel

Design loads are largely taken from the pre-existing fixed offshore wind turbines standard IEC 61400-3-1. This standard provides a comprehensive combination of environmental and operating conditions, which were complemented in different ways from a standard to another. IEC added loading situations specific to floating wind turbines: compartment damage, mooring line damage, stoppage and maximum operating conditions and a robustness check of the floating wind turbine under extreme conditions, with the turbine still producing electricity beyond its specified operating threshold. This latter case is the reflection of a wide-spread difference fixed and floating wind turbines, that the latter are designed to operate to specified wave / current conditions whereas fixed units typically operate up to the 50-year return period waves. These additional load cases are also present in DNV and BV. They are not explicitly

listed in NKK, LR and ABS but these standard call for specific verifications in damaged mooring and compartment conditions. Interestingly NKK standard also provides specific design situations for sea-ice conditions.

All standards propose the Loads and Resistance Factors Design method where material strength is divided by a safety factor which itself is material dependent- the material factor, and design loads are multiplied by another factor, the load factor. BV and IEC propose as an alternate to use the Working Stress Design method, where there is no load factor and a global safety factor on stresses that depends on the material, loading condition and failure mode. The LRFD method is however easier to use in actual projects, as wind energy converters' design analysis provide factored design loads for each component. The practicality of using homogeneous wind energy converter and floating structure design load definitions allow to improve communication in the design phase and ultimately the safety of floating wind turbines.

The use of concrete, although widely spread on several prototype (the Nipon hybrid spar in Goto, US small scale semi-submersible unit in the waters of the Maine, French Damping Pool floating floater) and more significantly in the world's first commercial floating wind turbine farm in Norway is not documented in all standards. ABS, DNV and LR propose a similar approach by providing a list of alterations to be applied to their general concrete offshore structures standards, for application to floating wind turbines. IEC, BV and NK, although not excluding the use of concrete as the main structural material, provide no guidance on concrete structures design while in the same time being very specific on steel structures scantling.

Mooring redundancy is considered optional in all standards except with Class NK. In the case of non-redundant mooring system, safety factors are simply increased to reduce the probability of failure. In the case of mooring systems however, this approach may not lead in all cases to increased safety as stiffer mooring lines also give rise to higher loads. More data on this can be found in the benchmark study summarised in this report. Stability is considered as optional in some cases as structures are unmanned in most operating conditions. DNV and BV relate to the operator's own risk analysis without specifying quantitative criteria for an acceptable risk whereas the IEC considers that damage stability is optional provided the risk of capsizing under damaged condition is less than the probability of capsize in intact conditions. NK, LR and ABS require stability that floating wind turbines shall sustain a single-compartment damage in any case. This requirement makes it mandatory to design the buoyant elements in such way that they are subdivised in sufficient watertight zones. However, standards that do not call for damage stability verifications explicitly require that the risk of punching a hull in way of boat transfer, maintenance zones or by a foreign object are evaluated and showed negligible.

Since the 2018 ISSC report, a consensus on the design load cases to be considered in floating wind turbines verification has been met. Although not yet fully explicit in standards, the underlying level of safety is homogeneous in all the standards sited for stability and structural strength. The case of mooring system strength is a little different, with approaches to redundancy and safety factors that give rise to large differences in the design of the mooring system. A consensus in moorings safety is of particular importance given probability of failure of mooring lines observed in hydrocarbons extraction applications.

4. WAVE ENERGY CONVERTERS

4.1 Recent development

At present, the number of wave energy device prototypes has grown to almost one thousand inventions. However, only two hundred of these have reached the stage of model testing (Mustapa et al, 2017). At the moment, WEC systems still suffer from high cost as compared to the conventional electricity generation, such as from coal power plant (Mustapa et al, 2017). Survivability in harsh weather condition is also another challenge on the way of the commercial deployment of these devices. In this context, several new solutions have been proposed by investigators and developers to overcome those barriers.

Crowley et al. introduced a novel design of ocean wave energy converter which is comprised of a floating, moored, spherical hull containing a mechanical pendulum arrangement from which power is taken when excited by incident waves. They performed theoretical modelling and experimental investigations to assess the performance of the device. An explicit expression is derived for the capture width of the proposed device in terms of physical and hydrodynamic parameters. This exposes the multiple resonant characteristics of the device which enable it to operate effectively over a broad range of wave periods.

de Almeida et al. carried out preliminary laboratorial determination of the REEFS novel wave energy converter power output. REEFS is a new wave energy converter that can harness both potential energy as well as kinetic energy. The REEFS structure comprises a nearshore immobile submerged caisson placed over the seabed at low depth. The REEFS concept is based on already existing hydropower and maritime technologies in order to speed up the development phase and reduce future production costs. Inside the REEFS structure,

there is a hydraulic circuit provided with several water intakes and outlets, as well as a power take-off (PTO) unit consisting of a hydraulic turbine.

Ning et al. proposed a novel cylindrical oscillating water column (OWC) WEC with double chambers to harvest the wave energy effectively in deep water. An analytical model is developed to investigate its hydrodynamic characteristics based on the linear potential flow theory and eigenfunction expansion technique. The comparison between results of the single- and dual-chamber OWC-WECs shows that the effective frequency bandwidth of the dual-chamber OWC-WEC is broader than that of the single-chamber OWC-WEC.

Rezanejad and Guedes Soares (2021a) devised a new concept of dual chamber floating OWC device. This device is composed by two chambers operating as OWCs. The fore chamber is faced to the incident waves. The mechanism of power absorption of this part is analogous to conventional OWC devices. The OWC part is supported by a plate that extends outside of the unit (Fig 1a). The second chamber, which is in the rear part of the FOWC device, has indirect interactions with the propagating waves. The chamber has the duct shaped similarly to the Backward Bent Duct Buoy (BBDB) devices (Fig 1a). Analogous to the conventional BBDB devices, this part is also interacting with waves downstream of the device. The wave energy is captured by the two chambers simultaneously and converted to pneumatic power in the air pockets inside the chambers above the water free surface. Comprehensive numerical and experimental studies (using 1:50 scale model, Fig 1b) are carried out to investigate the efficiency of the device in terms of converting the energy of the waves to pneumatic power (Rezanejad et al, 2021b; Rezanejad et al, 2021c). The influence of the power take-off damping as well as the wave characteristics on the hydrodynamic performance is investigated. The significant hydrodynamic performance of the introduced novel concept has been proven in the wide range of wave frequencies for both regular and random wave conditions. It is found that the fore and rear chambers of the device have the dominant role in absorbing energy of the waves in a specific range of wave periods. Their mutual interactions have a significant effect on the enhancement of the overall hydrodynamic performance.

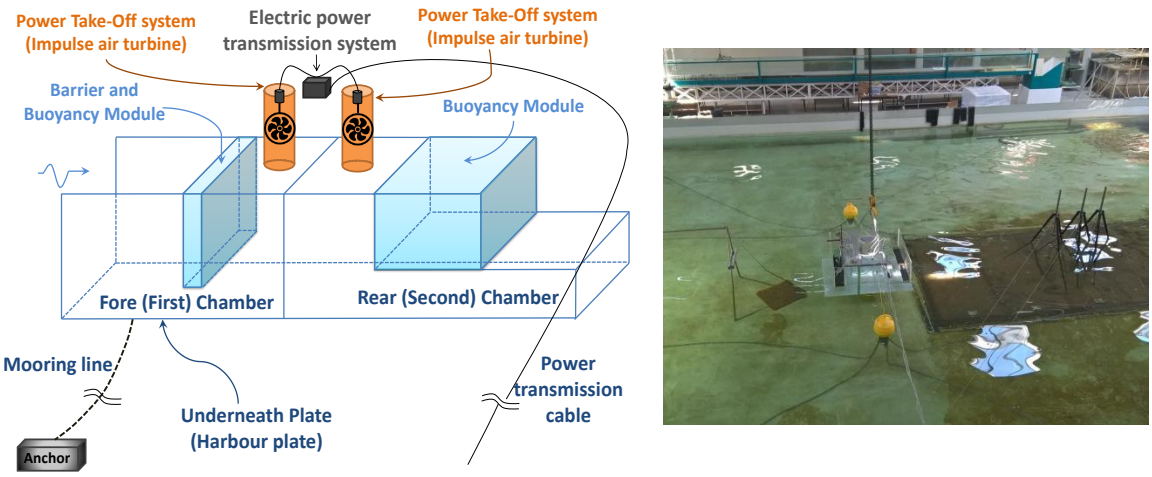

Figure 37: (a) Schematic plan of the dual chamber floating OWC device, (b) Floating OWC model in the wave flume (tested at University of Porto)

A two-degree-of-freedom (2-DOF) WEC composed of an eccentric dual-axis ring and power generators using circular Halbach array magnetic disks and iron-core coils was developed by (Wang and Lee, 2019). The WEC system was designed to convert kinetic energy from the pitching, rolling, and heaving motions of a mooring-less buoy. The eccentric dual-axis ring with appropriate weighting conditions enhanced power generation by revolving in biaxial hula-hoop motion, because it exhibited a higher angular velocity than when in swing motion.

A lift based Cycloidal Wave Energy Converter (CycWEC) was investigated by (Siegel, 2019) using numerical simulations to estimate its mean annual power absorption. Based on the power absorption as well as size and weight estimates a number of performance measures were derived in order to compare this novel WEC to other more established devices for which results have been published by (Babarit et al, 2012) using a similar benchmarking approach. Comparison of these measures with published data for eight more established WEC designs, including heaving buoy, oscillating water column and flap devices shows that the CycWEC performance in all metrics exceeds that of all other devices.

(Moreno and Stansby, 2019) carried out ocean basin tests to assess the capture width, response and energy yield for several sites for the 6-float wave energy converter M4. The M4 wave energy converter originally consisted of three in-line floats increasing in diameter (and draft) from bow to stern so that the device heads naturally into the wave direction with power take off (PTO) from a hinge above the mid float (Santo et al, 2020). (Moreno and Stansby, 2019) presented experimental comparison for a six-float system with two PTOs. Results for angular motion at the PTOs and mooring forces are presented. Wave conditions with different spectral peakedness and multi-directional spreading are applied and energy yield with electricity cost estimates made for 11 offshore sites. The capacity and LCoE could be similar to offshore wind energy for certain sites and with further optimisation LCOE could be generally similar or less.

(Tongphong et al., 2021) devised a novel WEC system, referred to as the ModuleRaft WEC. The WEC consists of a floating modular flap and four rafts hinged at the main floating structure. ModuleRaft WEC is unique due to its ability to convert both wave potential energy and wave kinetic energy by utilizing the pitch motion of rafts and floating modular flap. The motion characteristic, performance and optimization of the ModuleRaft wave energy converter are investigated under regular wave conditions using ANSYSAQWA. Comparing WEC with and without rafts, it was found that the capture factor of the modular flap with rafts is much better than the conventional floating modular flap-type WEC.

4.2 Numerical modelling and analysis

4.2.1 Load and motion response analysis (effect of arrays)

The selected publications listed in this sub-chapter relative to work being disseminated in the 2018-2021 period include various approaches that are also targeted at different analysis to be made, but that can be divided in optimization and hydrodynamic studies. The latter, can be somewhat discretized in the following:

- So called Numerical Wave Tank (NWT), where focus is made on nonlinearities of the wave-array structures interactions.
- Wave-propagation models, with the aim of including site specific properties, such as bathymetry and coastal morphology in general.
- Linear diffraction-based approaches using Boundary Element Methods (BEM), where focus here has be taken on array effects on moorings.
- Coupled models using at least two methodologies, typically wave-propagation models coupled with BEM.
- State-space models, where focus here is set on specific developments targeting this approach.
- Surrogate hydrodynamic models, especially attractive for optimization studies where the hydrodynamic effects are wrapped up in a simpler formulation.
- Analytical or semi-analytical approaches, targeted at fast prediction and analysis of WEC array behaviour without loss of accuracy within the limitations of the model assumptions.

The selection of research works described in this sub-chapter are an attempt to provide an overview of the recent work being carried out in the numerical prediction of the behaviour of WECs in array configurations and on implementations of array optimization algorithms. Focus here is set mainly on the models themselves and their implementation and not on the conclusions of the specific case studies being addressed.

Numerical Wave Tank

(Devolder et al., 2018) used the Computational Fluid Dynamics (CFD) toolbox OpenFOAM to perform numerical simulations of multiple floating point absorber wave energy converters arranged in a geometrical array configuration inside an NWT. The NWT was validated for fluid-structure interaction (FSI) simulations by using experimental measurements for an array of two, five and up to nine heaving WECs subjected to regular waves. Although results are shown to be in good agreement with experiments, the computational burden is considerable and probably impractical for optimization studies, as pointed out by (Goteman et al., 2020) in their review on advances and challenges in wave parks optimization. A similar conclusion is reached by (Windt et al., 2018) in their review of computational fluid dynamics-based numerical wave tanks applied to ocean wave systems.

Wave propagation models – phase averaging

Within phase averaging models approaches, (McNatt et al., 2020) compared the wave field generated by the spectral wave action balance code, SNL-SWAN, to the linear-wave boundary-element method (BEM) code, WAMIT. SNL-SWAN is a modified version of the open-source SWAN code, developed by TU Delft, that includes a WEC obstacle case that is built on the established concept of using SWAN's transmission coefficient to emulate the wave-WEC interactions. Comparisons were made over a range of incident wave conditions, including short-, medium-, and long-wavelength waves with various amounts of directional spreading, and for three WEC archetypes: a point absorber, a pitching flap terminator, and a hinged raft attenuator. Results showed that in the near-field, the difference between SNL-SWAN and WAMIT is relatively large (20% to 50%), but in the far-field from the array the differences are as low as 1%-5%.

(Luczko et al., 2018) presented a methodology (using SNL-SWAN) which spectrally resolves the individual WEC's energy conversion characteristics and has the flexibility to be applied to any emerging WEC design. Two novel WEC obstacle cases were implemented, and outputs compared with the traditional technique were WECs are represented by static obstacles with the transfer and extraction of energy defined by a static transmission coefficient: one considering the WEC's intercepted power (the rate of energy extraction from the waves), another with the captured power (the rate of energy conversion by the PTO). An array of 5 Bent Duct Buoy Oscillating Water Column subject to irregular waves was used as case study. Although results differed between the cases, the authors conclude that a validation exercise is needed to help assess the validity, uncertainty and limitations of the obstacle cases and even of other previously disseminated techniques.

(Atan et al, 2019) presented a methodology for studying the effect of arrays of wave energy converters on the nearshore wave climate using SWAN. A single unrestrained floating rectangular prism representing a point absorber WEC, which operates in the heave and pitch motions, was modelled in a NWT for determining the obstacle transmission coefficient to be implemented in SWAN. Three array configurations with 12 WECs were simulated for the Westwave test site (Ireland).

Also focusing on the effects of WEC arrays on the far field, (O'Dea et al. 2018) studied the impact of wave energy converter arrays on wave-induced forcing in the surf zone using SWAN for different array designs and locations. A frequency dependent power transfer function for a point absorber was established experimentally and used for setting the transmission coefficient in SWAN. Conditions that generate alongshore radiation stress gradients exceeding a chosen impact threshold on a uniform beach were identified.

Wave propagation models – phase resolving

(Rollano et al., 2020) made a direct comparison between the application of a phase-resolving wave model, FUNWAVE-TVD, and a phase-averaging model, SWAN, to simulate the wave environment associated with a hypothetical WEC array and evaluate their influence on power output estimation using WEC-SIM. The wave elevations were fed individually to each WEC in WEC-SIM and no interaction between WECs was accounted for. This raises uncertainties on the output estimates, particularly in the case of SWAN originated wave elevations, which are randomly phased for inclusion in the time domain model used in WEC-SIM. The result is that high energy waves occurring simultaneously across the array are improbable using the SWAN approach, which is not realistic. On the other hand, introducing WEC array interaction for inhomogeneous wave fields arising from phase resolving models in nearshore areas was thought to be an unresolved issue by the authors, with a solution being published later in (Rodrigues, 2021).

Another interesting application of a phase resolving model was that of (Rijnsdorp et al., 2020) who studied the coastal impacts by nearshore wave farms. The modelling was based on the non-hydrostatic wave-flow model SWASH that accurately accounts for the relevant (nonlinear) physical processes which dominate the coastal region – essentially, a direct numerical implementation of the RANS equations. 5, 10, and 14 WECs array configurations of three-tethered submerged point absorbers were included in the simulations with optimal PTOs. 18 different farm layouts at three different offshore distances to a beach were simulated. Although only one wave condition and a very simple rectangular domain were considered, this set needed the computational capabilities of a supercomputer. By use of a bulk longshore sediment transport formulation, a reorientation of the shoreline in response to the wave farm configurations considered was predicted.

BEM hydrodynamics based models – array effects on mooring loads

The application of BEM models to the case of WEC arrays being the most direct and traditional approach, reference here is made to two selected publications which give some interesting conclusions on the array induced effects on mooring lines.

(Oikonomou et al., 2020) presented a numerical analysis in the frequency domain of a triangular array of spar-buoy OWCs, with bottom and inter-body mooring connections, for regular and irregular waves. The array performance was compared to an unmoored and an independently moored array. Hydrodynamic coefficients and excitation forces were obtained using WAMIT and a linearization of the drag forces was applied. For regular waves, the analysis showed that the unmoored array was influenced by the hydrodynamic coupling between the three bodies in surge, while no significant differences were observed in the heave oscillations within the array between both mooring configurations.

(Yang et al., 2020) studied the influence of interaction effects on the power performance and fatigue of mooring lines for WECs in array configurations. The DNV GL SESAM software package was used to simulate the array in time domain. Diffraction and radiation matrices were obtained from WADAM. Two approaches were implemented in parallel and compared to perform the time-domain simulation: a) the uncoupled method, where SIMO (time domain simulation) and then RIFLEX (slender element FEM) are used in this order; b) the coupled method, where the SIMO-RIFLEX coupled code is used. Four 2-WEC models and two 10-WEC models were studied, among which different separating distances and mooring configurations were considered. The 10-WEC array systems showed that the effect of the hydrodynamic interaction on the average power absorption of the 10 WECs ranges from 17% to 23% depending on the incident load direction for the simulated environment conditions. Fatigue analyses showed a stronger influence of the hydrodynamic interaction, in which the predicted fatigue damage can be varied by more than tenfold.

Hybrid/coupled methods

Typically, hybrid (or coupled) methods aim at to numerically model both near and far field array WEC effects. BEM diffraction solvers are best suited for modelling the near field, where the detailed wave-structure interactions are important for assessing the WEC behaviour. However, introducing, say, bathymetric variation throughout the array is challenging if not impossible in practice when using these methods. On the other hand, wave propagation models are more suitable for investigating far field effects of WEC farms in large areas, given the possibility to include detailed bathymetric and coastal morphology, among other more complex phenomena depending on the solver. However, WECs are typically introduced as "artificial" obstacles in the domain with a transmission coefficient and assessing the array behaviour in an accurate way is challenging.

(Verao Fernandez et al., 2018) presented a coupled methodology that couples a BEM (WAMIT) with a mild-slope phase-resolving method (MILDwave), focusing on varying bathymetry. In essence, MILDwave handles the far-field wave propagation and diffraction problems while WAMIT handles the radiation problem locally at the WEC which is then transmitted to the far field through an interface surrounding the body. The time domain-based procedure seems to use a cascading progression of diffracted and radiated waves between WECs, which needs to be truncated for practical purposes; however, details are not present regarding this aspect. (Stratigaki et al., 2019) extends the method to consider a novel formulation for generating the perturbed wave field induced by an oscillating WEC in the wave propagation model.

(Belibassakis et al., 2018) presented a novel method for estimating the performance of WEC arrays in variable bathymetry. Contrary to the abovementioned two studies, no mild slope assumptions are introduced for the bathymetry; furthermore, a local BEM solver is introduced that also accounts for bathymetric details in the local area surrounding each WEC, valid for arbitrary WEC geometries. Although numerical results are presented concerning the wave field

and the power output of only a single device in inhomogeneous environment, extensions of the method to treat the WEC arrays in variable bathymetry regions are also presented and discussed. A study using this method to optimize WEC geometry was later presented in (Bonovas et al., 2019).

State space models

(Gaebele et al., 2020) presented a state-space model of an array of oscillating water column wave energy converters with inter-body hydrodynamic coupling between all distinct bodies considered without making simplification in the devices' geometries, as well as connecting them to a nonlinear air chamber/turbine model. Only three WECs were considered, and the used mooring arrangement did not allow for close distances between devices. According to the authors, this should be taken into consideration in their conclusion that interaction effects are negligible in irregular waves but not for regular waves.

Faedo et al., 2020) presented a multi-input, multi-output (MIMO) parameterisation strategy based on a system-theoretic interpretation of moments to be applied in WEC arrays. Specific emphasis was set on motion simulation and wave excitation force estimation, providing a low dimensional and accurate model for the array dynamics. The approach is said to allow for the computation of state-space representation characterising the input-output dynamics of WEC arrays which exactly matches the target steady-state behaviour of the array at a set of user-selected frequencies.

Surrogate models

Simplified models for the hydrodynamics in order to accelerate the optimization of other parameters in the arrays (e.g. PTO control) have been proposed. An example is that (Zou and Abdelkhalik , 2020), who implemented a surrogate model composed of real and artificial masses interconnected with springs and dampers for which an optimization procedure is used to perform the system identification resorting to data obtained from ANSYS AQWA simulations. Another is the wake model used by (Liu et al., 2021) for the optimization of oscillating wave surge converter (OWSC) arrays using differential evolution algorithm. In this study an SPH method wa used considering an OWSC with varying flap width, PTO damping and wave heights, to provide data to an analytical model of the wake which was then used in layout optimization of the array. The study was extended to also consider varying regular wave periods, along with a description of GPU accelerated algorithm, in (Wang and Liu, 2021).

Analytical and semi-analytical models and analysis

(Flavià et al., 2018) presented the implementation of (Yoshida, 1990)'s strategy to compute the diffraction transfer matrix (DTM) and "radiation characteristics" (RC) in the BEM solver NEMOH, for application in a semi-analytical direct matrix interaction theory. The method solves the scattering about each unique body in the array using partial incident cylindrical waves. For this, the body boundary condition was modified where normal velocities at the collocation point of each panel were implemented as the derivative of the incident partial wave functions. A second method by (McNatt et al., 2015) was used for comparisons. This second method uses a procedure to attain DTM from simulations using planar incident waves, therefore not requiring any special consideration in terms of the solver; however, the wave evanescent modes are not included. A very good agreement regarding the wave progressive terms was found, and the method implemented in NEMOH was then used to assess the importance of the wave evanescent modes particularly in the radiated wave fields. These were found to be significant when the bodies are in close proximity, as expected.

In addition to constant water depth, a limitation of the use of standard diffraction BEM models in arrays of structures at sea is that the wave field is homogenous across the whole array. This means that either long crested or short crested seas always assume a coherent wave distribution with straight wave crests. This has implications in the frequency dependent excitation forces, which are computed in this way and thus interaction effects on the diffraction problem cannot be properly accounted if the wave system incident in the individual bodies in the array are not the same. The implementations of direct matrix methods also typically include this limitation. To solve this problem, (Rodrigues, 2021) demonstrated that the semi-analytical direct matrix method formulation, initially developed by (Kagemoto and Yue, 1986), is able to tackle such problems, with minimal modification to its standard implementation. The algorithm by (McNatt et al., 2015) was modified to allow for the inclusion of arbitrary wave systems (direction, amplitude, phase) for each individual wave with accurate excitation forces being computed coherent with the inhomogeneity of the system. The procedure was validated with WAMIT results for a range of frequencies where interaction is significant. Results were in excellent agreement, despite the absence of consideration of wave evanescent modes. A case study with frequency components inhomogeneity in a hypothetical array of WECs was also presented. The approach seems very promising especially for its use in hybrid approaches coupling BEM solvers with wave propagation methods, where wave inhomogeneity arising from coastal morphological effects is no longer an issue in terms of properly accounting for intra array hydrodynamic linear interactions.

Another interesting development is that by (Tokić and Yue, 2019), who studied the hydrodynamics of periodic WEC arrays. A multiple-scattering method of wave–body interactions applicable to generally spaced periodic arrays, where the sub-array configuration is arbitrary, is also presented. They show that array amplifications can be as high as O(10) for heave oscillating WECs used in their study. Furthermore, prominent decreases in array gain were found to be associated with Laue resonances, involving the incident and scattered wave modes, for which an explicit condition was obtained. Additionally, it was theoretically demonstrated that Bragg resonances can result in large decreases in gain with as few as two rows of strong absorbers. For a special class of multiple-row rectangular WEC arrays, numerical results showed that motion-trapped Rayleigh–Bloch waves can exist and be excited by an incident wave, resulting in sharp narrow-banded spikes in the array gain. Also worth mentioning is the work by the same authors in (Tokić and Yue, 2021) on the energy extraction of randomized array configurations that are obtained by introducing zero-mean position perturbations to line arrays of uniform spacing. Substantial q-factors in monochromatic and irregular incident seas were obtained. The authors also show and provide a heuristic explanation for why uniform line arrays with spacing optimized for a given incident spectrum generally outperform randomized arrays of any mean distance between WECs and position perturbation in that wave spectrum.

Considering nonlinearities, (Michele et al., 2019) applied a weakly nonlinear theory for a gate-type curved array in waves to the case of oscillating surge WECs with curved geometry. They report that nonlinear synchronous resonance of curved WECs yields constructive interactions in terms of generated power that can be significant for design purposes. The case of subharmonic resonance was investigated where an optimum criterion to find the power take-off (PTO) coefficient which maximises power extraction was defined. Large efficiency was obtained, with the capture factor reaching much greater values than the theoretical maximum of a two-dimensional absorber described by the linear theory. However, in this case the performance of curved gates is sub-optimal with respect to that of flat gates.

Optimization

A paradigmatic study is that of (Giassi and Göteman, 2019), who performed a layout design of cylindrical heaving cylindrical WECs arrays by a genetic algorithm using discrete and

continuous optimization approaches. Optimization of single device, namely on radius and draft of the buoys, and the damping coefficient, was also performed. The devices are all similar throughout the array. A tendency for the WECs to align themselves perpendicularly to the wave propagation direction was generally observed, although staggered if space constraints for the entire farm area are present. This agrees with several other previous studies. A noteworthy characteristic of this study is the application of a distance cut-off approach for the interaction between devices, although arrays of only up to 14 WECs were considered. The maximum obtained q-factor was 1.09, however the same single sea state was used for all cases. In contrast, (Murai et al., 2021) performed array optimizations in the frequency domain with 3 and 5 units, considering full intra-array interactions and a site scatter diagram, arriving at q-factors in excess of 1.15.

Extending the optimization from the farm layout to include other hydrodynamic related parameters, such as device geometry, was presented by (Lyu et al., 2019) who also included two types of PTO control (impedance matching and derivative control) for arrays of up to 7 cylindrical WECs. The device dimensions are not uniform throughout the array in the optimized solutions of the Genetic algorithm deployed. The numerical test cases demonstrate that a higher q-factor is achieved when optimizing the buoys dimensions (draft and diameter) simultaneously with the array layout: an increase of the q-factor on average by approx. 40% and 10% when using optimal and derivative control, respectively.

A brief mention is due for optimization procedures that aim at providing a more encompassing view, namely including parameters that affect the total system revenue such as electrical cable lengths, distance from grid connection point, etc, in addition to hydrodynamics. Noteworthy studies considering these aspects are that of (Sharp and DuPont, 2018) and (Giassi et al., 2020). An interesting conclusion from (Giassi et al., 2020) s that the hydrodynamical interaction has a large impact on the optimal design of wave energy parks. The length of the intra-array cable does not play a significant role in the economical layout optimization routine at least for the wave energy park system in their study, as converters inside the park are grouped in clusters around substations via a k-means clustering algorithm, which allows to minimize the intra-array cable length under the input of real wave climates.

4.2.2 Power take-off analysis

The Power Take Off system is the key point of wave Energy converters. It is often a weak point of the structure associated to pivoting or sliding function or connected to the mooring lines. The PTO is submitted to a high level of oscillating loads and therefore to fatigue cycles. For similar reasons, the watertightness of moving electrical components is an issue.

The simplest model of PTO is a linear damping which is easy to introduce in the analytical formulation and numerical schemes and which power is easy to calculate in the frequency or time domain. But more complex PTO can be introduced including nonlinear damping, inertia and stiffness effects.

A detailed description of some PTO principles, WEC concepts and developers is given by Ahamed et al (2020) with the advantages, limits and weaknesses of the different PTO.

Calvario et al (2020) depict the implementation of an oil-hydraulic based power take off for different kinematic schemes and focus on a wave surge converter. configuration. Nonlinear relationship between the body dynamics and the motions of the rod-crank mechanisms are developed including the hydraulic pressures, flows and control. The hydrodynamic parameters of the main body rely on a linear diffraction and radiation approach in the frequency domain reformulated in the time domain for simulation of the overall system.

Nielsen et al (2017) apply resistive and reactive controls to the WAVESTAR WEC PTO modelling the losses that are inherent to the mechanical to electrical conversion. The hydrodynamics of the system relies again on a linear formulation of the incident, diffracted and

radiated waves actions on the floater. A state-space model is built including the other parameters like the solid body inertias and the hydrostatic stiffness.

According to the Froude law, any energetic power quantity is scaled by the ratio $E^{7/2}$ with E the characteristic length ratio. The captured power then decreases from full scale to model scale in the case of wave tank testing. Table xx shows the values of the scaled power for a 100kW full scale target and for several scale ratios. Obviously, too large scale ratios reduce the power to negligible values that cannot reliably be measured in a wave tank. More over the technology that can be used to simulate the PTO at very low power levels is very different from the full scale one and even can be inexistent. An ersatz is then used to simulate the PTO like a damping induced by a viscous effect which is nonlinear and must be carefully calibrated. For scale ratio larger than 10-20 the effect of parasitic Coulomb friction can be larger than the expected damping.

Table xx : Evolution of a rated power according to the scale ratio

L_{real}/L_{model}	1	5	10	20	25	50
P_{real}/P_{model}	1	280	3162	35777	78125	883883
Power (W)	10^5	358	32	2.8	1.3	0.1

An example of experimental and numerical simulation of a WEC with different PTO models is given by Dong et al (2020). The system consists on a quite classical couple of guided heaving bodies. The relative heave motion between the two concentric cylinders is tuned by a hydraulic PTO located on the side of the wave tank because it was too heavy to stand onboard the floaters. The numerical modelling of the hydrodynamics loads on the floaters relies on more time on a linear approach. The PTO action can be simulated by a linear damping or by a nonlinear function of the relative heave velocity that can be nearly constant on intervals of constant velocity sign. The scale ratio considered in the laboratory tests is $L_{model}/L_{real} = 1/9$ and the power magnitude measured at model scale is below 6 W which according to the power ratio on table xx corresponds to a full scale maximum power around 13 kW. This scale ratio allows a realistic experimental PTO and a significant level of captured power.

4.2.3 Mooring analysis

The main role of a mooring system of a WEC is that of stationkeeping, i.e. to avoid the drifting of the device due to the action of waves, current and wind. In a similar way to the design of the WEC unit itself, the mooring system design is inherently related to the location of the installation in terms of its bathymetry and environmental conditions. These premises are common to other offshore structures. However, as all WECs ultimately aim at absorbing power from waves, the loads on WEC moorings are more demanding, especially if the devices are meant to operate in near resonance conditions, with the additional difficulty that the operation of the floating unit becomes more prone to be affected by the mooring. In the last 3-4 years, research work on moorings seems to be mainly driven by the objective of reducing costs of the mooring system, either by using new materials and solutions, increasing survivability and reliability, optimizing floater-mooring interaction, etc.

Reviews, guidelines and standards

(Xu et al., 2019) made a thorough review of mooring design for floating wave energy converters. The design essentials of WEC mooring systems are discussed and a mooring system design procedure for WECs is proposed, including the introduction of related design codes and mooring analysis methods. Different mooring systems and mooring materials are introduced and discussed. Recommendations are made for the suitable mooring design according to the WEC's dimensions and working principles. It is shown that the elastic synthetic rope has great

potential in the application of WEC mooring system, and the hybrid mooring system could be a good solution for WEC station keeping problem.

A more introductory, yet recent, review worth mentioning is that by (Qiao et al., 2020). Mooring materials, configurations, requirements, and modelling approaches for WECs are explained. Design of mooring systems, including the design considerations and standards, analysis models, software, current research focus, and challenges are discussed. The authors corroborate the conclusions of (Xu et al., 2019), stating that hybrid mooring, consisting of clump weights, buoys, and mooring lines, to be an appealing option of station keeping for WECs, demonstrating excellent results in reducing mooring loads and absorbing environmental energy.

Focusing on mathematical modelling of mooring systems for WECs, (Davidson and Ringwood, 2017) presents a review of this subject. A compilation of relevant material developed in other offshore industries is presented, as well as the published usage of mooring models for WEC analysis.

Part of the EU project OPERA (Open Seas Operating Expereience to Reduce Wave Energy Cost), a set of recommendations targeting WEC mooring guidelines and standards has been published as deliverable D2.4 (Khalid et al, 2019). The document includes recommendations for WEC mooring guidelines and standards, assessment of gaps in knowledge based on findings from open-sea demonstrations to inform about possible additional requirements towards existing or new wave energy codes or standards, and provides recommendations for the wave energy industry.

Reliability, probabilistic design and uncertainty

Traditionally, a considerable computational effort is necessary to build up probability density functions for tension loads on moorings in WECs by running simulations using the Monte Carlo Method targeting reliability assessment of these components. (Paredes et al., 2019) circumvents this issue by approaching the problem by resorting to general Polynomial Chaos where the number of required simulations is greatly reduced. The same authors use the same approach to quantify uncertainty in mooring cable dynamics (Paredes et al, 2020).

Variation Mode and Effect analysis was applied to the specific case of CorPower's mooring pre-tension cylinder in (Johannesson et al.. 2019). The methodology was compared to the use of a corresponding pressure-vessel standard in what regards reliability design focusing on safety judgements. The methodology is said to provide a better ground for improvement work, design updates and maintenance planning.

The influence of mooring design on the output of wave energy converters has been studied somewhat substantially in the past years. On the other hand, the opposite approach is not very common. (Palm and Eskilsson, 2019) studied the influence of floater geometry on snap loads on mooring systems for WECs. The results showed that these can be considerably reduced by adjusting the geometry thus increasing the reliability of the system.

On the fatigue analysis, (Parish et al., 2017) used a validated numerical model to quantify the load reduction achievable by substituting a novel elastomeric tether in place of a conventional fibre rope mooring. Results show that the peak mooring loads are reduced substantially, albeit increasing, to a lesser degree, the mean peak excursion in surge of the floater.

The influence of hydrodynamic interaction on the power performance and fatigue life of the WECs' mooring lines in array configurations was studied by (Yang et al., 2020). Four 2-WEC models and two 10-WEC models, among which different separating distances and mooring configurations were considered, were investigated. The models were simulated for various environmental loading conditions. The results from each simulation were evaluated in terms, among others, of accumulated fatigue damage in each mooring line. The hydrodynamic

interactions show a larger impact on the 10-WEC simulation models. To account for the hydrodynamic interactions in the simulations using the 10-WEC models, the fatigue damage in the mooring lines is varied at an average of 15% and a maximum of an order of magnitude difference. The results obtained from the 2-WEC simulation models, the results showed a clear influence of the hydrodynamic interaction and a larger variation in the results among the simulated environment conditions. The inclusion of the hydrodynamic interaction in all of the simulated load cases caused an impact on the fatigue interaction factor, which ranged from an 80% reduction to an increase in the accumulated fatigue damage by a factor of 4. Fatigue analyses for the 10 WEC scenario showed a stronger influence of the hydrodynamic interaction, in which the predicted fatigue damage can be varied by more than tenfold.

Numerical modelling and optimization

MoorDyn is an open-source lumped-mass mooring dynamics mode which interfaces with the well-known WEC-Sim matlab based open source code for design of WECs. Increased capabilities for this code, namely modelling friction between mooring lines and the seabed and modelling mooring systems attached more than one floater, are presented in (Hall, 2017). A mooring line connecting two bodies is used to demonstrate these capabilities, also including sea-bed friction. Results show the effect possible that this friction can have on the mechanical power dissipated by the moorings in a shared-mooring WEC array.

Also considering WEC arrays with shared moorings, analysis of the effects of moorings in the responses of an array of three spar-buoy OWCs was carried out by (Oikonomou et al., 2017) and (Oikonomou et al., 2020). Two different mooring configurations were studied (independent and inter-body moored devices) and a stochastic analysis was undertaken for irregular waves. Difference between configurations was 2-3% in terms of efficiency, but average heave RAO decreased by 7-8% at the peak frequency when including the inter-device mooring connections.

(Thomsen et al., 2017) performed a screening of available tools for dynamic mooring analysis of WECs. A number of relevant commercial software packages for full dynamic analysis were tested, focusing on each one's ability of fulfilling the requirements of modelling, as defined in design standards, and thereby ensuring that the analysis can be used to obtain a certified mooring system. According to the author's, DeepC and OrcaFlex were found to best suit the requirements, while OrcaFlex would satisfy all of them.

Regarding optimization, (Thomsen et al., 2018) developed a methodology for cost optimization of mooring solutions for large floating WECs. The study used four Danish WECs to find an inexpensive and reliable mooring solution for each device. A surrogate-based optimization routine to find a feasible solution in only a limited number of evaluations and a constructed cost database for determination of the mooring cost was developed. Based on the outcome, the mooring parameters influencing the cost were identified and the optimum solution determined.

Worth of notice is the release of the alpha version of the Staion Keeping tool developed within the closing DTOceanPLus European project (Luxcey et al., 2020). The tool deals with the full design of: a) Foundation base for fixed devices: gravity foundation base, pile; b) Mooring system and anchors for floating devices: mooring line, drag anchor, pile, dead weight anchor, suction anchor. Functionalities include: static analysis, dynamic analysis, ULS analysis, FLS analysis, mooring system design, soil properties, foundation suitability, foundation design, hierarchy and bill of materials, and environment impact.

Experimental studies

Experimental campaigns of WECs including accurate mooring systems provide a way for validation of numerical based approach design of WECs, giving confidence to results regarding predicted structural integrity of the mooring system.

(Barrera et al., 2019) made a thorough experimental setup description and analysis of their investigation of the performance of mooring systems in terms of tensions, movements and

energy absorbed by means of an experimental test campaign under different loading conditions in a flume tank. These effects were evaluated through imposed movements at the fairlead, through purpose-built actuator systems, with and without currents and hydrodynamic loads (waves and currents). In addition, the influence of different weight of mooring lines and seabed friction coefficient was investigated as well. A noteworthy conclusion, among others, is that the standard procedure of modelling chain stiffness with a spring induces discrepancies between modelled and prototype results in terms of snap loads, for the propagation speed of the tension shock and the tensile stiffness of the cable governs both the peak load magnitude and the period of slack in the cable. Therefore, the spring only models the stiffness of the whole cable in a quasi-static manner, and as a consequence, the resulting snap load cases have uncertain magnitude and are most likely over-predicted compared to prototype scale.

(Xu et al., 2020) presented an experimental assessment of three hybrid mooring systems for a heaving-buoy wave energy converter in waves. The effects of wave period, incident wave height and mooring configuration were evaluated. To study the short term extreme dynamic tension, the traditional Weibull distribution, Weibull distribution based on tail data and peaks-over-threshold method are applied. The results showed that the Weibull distribution failed to present accurate extreme dynamic tension prediction when the snap events occur frequently, while the other two methods showed good performance despite of number of snap events. Based on the results of energy production performance and extreme dynamic tension, a novel mooring line design was suggested, aiming at reducing mooring dynamic tension. In (Xu and Guedes Soares, 2020), two of these mooring systems are analysed in terms of the effects of T-N curve and snap loads on mooring fatigue damage. Uncertainties in mooring fatigue estimations are discussed.

An interesting scaled experimental study on nylon compact mooring systems loosely based on the SALM concept applied to a floating dual chamber water column was presented by (Xu et al. 2020b). A catenary system was also tested, while the difference between both compact systems was the addition of a clump weight above the buoy to reduce snapping loads. It was shown that the compact systems had a detrimental effect in the efficiency of the WEC in low sea states, while the opposite was true for large wave heights. On the other hand, fatigue loads were greatly reduced with the option for the compact systems.

Considering arrays, (Gomes et al., 2020) present the experimental study of different configurations of a five-device array of spar-buoy oscillating-water-column wave energy converters in a wave basin, focusing on the analysis of the devices motion and the mooring line loads. The study compares the performance of a single isolated device, an array with independently-moored devices and three arrays with inter-body connections, with different levels of connectivity in the mooring arrangement. Results showed good performance for all configurations when subjected to moderate sea conditions. Under extreme sea conditions, high peak tensions were observed in the lines of all array configurations, but particularly large in the inter-body lines. The authors argue for longer inter-WEC moored lines to mitigate the phenomenon.

4.3 Physical testing

4.3.1 Laboratory testing and validation of numerical tools

Testing of power take-off (PTO) components

(Fleming and Macfarlane, 2017) conducted 2D PIV model test experiments on a series of forward-facing bent-duct type oscillating water column (OWC) models with varied underwater geometry. They investigated conversion losses and device performance by modifying the underwater geometry. Four models were tested; the base model and three variations had additional segments to afford different chamber lengths and lower/upper lip angles (10, 20, and 30 deg.). Performance comparisons were undertaken using phase-averaged wave probe,

pressure transducer, and PIV data. Additional qualitative analysis of velocity fields was performed using temporal averaging.

(Yurchenko and Alevras, 2018) suggested a novel WEC system based on the rotating mass system having low gravity. They showed that numerical results of deterministic and stochastic modeling reflect an advantage of the proposed design, and the numerical results were compared with experimental results. From the results, the novel WEC system used both the heave and surge motions, and the motions could be excited the rotating mass in various wave periods and wave heights.

(Wang and Lee, 2019) proposed a 2-DoF WEC composed of an eccentric dual-axis ring and power generator using circular Halbach array magnetic disk and iron-core coil. The WEC was designed to convert kinetic energy from the vertical motions, which are heave, roll and pitch, of a mooring-less buoy type. The designed WEC was verified from model test, and 0.56W power was generated in the frequencies of buoy motions from 0.7 to 1.0Hz.

(Sarmiento et al., 2019) presented experimental testing results performed to validate the technical feasibility for a new floating semi-submersible platform which combines wave energy converters (3 OWC) and a 5MW wind turbine. To investigate the global performance of the platform as well as the performance of OWCs, a wave tank testing was carried out under the incidence of regular waves with and without winds, operational sea states, and survival sea states. The wind turbine was modelled as a drag disk to give proper loads by the turbine and the PTO effect by the OWC was conceptualized by the orifice. They concluded that the platform natural period varies depending on the openness of the chamber and that the wind turbine operating state had a significant impact on the platform response and the mooring load compared to the OWC operating state.

(Bacelli et al., 2019) applied a real-time realization of pre-control algorithms to evaluate and optimize energy absorption. They presented an experimental method to evaluate the ability to execute basic control algorithms in WEC model tests. For controller tuning, a dry bench test was performed, and a wave tank test was performed. The trends of the dry bench test and the wave tank test were well matched, and the performance of a simple feedback controller was also shown to be effective.

(Liu et al., 2020) applied an impulse turbine in the model test of OWC chamber, not an orifice plate, in order to evaluate the performance of the OWC. This method can more strictly consider the interaction between the OWC chamber and the impulse turbine. The rotation of the turbine during the test was controlled by a servo motor, and the OWC internal wave elevation, changes in air pressure in the chamber, and torque output were measured.

Testing of a single device

- ***Power performance tests***

(He et al., 2017) conducted a series of wave-flume experiments in regular waves to examine the wave power extraction of a floating box-type breakwater with dual pneumatic chambers. The effects of wave period, chamber draft, water depth, and arrangement of chambers on the power extraction were examined. The results showed that the power extraction was mainly due to the water column oscillation inside the chamber, and differentiation in the designed natural periods of dual chambers could widen the efficiency bandwidth of power extraction. The front chamber always played a prominent role in power extraction, and the power extraction of the rear chamber was only a supplement. It showed that the water column oscillation was more dependent on the wave period rather than controlled by the wave scattering under different water depths.

(Elhanafi et al., 2017) conducted an experimental and numerical hydrodynamic performance assessment of a 1:50 scale model offshore floating–moored Oscillating Water Column (OWC) wave energy converter. The device was a tension–leg structure with four vertical mooring lines.

The performance of the OWC device was investigated for several design parameters, including regular and irregular wave conditions of different heights and periods, power take-off (PTO) damping, and mooring line pretension. A 3D Computational Fluid Dynamics (CFD) model using RANS–VOF approach in STAR-CCM+ was constructed and validated against experimental results for regular waves. The device performance was compared to that of a fixed device of the same geometry, and the surge motion of the floating device improved the power extraction efficiency.

(Vyzikas et al., 2017) investigated the behavior of different designs of OWC, making geometric modifications to the classic design of OWC and the U-OWC. The multi-chamber OWCs are fixed on the seabed and have a slit opening at the seaward side. The devices were tested in uni-directional regular and irregular wave conditions, with and without power take-off (PTO) mechanism, essentially also testing absorbing seawalls. They suggested potential shape improvements towards an overall optimization of the devices that take into account both the hydrodynamic efficiency of the OWC and other design aspects, such as the wave run-up, and they also endeavored to highlight potential benefits from incorporating OWCs in coastal defense as absorbing.

(Ning et al., 2019) investigated the hydrodynamic performance of a land-based dual-chamber oscillating water column (OWC) system by scaled model experiment. It was showed that the dual-chamber OWC is favorable with increases in both the peak efficiency and the effective frequency range. The hydrodynamic analysis on the dual-chamber OWC using fully nonlinear numerical wave tanks (NWTs) within the framework of potential flow theory were also carried out to cross-check the experimental results.

(Zhao et al., 2019) proposed a breakwater integrated WEC system in which an array of oscillating buoys are arranged on the weather side of a breakwater. The performance comparison between the conventional WECs and the breakwater-integrated WECs was experimentally discussed, and those results were verified by comparing with the numerical simulations in terms of the motion RAO of the WEC devices. Influences of the buoy draft and spacing on the hydrodynamic performance, which was found to have a larger heave response as the spacing was narrower or the draft was deeper, was studied. In addition, it was shown that the presence of the breakwater amplifies the energy conversion performance of the WEC array by comparing the hydrodynamic performance without and with combining the WEC to the breakwater.

(Çelik and Altunkaynak, 2019) carried out a comprehensive experimental campaign to study the effects of different underwater chamber openings and the PTO damping on the efficiency of an OWC device under different wave conditions. A broad range of the opening height and the orifice diameter were implemented into the experimental model, and the performance of energy conversion was evaluated under various regular incident waves. They showed that obtaining the optimal energy conversion performance does not depend on a unique optimal damping state but depends on the incident wave characteristics, however, for a range of wave steepness, optimal damping further varies with the opening height of the chamber.

(Martin et al., 2020) applied an additional underwater body to the buoy in order to improve the performance of the point-absorbing WEC. The underwater body may change the resonance frequency by increasing the wave force. It can be used to increase the excited force and provide resonance adjustment. Model tests were conducted using the 1:30 scale model WEC, and the experiment showed that the device with additional underwater body could generate twice as much power as the single device. The WEC with additional underwater body have a capture width of up to 58% at 59 kW/m and 51% at 36 kW/m.

- ***Numerical model validation tests***

(Zabala et al., 2017) presented a new tank calibrated wave-to-wire model based on a six degrees-of-freedom time-domain simulation of the spar-buoy OWC, including a nonlinear model of the self-rectifying biradial turbine and the mooring lines, and assessed the spar-buoy performance. Then, they also presented a numerical model calibration procedure, and this hydrodynamic model has been adjusted based on an extensive 1:16 tank testing performed at NAREC.

(Rezanejad and Guedes Soares, 2018) calculated 1st energy conversion efficiency of an OWC from a dual-mass systems. The dual-mass system were designed from mass-damper-spring system, and the analytical results by the dual-mass system were directly compared with experimental results. They showed the OWC located in the stepped bottom acted as a single-mass system in short wave periods and by long wave periods it performed as the dual-mass system.

(Xu et al., 2059) presented the evaluation results for hydrodynamic performance of the floating-point absorber (FPA) in terms of both of survivability and operability. Physical models were built and tested in wave tanks, and both the BEM-based potential flow analysis model and the RANS simulation were used for analyzing the WEC behavior in regular waves and for evaluating the WEC survivability in extreme waves. The experimental and numerical results showed that nonlinear effects which is caused by viscous damping and interaction between waves and the FPA, significantly influence the system response and power absorption performance.

(Bingham et al., 2021) presented a set of experimental results which were measured by KRISO OWC tests and the comparison with numerical predictions based on weakly-nonlinear time- and frequency-domain potential flow methods and CFD as a benchmark test. The effects of air compressibility were found to be small for the pneumatic pressure, but produced significant nonlinear effects and a significant phase shift for the internal chamber surface motion. All numerical models captured the time-averaged quantities well, but only the compressible CFD model was able to accurately reproduce the detailed response.

- ***Survivability tests***

(Ashlin et al., 2017) performed model tests, and horizontal and vertical wave forces on an OWC caisson model were measured according to wave steepness. To measure the horizontal and vertical wave forces, four pressure transducers were attached on the front wall of the OWC caisson, and two pressure transducers were attached on the roof of the OWC caisson. Also, the measured horizontal wave forces were directly compared with Goda's empirical formula. From the results, it could be found that the total horizontal wave force was about 2.5~3.0 times the total vertical wave force, and the measured shoreward total horizontal wave force was higher by about 46%-90%, compared to shoreward horizontal wave force from Goda's empirical formula. However, the measured seaward total horizontal wave force was observed to be always greater than the seaward horizontal wave force from Goda's empirical formula by about 5~50%.

(Pawitan et al., 2019) suggested a model to estimate forces acting on an OWC chamber in a caisson breakwater. Horizontal forces on the front and rear walls of the OWC were measured in experiments, and the experimental results were directly compared with Goda's empirical formula. From the results, the estimation model for horizontal forces on an OWC chamber was suggested.

Testing of an array

(Nader et al., 2017) presented an experimental approach for understanding the performance of WEC arrays to develop a methodology to model an array of WECs accurately. They applied the phenomenological theory to the experimental hydrodynamic investigation of an array of generic WECs by separating the problem into its diffraction and radiation problems. Then, using a postprocessing analytical model, the q-factors, the parameter representative of the array

performance, for several configurations were derived. Furthermore, a bespoke stereovideogrammetry method was applied to verify and analyze the wave field around the lee of the array.

(Zhao and Ning, 2018) suggested a novel system consisting of a front oscillating WEC and a rear fixed pontoon. They performed model tests according to different draft ratios between the front and rear pontoons, and the experimental results were compared with experimental results for a single oscillating WEC system. From the model test, the novel system improved the capture width ratio (CWR) effectively without compromising the coastal protection performance in comparison with the single WEC system, and the effective wave period range for the transmission coefficient and CWR could be broadened by improving the CWR in short wave periods.

(Kamarlouei et al., 2020) presented the model test results of multiple wave power generation systems attached to floating offshore wind platforms. Twelve floating buoy attached along the floating offshore wind platforms at a scale of 1:27 showed that the interaction between the buoy and the platform had a positive effect on the platform heave and pitch motions.

4.3.2 Field testing

As a consequence of environmental pollution and climate change, there has been an increasing interest in developing technology to efficiently make use of renewable energy. Wave energy is one of the four main sources of marine renewable energy including wave energy, tidal energy, thermal energy and wind energy. Wave power flux can be well probabilistically forecasted 48 h in advance and the average annual power flux per unit length of wave front of wind-driven waves ranges from 10 kW/m to 100 kW/m (He et al, 2013). A typical wave energy power plant potentially can have a capacity that is comparable to the capacity of a typical conventional power plant. Therefore, field testing for wave energy converter (WEC) has been a growing area of research in recent years.

Many Europe countries have achieved significant progress in research and application of WECs. In 2018, the Penguin WEC2 was towed to the European Marine Energy Centre (EMEC) in Orkney, Scotland, where it was deployed alongside Wello's original Penguin WEC. Funded by the European Union's Horizon 2020 research and innovation program, the CEFOW project aims to build and deploy an array of three Wello Penguins at EMEC's grid-connected wave test site at Billia Croo, on the west coast of Orkney. The first of the three Penguin WECs was successfully installed by local marine contractor, Green Marine, in April 2017 and has safely remained on site since then, surviving wave heights of over 18 meters. Learning from the WEC1 demonstration has fed into the development of WEC2 which has been optimised for power generation. The device has been built at the Netaman shipyard in Tallinn (See Fig. 2). Using dry mate connectors, a bespoke four-way smart subsea hub will interconnect the dynamic umbilical cables from each WEC to EMEC's marine export cable. Power will then feed into EMEC's onshore substation and on into the national grid. The hub incorporates subsea switchgear enabling the disconnection of a single device while allowing the other two to continue generating. In November, a marine licence was granted for the installation, operation and decommissioning of the three-WEC array and the subsea hub (EMEC, 2018).

The bottom hinged Oscillating Wave Surge Converter (OWSC) proposed by Queen's University Belfast has been installed at European Marine Energy Center, Orkney, Scotland, and the next-generation devices called WaveRoller [Reference is missed] has been designed based the hydraulic power take-off system, as shown in Fig. 3. Another new WEC has been tested in Portugal based on the direct mechanical drive system which is called as CECO (Rosa-Santos et al, 2019). The novelty of the CECO is that it consists of two floating modules which help to generate electrical energy simultaneously from kinetic and the potential energy of the ocean waves.

Fig. 2 Wello Penguin WEC2 being lifted into the sea in Tallinn, Estonia

Fig. 3 The photograph of WaveRoller device

A Danish company named Wave Dragon Aps [Reference is missed] developed and installed the Wave Dragon device (as shown in Fig. 4) in Nissum Bredning, Denmark, which is an overtopping type device and was the first offshore floating slack-moored WEC in the world. Some EU countries including Denmark, UK, Portugal, Germany, Sweden, Austria and Ireland jointly supported this Wave Dragon project. The device consists of two arms that assist water to gather in the reservoir, whose level is higher than the surface level of the ocean and turbine by using a submerged ramp.

Fig. 4 The photograph of Wave dragon deviceA new wave energy technology CETO 5 prototype with 5 MW peak design capacity, developed by Carnegie has been installed in Fremantle between Garden Island and the Five Fathom Bank, Perth, Western Australia, which was the world's first wave energy project that produced energy and desalinated water together in the same time at commercial scale [Reference is missed].

There are a couple of hybrid wave-wind systems that have been proposed in some EU countries. Green Ocean energy, a marine energy company based in Scotland, is developing a wave-wind energy device known as Wave Tender (as shown in Fig. 5) and currently, it is projected to have a peak rating of 500kW-700kW (Ahmed et al, 2020) due to high yield per unit of sea area. The system consists of wind turbines to generate energy from the air in the top of the ocean surface and hydraulic cylinders to convert wave energy. A Poseidon system demonstrator has been constructed by the Danish company Floating Power Plant in which a range of pitching type WECs are mounted on a secure cross-type base. Moreover, a Norwegian company is developing a W2power system that incorporates a point-absorber type WEC and two wind turbines (Rusu and Onea, 2018).

Fig. 5 Wave Tender

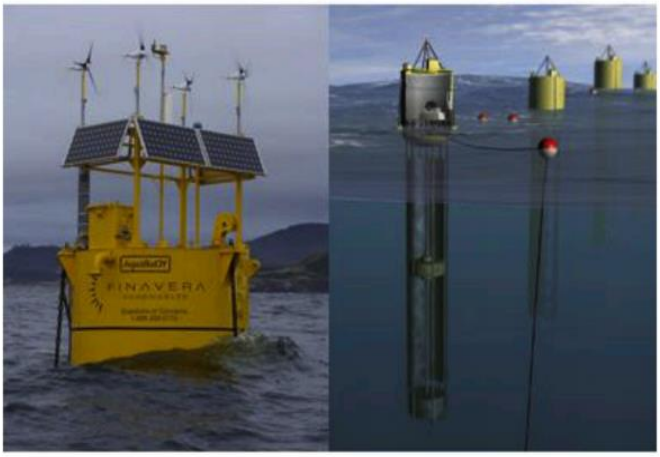

Fig. 6 The photograph of AquaBuoy

The UK based wave energy developer company Archimedes Wave Swing (AWS Ocean) designed a series of AWS WECs and they were first deployed and tested in Portugal [Reference is missed]. The AWS is basically a fully submerged air-vessel which was mainly developed in the Netherlands. The Dutch company Teamwork Technology first conceived of the original concept of the AWS. It consists of two parts; the top part is free to move but the bottom part is fixed to the seabed. The floating component moves up and down because of the water pressure which is created as the wave passes over the AWS. The linear generator generates energy from this relative motion between the top and bottom parts. The AWS was the first commercial wave energy converter that used a linear electrical generator in a PTO system.

Hydro turbine methods have also been used in the Aquabuoy [Reference is missed], as shown in Fig. 6, to generate energy from ocean waves in the USA. In the Aquabuoy the pumped water was directed into a conversion system that consists of a Pelton turbine to drive a conventional electrical generator. Oregon State University developed 12 prototypes, and deployed and tested them over a period of more than one decade [Reference is missed]. The first device contained a spar and a float where the spar was moored, and the float moved up and down with the wave motion. The spar was a central cylindrical design housing a bobbin, wound with a three-phase armature and the float was an outside cylinder that consisted of 960 magnets. The inner surface of the float faced the outer surface of the spar and when the float moved up and down due to the wave motion then voltage was directly produced inside the armature.

In 2009, Australian marine energy company BioPower Systems cooperated with German Siemens to develop BiOWAVE terminator WEC (BioWAV,E 2020), as shown in Fig. 7. The converter is installed on a fixed platform on the seabed. The pendulum body can swing back and forth with waves to generate electricity and rotate around the vertical axis of the base to match the wave direction. At present, typical terminator WEC built offshore include the Langlee WEC in Norway (Perline et al, 2001), the WaveRoller WEC in Finland (WaveRoller, 2020) and the Duck WEC in the UK (DuckWave, 2020). (Zhang et al., 2021) introduced some typical multi-degree of freedom WEC (MDWEC) and their realization. In addition, Using the AHP evaluates the performance of existing wave energy power generation devices comprehensively from five different perspectives: energy capture, technology cost economy, reliability, environmental friendliness and adaptability.

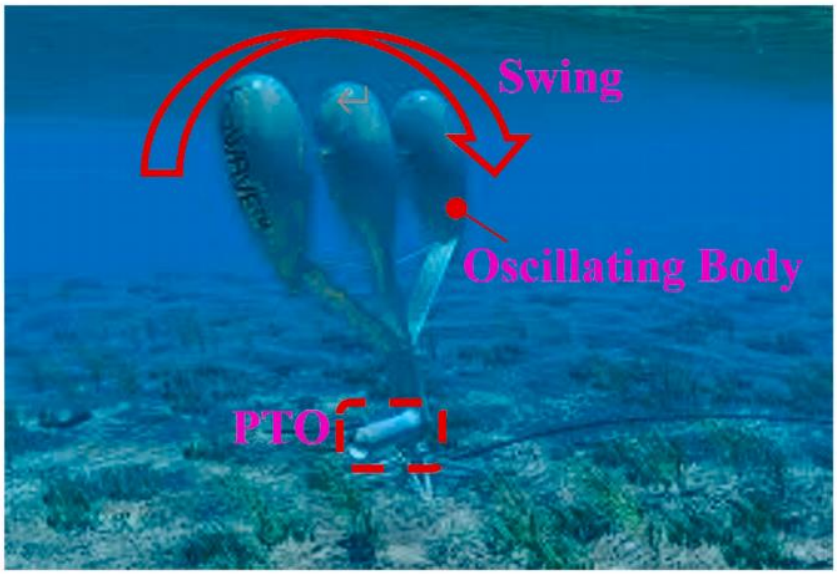

Fig. 7 BioWAVE WECA novel vertical augmentation channel housing a direct-drive cross-flow turbine, with nozzles on both the sides of the turbine, was designed as a wave energy converter (Weerakoon et al, 2021). The actual wave measurement data near the korea maritime and ocean university (KMOU), South Korea, are set as input conditions, as shown in Fig. 8(a). The design not only looks at using the cross-flow turbine for wave power applications but also proposes a new vertically configured augmentation channel through which the water flows vertically in and out due to wave action, as shown in Fig. 8(b). Thus, the flow at the inlet, at the outlet and through the turbine is in the vertical direction. This makes the design compact and the whole WEC occupies less space. The turbine is fully submerged in water and under the action of incoming waves generates power bidirectionally while rotating in just one direction.

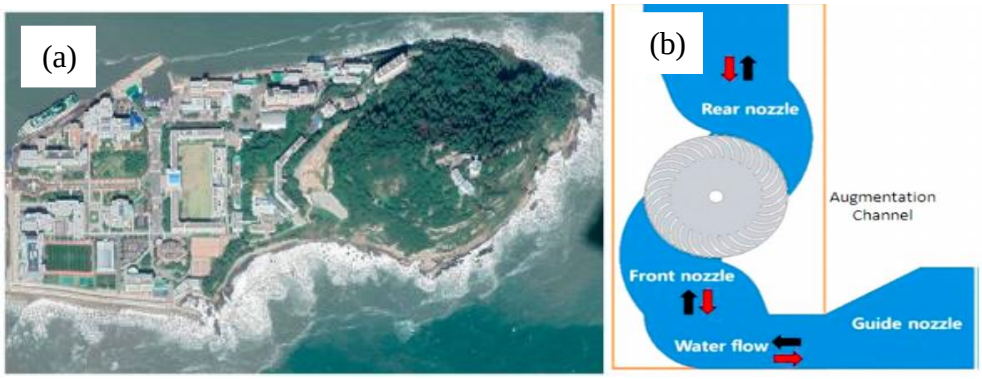

Fig. 8(a) Map of korea maritime and ocean university and (b) the vertical augmentation channel and the turbine blade

In recent years, open sea tests for well-design wave energy device in China were mainly conducted by research institutions. The wave energy electrical system at Dawanshan Island, 'HAILONG 2', designed by the research institution 710 is a type of raft-type wave energy device (see Fig. 9). The hydraulic equipment is edged between the adjacent rafts, driving the generator through the relative motion of two rafts. The demonstration operation of the device 'HAILONG 2' last for 180 days and finished in 2018. The average generating efficiency reached 20% according to the report (Hailong, 2021).

Fig. 9 The photograph of 'HAILONG 2'A multi-buoy offshore floating wave energy converter

named 'Sharp Eagle WANSHAN' was tested near Wanshan Island, Zhuhai (see Fig. 10). The test was led by Guangzhou Institute of Energy Conversion, Chinese Academy of Sciences. The device is 36 meters in length, 24 meters in width and 16 meters in height. The sea test in shallow water of 20 meters depth started in March and last about 3 months. The generating power was 30530.57 kWh in total (Sheng et al, 2019). The results also indicated that the generating efficiency was much higher in June because of the summer climate (see Fig. 11). Another sea test for 'Sharp Eagle WANSHAN' was conducted by the National Ocean Technology Center and Tianjin University (Wang and Yu, 2019). The test was located in the region with water depth of 30 meters, started in April and last for 40 days. The experimental data was analyzed by a proposed methodology, through which the predicted generating power reached 40171kWh per year.

Fig. 10 The 'Sharp Eagle WANSHAN'

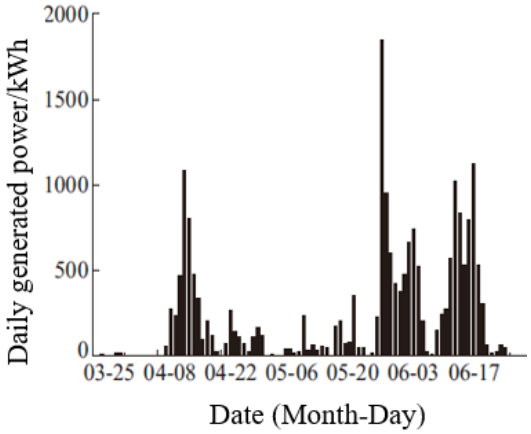

Fig. 11 The daily generated output bar chart

A novel floating array-buoys WEC (FABWEC) system (Sun et al, 2021) is presented (see Fig. 12) as the basic model and sea trials of a 10 kW full-scale prototype were practically performed at Taiwan Strait, China. The FABWEC system consists of an A-shaped floating platform, ten oscillating buoys, two sets of mechanical transmission and power generation mechanisms, an electromechanical control system and a single-point mooring system. The oscillating buoys located on both sides of the floating platform are the main energy capture mechanism of the FABWEC system. When the wave is transmitted to both sides of the platform, the oscillation amplitude of the central platform is much smaller than that of the oscillating buoys, leading to relative motions between them. And then the relative motions are dampened by pinion power take-off (PTO) systems to convert wave energy to mechanical energy.

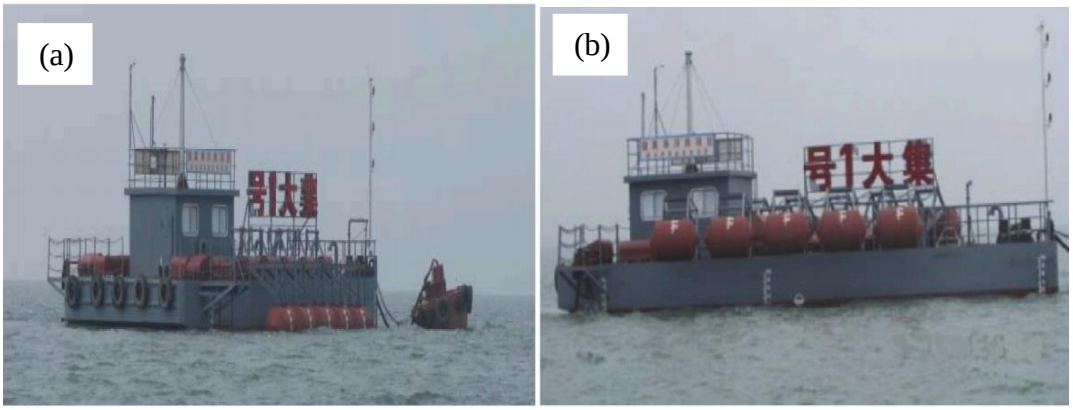

Fig. 12 The prototype of novel FABWEC system deployed at Taiwan Strait, China: (a) Oscillating buoys float on the sea surface to capture wave energy under normal operation mode; (b) Oscillating buoys are pulled out of the seawater under storm protection mode.

Some tests for prototypes were also conducted by universities. Shanghai Ocean University designed and manufactured a new type of wave-current energy device (Wang et al, 2020) which consisted of 1: blade wheel, 2: generator, 3: diffluence cover and 4: guide cover (see Fig. 13). The fluid flows into the device through the guide cover, and then the inside diffluence cover further leads the fluid to the blade wheel. A series of experiments were conducted to verify the rationality of theoretical design and the feasibility of power generation, including the flume tests for bilateral 20W and bilateral 50W prototype, and the open sea test for bilateral 500W prototype. The sea test was located at the wharf of the Shanghai electric Lingang heavy machinery equipment co. LTD (121.50oE, 30.85oN) and last for 2234 hours. The average generated power was around 1000W and the maximum power reached 1200W, confirming the good stability of power generation.

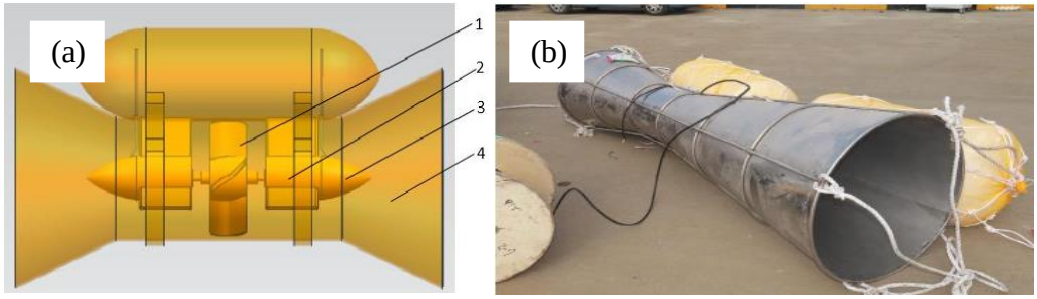

Fig. 13 The diagram of direct drive wave-current power generation device: (a) blueprint and (b) bilateral 500W prototype in kind.

'JIDA 2' is a float-type wave power acquisition device designed by Jimei University with length, width and depth overall are, respectively, 18 meters, 8 meters and 2.4 meters (Wang et al., 2019). The device is mainly a floating platform with mooring system, and the generators at both sides are motivated by levers and buoys (see Fig. 14). The sea test was conducted near Xiaodeng Island in 2018. The experimental data indicated that the efficiency of each generator was around 15%-17%.

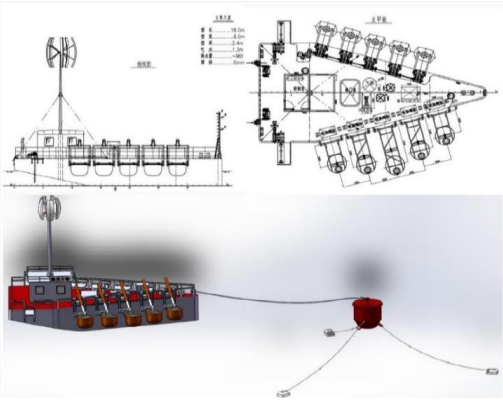

Fig. 14 The buleprint of 'JIDA 2'

Fig. 15 The buoy-rope-drum wave converter

A buoy-rope-drum wave converter (Li, 2018) proposed by Shandong University is a kind of oscillating buoy wave energy device (see Fig.15). The 2 meters height buoy floats up and down under wave motions, driving the incide generator transfers mechanical energy into electricity. The first sea test was performed in the shallow water of 20 meters depth and last over 100 days, while the generating efficiency was unsatisfactory. After the optimizing by numerical simulation, the counterweight at bottom was set to 700kg and another sea test was then performed. The results showed that the generating power reached 311W and 9043W under the circumstance of small waves and medium waves, respectively, which were 20times larger than those in the first sea test.

Shanghai Ocean University and China petroleum pipeline material equipment co. LTD co-designed a floating breakwater based on ocean wave power generation (Wang et al, 2019) and further performed a sea test for the 40W small prototype at Luchao port whart (see Fig. 16). The blades at windward side motivates the device rotating about the axis under the wave motion, while those at backward close automatically due to the gravity. The average power in the two-hour monitoring interval was 42W, with the maximum power of 54W. The peak output voltage of a 60s cycle under a better load was 52V, and the average voltage was about 20V, but the output voltage fluctuates sharply, and there was a voltage range of 0 at the interval of incoming tide.

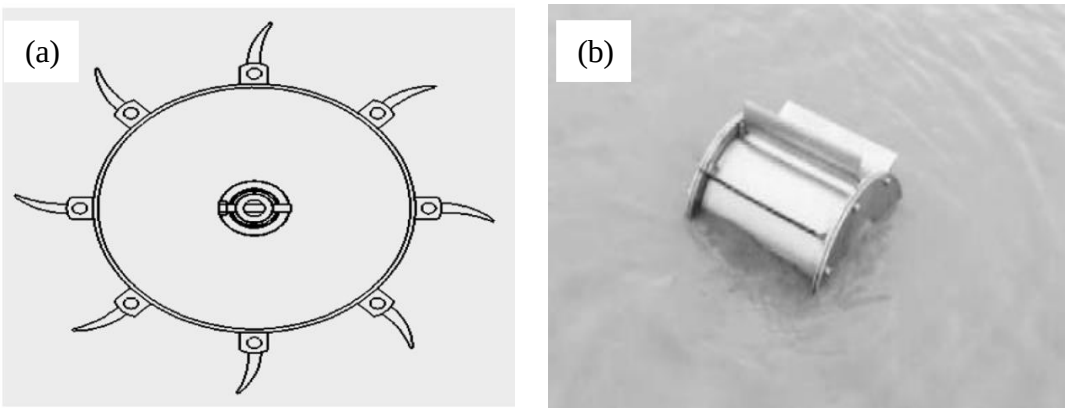

Fig. 16 The diagram of floating breakwater device: (a) blueprint and (b) 40W prototype in kind An innovative floating system which integrates an oscillating buoy type wave energy converter (3kW) designed by Harbin Engineering University with a cylindrical dual pontoon-net floating breakwater (FB) designed Jiangsu University of Science and Technology are proposed, as shown in Fig. 17. Each FB module having the length 15 m× breadth 20 m, consists of two 8 m (diameter) ×15 m (length) cylinders which is attached with four rows of plane nets underneath at intervals of 3 m. The dimensions of the wave energy converter are 2.2 m in length and 2.5 m in height. The full scale prototype has been constructed and the field test has been undertaken in

China Sea areas. A range can be observed for which the hydrodynamic efficiency of the system can achieve approximately 24% while the wave attenuating capacity was kept higher than 15% within the whole tested range of wave periods, and the integrated system performs in an effective manner.

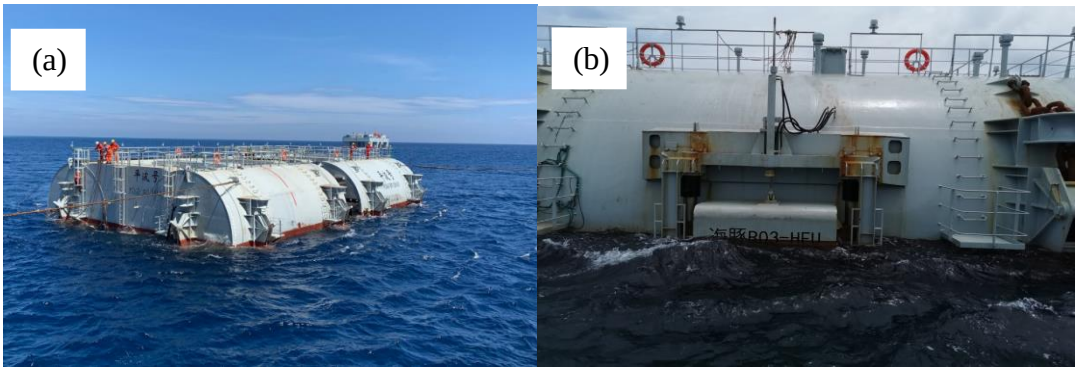

Fig. 17 Integrated system (a) Cylindrical dual pontoon floating breakwater and (b) 3kW wave energy converter

5. TIDAL AND OCEAN CURRENT TURBINES

5.1 Recent development

The European Marine Energy Centre (https://www.emec.org.uk/) gives a clear landscape of the different types of tidal devices and a quite complete list of the tidal energy developers.

Wani et al (2017) depict a state of the art of marine current turbines configurations, most of them bottom mounted.

IEA-OES writes annual reports and other documents that reports the strategies for developing the Marine Energies related activities. Some publications formulate best practices for the design processes.

In the recent years, beside seabed mounted devices, was noted an increased development of tidal devices supported by floating bodies or moored in midwater. The GEMSTAR project illustrates such a floating configuration described by Coiro (2019) (https://www.gemstar.it/). The MINESTO tidal kite illustrates another approach of tidal energy harnessing (Wani 2017).

The European H2020 project MaRINET2 (https://www.marinet2.eu/) gave opportunity to access experimental infrastructures for SMEs and academic teams. A round robin was organised for testing a common model of a scaled three bladed HATT in four different facilities with current, and even with combined waves and current (Gaurier 2019). The MaRINET2 project led to many publications especially during the EWTEC conferences in 2017 and 2019, some of the articles were later published in journals.

An important work is undergoing headed by the International Electrotechnical Commission (IEC) in order to provide guidelines for assessment of the marine energy converters.

5.2 Environmental Conditions (related to the boundary layers)

Tidal turbines primary focus is to harness current flows expected to be steady. Practically many reasons lead to nonuniform flows: turbulence, boundary layers on the sea bottom and even along the free surface, variable bathymetry, seabed roughness and obstacles, waves and wave-current interaction, tidal arrays interaction.

The evaluation of the complex current, waves and turbulence interactions is a common question for the developers of tidal tests sites and operational sites. There is a need for intensive measurements in time and space to build useful databases and validate the numerical methods.

Compelli et al (2019) develop mathematical formulations for irrotational and rotational flows for the purpose of deducing the free surface elevation from the pressure on the sea bottom in

the case of regular waves and a perfect fluid. The simple irrotational Airy waves model combined with a uniform current with modified dispersion relationship gives a quite simple formula for this pressure factor. It is expected that for small wave length compared to the water depth, the seabed pressure is too small to evaluate the free surface effect. A second irrotational model is developed using the stream function and suitable series. The resulting nonlinear formulation cannot be solved analytically and the assumption of a moderate current intensity is adopted. The numerical results still need to be validated by comparison to measurements in real conditions.

The numerical procedure used by Venugopal et al (2017) to evaluate the complex flow at Fall of Warness in Scotland relies on the MIKE 21 and MIKE 3 software (Danish Hydraulic Institute, Denmark). The first software is used at the North Atlantic scale to simulate the boundary conditions of the second one at the Orkneys islands scale with a refined mesh. The numerical and experimental free surface elevation measured with an ADCP at a given location are in good agreement. The numerical simulation demonstrates the important interaction of the current and waves and variations of the moderate sea state's significant height, peak period and mean direction with the ebb and flow of the tides. More simulations are needed to validate the model for higher sea states.

Jakovljevic et al (2017) numerically simulate wave and current interaction in storm conditions and obtain results which are qualitatively correct but still need experimental validation.

The Alderney Race is considered as a target site for the deployment of operational arrays of tidal turbines and a possible massive capture of energy. Sentchev et al (2019) used the MARS 2D software at regional scale to simulate the current flow. Thanks to the Optimal Interpolation technique, the ADCPs measurements at fixed locations or onboard travelling vessels help to improve and validate the numerical results and the estimation of the available tidal energy.

In the same Alderney race area, Lopez et al (2019) use two High Frequency radars able to measure surface currents on a large area and measurements with ADCP at specific locations and numerical modelling results (MARS 3D and WAVEWATCH III software) are compared.

Strong currents in Alderney Race may reach 5 m/s and are able to convey sands, gravels and even rocks, and ADCPs located on the seabed! Gaurier et al (2017) experimentally simulate the trajectories of calibrated particles in a flume tank and their interactions with a HAWT.

Considering the roughness of the seabed, Grondeau et al (2017) use the Lattice Boltzmann to simulate the interaction with a strong current and the development of the boundary layer. The numerical results are compared to the results of a documented test campaign run at reduced scale for arrangements of cubic blocks located in a water-circulation tank. A good agreement is found when considering the average values of the turbulent components for Reynolds number below 105 according to the water depth. Simulations for higher Reynolds number up to 108 are necessary in real cases and need to be done.

5.3 Tidal turbine loads and response analysis (effect of arrays)

According to the list of environmental flows and interactions, multiple loads are applied to marine current energy converters. Their structures combine slender elements, bluff bodies, rotating parts and the fluid-structure interactions are consequently complex. The energy efficiency is the main parameter from an economical point of view but many other loads and responses are technical key points for the operation, the fatigue and the survivability of the systems.

5.3.1 Numerical methods

Calculation methods for tidal turbines take profit from the developments for marine propellers and for wind turbines. In the order of appearance and accordingly with the development of computational power, the numerical methods were first based on perfect fluid approach with

rotational flow and use of the Boundary Element Method. The Blade Element Method is based on a two-dimensional formulation of the loads on blades profiles and integration along the blade radius with corrections accounting for the effects around the blade tips and close to the hub in the case of HATT. Drag and lift coefficients are those of real profiles. Recent developments use Computational Fluid Dynamics and simulate the turbulence effects associated to the incoming flow, the boundary layers along the blades, stalling and the wake. Fluid structure interactions take into account the materials stiffness, inertia and damping. Attention should be paid to the Reynolds scale effects when simulating full scale or model scale turbines.

Ellis et al (2019) compare two CFD software, OpenFOAM and ANSYS CFX, for the prediction of a HATT efficiency. In this case, a single mesh generated for ANSYS CFX is used for the different parameters and OpenFOAM gives larger loads. Nevertheless, both numerical results show an acceptable agreement with the available experimental results. Improvement could be done by adapting the mesh geometry for the various considered tip speed ratios.

With the OpenFOAM CFD solver, Feinberg et al (2019) study the crossflow on a VATT and the free surface effects which are generated. Lift, drag and power coefficients are computed for different water depth and two different boundary conditions on the upper surface, no slip condition or free surface. In this last case, a bore is generated in the wake of the turbine.

Encarnacion et al (2019) apply a Blade Element Momentum method to simulate a HATT. A current profile shaped by a power function z1/7 of the altitude z starting from the sea bottom is chosen and the incoming regular waves velocity field is stretched up to the instantaneous wave elevation. Less energetic sites are also considered with a modified current profile shape z2/7.

Lloyd et al (2019) use ANSYS CFX CFD software to simulate the free surface effects in a channel with current and a reduced scale model. Seven meshes are tested and two different conditions at the free surface are considered including free slip condition. It is found that the numerical results overestimate the experimental loads by several percent and that the free surface condition induces more loads fluctuations on the blades and torque than the free slip condition. The thrust on the hub is also sensitive to the free surface condition.

5.3.2 Laboratory tests and field measurements

As far as possible the recommendations of the ITTC (2017) Specialist Committee on Hydrodynamic Testing of Marine Renewable Energy Devices should be followed (Day 2014).

Gupta et al (2019) investigate the action of waves and current on blades of a two bladed HATT. The current effect was simulated by towing the model in a 100 m long wave tank. The waves are not modified by the forward velocity and the encounter frequency is considered. The authors find that the waves load can be approximated by the Morrison formula and further analysis will focus on the comparison of the loads and waves phases.

With similar objectives, Martinez et al (2019) investigate the behaviour of a three bladed HATT in a water circulation tank combining current and waves. The advantage of a closed loop water flow is the possible simulation of current and waves during long time periods. Inflow turbulence can be stimulated by grids or obstacles located in the flow before impacting the tidal turbine model. With a proper arrangement of the wave maker, waves can be generated over the current. In this case a real wave-current interaction with modified wave length is possible while only the encounter frequency can be modified in a towing tank. The scaled model used is able to control the rotating speed and the pitch angles of the blade, load measurement sensors are associated. Both regular and irregular sea states are tested. Average thrust and torque are merely influenced by the waves. Variations of thrust and torque are larger when the torque control is activated compared to the speed control situation.

Pinon et al (2019) compare the performance at model scale (~1/30) under turbulent current of three HATT with three different designs including an open-geometry. Two different turbulence intensities, a low value corresponding to the minimum controlled turbulence in the tank and a second one obtained without straighteners, are simulated in the water circulation tank. The turbulence of the current has a small effect on the average loads but a more important one on their fluctuations.

Walker et al (2019) test a scaled model (1/81) in current and waves. The influence of the wave direction, upstream or downstream, is investigated and show that favourable instantaneous addition of current and waves velocities increases the corresponding maximum power.

TATT interactions in current flow are investigated by Provan et al (2019). Current velocities are measured at various places in the water circulation tank close to the turbines and in the wake downstream. Maps of velocity fields details the interaction in two turbines arrangement cases and will be used for CFD validation.

The Tidal Stream Industry Energiser (TIGER https://interregtiger.com/) European project aims at driving collaboration and cost reduction

through tidal turbine installations. A total of six tests sites in France and UK is involved. Among the technology fields of interest for the tidal structures are steel manufacturing, composite blades, anti-fouling and anti-corrosion, reliability of tidal turbines. The effect of the growth of fooling primarily is rarely analysed in tank testing, it modifies the hydrodynamics diameters of the support structures and may increase the resulting current and waves loads. It also modifies the performance of the blades but it is expected that the rotating blades experience less marine growth at distances large enough from the hub. The TIGER website disseminates many articles, some of them, or related ones, can be found in the references of this committee report.

Starzmann et al (2019) report their experiences at full and model scale of the SCHOTTEL Instream turbines. Tests were designed and the measurement were analysed according to the ITTC and IEC recommendations. Two diameters, 4 and 6.3 m, are part of the full scale testing, while 1/8 and 1/12.6 scaling is obtained with a single reduced scale model with a 0.5 m diameter. Full scale trials happen in two different sites with different turbulence intensities, about 10 % for the 6.3 m diameter and close to 30% for the 4 m diameter. Some Reynolds effects are detected due to the different diameters and flow velocities, but, globally, the Blade Element Momentum prediction is close to the experimental data.

Frost et al (2017) analysed field measurements and laboratory measurements with the same 1.5 m diameter turbine.

Measurement of hydrodynamic loads on a full scale tidal current turbine generally needs to incorporate numerous strain gauges in the support structure or directly into the blades. An alternative method is proposed by Li et al (2020). The dynamic equations of a system consisting on a floating body supporting an HATT is used to relate the external forces to the floater motions. The mooring system is carefully described, he hydrodynamic parameters of the floater are computed. The current speed is measured by an Acoustic Doppler Current Meter and the rotor rotating speed is measured by an encoder. A group of sensors is used to measure the floating body motion and computation of its velocity and acceleration components. As far as the structural inertia of the system is known, the external loads on the turbine are the last unknowns and can be deduce from the dynamic equation. This indirect method looks promising to evaluate the mean forces and torques applied by the turbine on the floating body but need further analysis to evaluate its ability to detect the fatigue parameters and discard noise from relevant information.

5.4 Ocean turbines

As opposed to tidal current which flows in opposite directions, ocean current basically flows in one direction. Also, the flow velocity of ocean current is more steady than that for tidal current, for which the flow velocity changes alternatively. Thus, it is expected that ocean current turbines should arrive at higher capacity factor than tidal current turbines. However, ocean current dominates at deeper waters than for tidal current. Thus, a floating-type ocean current turbine system will be promising rather than a bottom-fixed type, although bottom-fixed turbines are main stream for tidal current turbines.

Dodo et al. (2021) described development and design of a floating-type ocean current turbine system and at-sea demonstration test (see Figure 1). The Kuroshio Current which flows through southern part of Japan is one of the strongest ocean currents in the world. To utilize this plentiful energy, they developed the floating-type ocean current turbine system “Kairyu” under the government funding of NEDO (New Energy and Industrial Technology Development Organization). They completed the 100 kW class turbine demonstration test in the Kuroshio Current. They reported design methodologies and the results of the at-sea demonstration test. In particular, they focused on the structural design to enable stable floatation in water, the control of weight distribution and the center of floatation, and the pressure-resistant design of the shell structure to secure water-tightness in the deep sea.

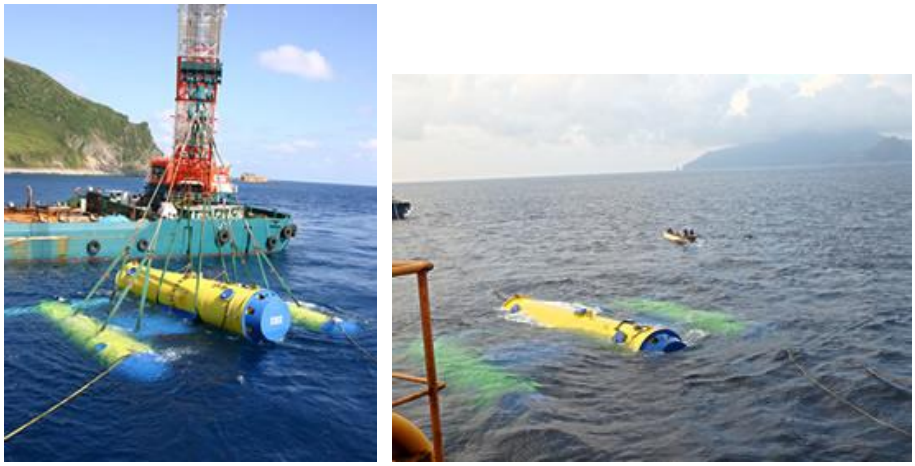

Figure 1: The preparation work for the demonstration test of the ocean current turbine “Kairyu” near Kuchinoshima Island (IHI and NEDO, 2017).

For assessing ocean current characteristics at the demonstration test site of Kuchinoshima Island, Imamura et al. (2018, 2019) made field measurements of ocean current at the site. They used Acoustic Doppler Current Profiler (ADCP) and Acoustic Doppler Velocimeter (ADV) for measuring velocities in ocean environments. Power Spectral Density (PSD) of the current speed, turbulence intensity and its profile in the vertical direction, and spatial and temporal structures of the turbulence were discussed. Further, comparison of numerical simulations and field measurements have been made in Imamura et al. (2018), and basically good agreement was observed.

For the above-mentioned 100 kW system, the rotor diameter was about 11 m. When such a system is scaled-up to 1 MW, the rotor diameter is expected to become 40 m. Thus, Yahagi and Takagi (2019) considered moment loads acting on a blade of an ocean current turbine. They focused on the effect of shear flow on an ocean current turbine, and highlighted the periodic fluctuation of moment loads at the blade root induced by the shear flow. Shear flow experiments in a circulating water channel were made, and the comparison with numerical

computation were conducted. Through the comparison, it has been concluded that the moment loads are well estimated by the present CFD method.

Sato et al. (2021) showed control of a Twin-Turbine Submerged Floating System (TTSFS) with Model Predictive Control (MPC). In a turbulent ocean current flow, the TTSFS is perturbed and the output power fluctuates. Thus, they aimed to show the possibility to mitigate motions of the TTSFS and the fluctuations of the output power simultaneously in turbulent flow, using blade pitch control and torque control of the generator. Based on the simulation results, it was concluded that motion control is necessary to prevent large asymmetric motion which may affect the integrity of the mooring system.

5.5 Design rules and standards

General standards and other guidelines related to offshore structures from American Bureau of Shipping (ABS), Bureau Veritas (BV), DNVGL and Lloyd's Register (LR) can be used: ABS documents 1001, BV documents NR445, DNVGL document RU-OU-0102, LR Regulations for the Classification of Offshore Units.

Several specific rules help the development of novel concepts or are dedicated to tidal turbines: ABS document 116, BV documents NI631 and NI603, DNVGL documents OTG-19 and SE-163.

Additional rules are very useful for the design of mooring with a focus on textile mooring lines: ABS documents 292 and 90, BV documents NR493 and NI432, DNVGL documents OS-E301 and OS-E303.

Bureau Veritas (NI603) gives specific guidelines for current and tidal turbines including tables of lift and drag coefficients for several particular blade profiles.

The International Electrotechnical Commission (IEC) provides a wide range of technical guidelines including current energy converters.

IEA-OES reports contain relevant recommendations for the development of Tidal devices.

Germain et al (2017) introduce the Interreg 2 Seas Met-Certified project which will proceed to four experimental campaigns in laboratory according to the IEC 62600-202 testing procedures. The four devices tested in laboratory tanks are a Horizontal Axis Tidal Turbine (HATT), a Vertical Axis Tidal Turbine (VATT), a Floating Tidal Energy Converter (FTEC) and an Undulating membrane. The first tests result at Ifremer water-circulation flume tank deals with the HATT able to reach TRL5-6 because of the ability of the model to simulate blade pitching and individual measurement of blade loads, keeping in mind the influence of the Reynolds scaling and other bias that may occur.

Frost et al (2017) describe the comparison of tests in Strangford Narrows and tests at CNR-INSEAN towing tank, according to IEC 62600-202 procedures. The main difference is the incoming flow on the tested 1.5m diameter tidal turbine rotor: a natural incident flow in the tidal tests site and a flow simulated by a carriage velocity in the laboratory. The power and thrust coefficients measured in Strangford were lower than the values measured in the towing tank. The turbulence parameters and signal noise need a particular attention.

Sutherland et al (2017) did flow measurements to characterise the Orkney tidal site in accordance with the same IEC 62600-202 document. Schaap et al (2019) report about the work of the IEC Technical Committee TC114. This includes references to the EMEC standards and guidelines. Scheijgrond et al (2019) report about the interaction between the Met-Certified project and the IEC activities.

6. OTHER OFFSHORE RENEWABLE ENERGY TECHNOLOGIES AND HYBRID SOLUTIONS

6.1 Other offshore renewable energy technologies

In this section 6, other offshore renewable energy technologies and hybrid solutions are reviewed. In particular, hybrid solutions are discussed in 6.2 and Ocean Thermal Energy Conversion (OTEC) in 6.3. As technologies other than hybrid solutions and OTEC, floating solar technologies are briefly introduced here.

Cazzaniga et al. (2018) performed the analysis of the performance of photovoltaic (PV) installations mounted on a floating platform. They presented and discussed different design solutions for increasing the efficiency and cost effectiveness of floating photovoltaic (FPV) plants. Ranjbaran et al. (2019) made a review on floating photovoltaic power generation units. In this paper, an analytical analysis and updated review that studies different aspects of FPV systems as a power generation system is presented. Also, a comparison between the ground mounted and floating PV systems is presented and the gaps of the reviewed subjects are indicated. Oliveira-Pinto and Stokkermans (2020) presented a brief state-of-the-art review of the FPV sector and the background that supported the selection of the sites and technologies further described in their paper as case studies. The economic feasibility of the selected FPV technologies and of the in-land reference systems was also analyzed.

With the rapid expansion of the market for floating solar photovoltaic (FPV) systems, DNV GL (2021) has recently issued the recommended practice on design, development and operation of floating solar photovoltaic systems. The RP focuses on FPV systems located in sheltered, in-land water bodies, while still being applicable for near-shore locations. A near-shore water body is intended as any water body, with salty, brackish or fresh water, geographically located close to a shoreline, in reasonably sheltered areas and with significant wave heights up to 2-3 m. However, any offshore location, or location with harsher conditions, is considered explicitly out of scope of the RP.

6.2 Hybrid solutions

In recent years, some research and development activities have been focused on offshore multi-use platforms (to generate renewable energy together with other applications) as well as combined renewable energy systems. In this case, the CAPEX (Capital Expenditures) and OPEX (Operating Expenses) are shared between all the sub-systems incorporated in the platform that can cause reductions in energy production costs and boost the application and commercialization process of offshore renewable energy technologies.

6.2.1 WEC systems combined with floating breakwaters

Floating breakwaters are typically used in areas with high water depth as an alternative option for conventional breakwaters to protect coastal areas from waves. However, they can only protect sheltered areas from the waves in a limited range of wave frequencies, which is one of their prominent drawbacks. In this case, employing a Wave Energy Converter (WEC) system into the structure of the floating breakwater can improve its effectiveness in terms of protecting the sheltered area and simultaneously generate clean energy. The performance of floating breakwater device to attenuate the waves is expected to be increased in this case, as some portion of the energy of waves is captured by the WEC system in addition to the reflection and dissipation mechanisms (to not allow waves passing through the device). On the other hand, the renewable energy production cost by the WEC system is expected to be reduced due to sharing construction and operational costs with the floating breakwater device.

In this context, Howe et al. (2020b) investigated the performance of a π-type floating breakwater integrated with multiple Oscillating Water Column (OWC) WECs through model scale hydrodynamic experimentation. The wave energy extraction characteristics of the installed devices are explored across parameters including device configurations, breakwater width,

power take-off damping, wave height and motion constraints. The major findings indicate that OWC device spacing is a key parameter in the design of multi-device structures, as device-device interaction can have constructive or destructive interferences on the energy extraction (Howe et al., 2020a). Rezanejad and Guedes Soares (2021) introduced a new concept of dual chamber floating OWC device that can simultaneously be used as floating breakwater. They performed numerical simulations to estimate the transmission coefficient of waves passing through the device and compared the obtained results with the corresponding values for the typical box-type floating breakwater device with equivalent physical characteristics (width, moment of inertia, etc.). They concluded that the dual chamber floating OWC system has inherently higher performance compared to the conventional box-type floating breakwater in terms of protecting the sheltered area from waves.

6.2.2 Floating wind turbines combined with WECs

Simultaneous renewable energy production using both wind and wave energy resources on a unified platform is a topic that some research studies have been focused on in recent years. Two different types of WEC devices are typically used with floating wind turbines to generate renewable energy: (1) Oscillating Water Column devices (2) Heave type point absorbers (called Torus type WEC device is some research studies in the literature).

Perez-Collazo et al. (2018a) and Perez-Collazo et al. (2019) introduced a novel hybrid system that integrates an OWC wave energy converter with an offshore wind turbine on a monopile substructure. They performed an experimental investigation to characterise the hydrodynamic response of the WEC sub-system under regular and irregular waves. They also investigated the hydrodynamic response of the WEC sub-system in a similar hybrid wind-wave system on a jacket-frame substructure (Perez-Collazo et al., 2018b). Sarmiento et al. (2019) introduced a new floating semi-submersible structure which combines wave energy converters (3 Oscillating Water Columns) and wind harvesting (5MW wind turbine). The multi-use platform was characterized under the incidence of regular wave tests (with and without wind), operational sea states and survival sea states (combining waves, currents and wind) and the corresponding experimental data such as natural periods, movements and loads on the mooring system are presented. Elginoz and Bas (2017) carried out life cycle assessment of a combined wind and wave energy production platform. Cheng et al. (2019) studied several combined concepts of floating horizontal axis wind turbines (HAWTs) with a WEC system. By also studying the floating vertical axis wind turbines (VAWTs), they concluded that VAWTs have a good potential for cost-of-energy reduction compared to floating HAWTs.

Wan et al. (2017) proposed a combined wind and wave energy converter concept which is composed of a 5 MW spar floating wind turbine and a torus-shaped WEC device. They performed numerical and experimental studies on the proposed concept in the both operational and survival modes. Ren et al. (2018) undertake investigations on a monopile type wind turbine and a heave-type wave energy converter. Hydrodynamic responses of the devised system under typical operational seas cases have been investigated by using both time domain numerical simulations and 1:50 scale model tests. Ren et al. (2020) devised a novel hybrid concept by combining a tension leg platform (TLP) type floating wind turbine and a heave-type wave energy converter. Dynamic responses of the system under operational seas cases (in South China Sea) have been studied by implementing both the numerical (time-domain simulation) and experimental (1:50 scale model tests) approaches. O'Kelly-Lynch et al. (2020) reviewed normative design methodologies and presented a simplified concept to assess the structural steel design implications of incorporating a point absorber wave energy device to a monopile for selected sites off the East and West coasts of Ireland. Their research work provides a review-driven methodology as a tool to obtain an initial design-based estimate of LCOE (Levelized Cost Of Energy) comparisons for similar devices and allows making robust decisions on development or choice of devices for a particular location.

6.2.3 WEC devices with other renewable energy producing systems

The use of energy from the sea wave to produce electricity via wave converters is one of the most interesting methods to meet the electrical demand in coastal cities. Hybridization of wave energy with other renewable resources, such as solar, wind, or tidal currents, is a reliable way to generate and provide electricity for remote cities (Jahangir et al., 2020). In this regard, Jahangir et al. (2020) carried out a techno-economic and environmental analysis for a hybrid renewable energy system consisting of Wave Energy Converter/PV/Wind Turbine/Battery aiming to provide electricity for 3000 households in three different locations of Iran (including the Persian Gulf, the Gulf of Oman, and the Caspian Sea). Talaat et al. (2019) presented dynamic modeling and control of a PV/Wind/Wave energy hybrid system. Experimental test-bed is established for these three different types of renewable energies to study how to integrate them and unify their energy production. Li et al. (2018) studied the hydro-aero-mooring coupled dynamic analysis of a new offshore floating renewable energy system, which integrates an offshore floating wind turbine, a wave energy converter and tidal turbines. Simulation results show that the combined concept achieves a synergy between the floating wind turbine, the wave energy converter and the tidal turbines. Compared with a single floating wind turbine, the combined concept undertakes reduced surge and pitch motions. The overall power production increases by approximately 22%-45% depending on the environmental conditions.

6.3 OTEC

Ocean Thermal Energy Conversion (OTEC) is a process of harvesting energy from the ocean by utilizing the temperature difference between surface warm water and deep cold water. A brief review of OTEC including latest 1-MW OTEC demonstration test is shown in OES (2021). Figure 1 shows the 1-MW sized OTEC plant on the barge (South Korea's "K-OTEC1000") with the riser (Seo and Kim, 2021). The 1-MW OTEC barge plant was designed as a temporary test facility for the heat exchangers and turbine. This floating test was to check the performance of the process equipment prior to its transportation to Kiribati in the Central Pacific Ocean for a land-based project, which is still planned to be undertaken, but has been delayed (OES, 2021).

For upscaling a floating OTEC plant toward its commercialization, ship conversion similar to a Floating Production Storage and Offloading (FPSO) vessel can be a potential solution. Kibbee (2013) presented an overview of internal R&D that SBM has carried out on OTEC during 2011 and 2012. They have worked to develop a Cold Water Pipe (CWP) design for a 10 MW plant that can be manufactured, installed, and operated with available technology. Analysis of the 4-meter diameter fiberglass reinforced plastic CWP showed manageable stress and angle response to the environment. The CWP system included a sealed gimbal device at the interface of the ship and CWP. They identified that this specialized ship - CWP interface device must be developed to enable the operation of a ship in OTEC service, just as a high-pressure fluid swivel had to be developed to enable operation of a weathervaning ship in FPSO service. Song (2018) considered an alternative solution involving the application of OTEC power generation system for designing an FPSO vessel to be installed in a deep-sea area. The closed-, open-, and hybrid-cycle OTEC systems were simulated under the same conditions, for comparison purposes. It was confirmed that the closed cycle is the most effective cycle for producing electricity, and that the open cycle is an alternative option for facilities that are required to produce both electricity and fresh water. It was also suggested that an FPSO be converted to an OTEC plant at the end of the life cycle of an oil field, based on the simulation results of a 100 MW OTEC plant. Adiputra et al. (2020) considered preliminary design of a 100 MW-net OTEC power plant to be from an oil tanker ship conversion. The process of designing 100 MW-net OTEC power plant yielded results implying that Suezmax oil tanker type is sufficient to be the plantship.

Figure 1: The 1-MW OTEC plant on the barge with the riser (Seo and Kim, 2019).

The Cold Water Pipe (CWP) still remains as a key technical challenge since a commercial scale OTEC plant requires a pipe diameter of about 10 m and a length of 1,000 m to pump about half the average discharge of the Colorado River from the deep ocean to the surface and through heat exchangers (Halkyard et al., 2014). Thus, the United States (U.S.) Department of Energy (DoE) and Lockheed Martin sponsored a 1:50 scale wave basin model test of a commercial OTEC platform with an elastically scaled model of a 10 m pipe. The purpose of the test was to validate the use of current software for the large CWP diameters in the designs of pilot or commercial systems in the near future. Halkayard et al. (2014) briefly reviewed past work on the OTEC cold-water pipe and presented the current state of the art in numerical modeling and the results of the model tests. Overall, the results supported the numerical methods being used and the current design practices appear to be valid. However, these tests did not address all of the issues of CWP responses, e.g. the effect of current and waves, the issue of vortex induced responses and the effect of flow internal to the pipe.

The large amount of mass of internal flow in CWP may trigger instability which leads to the failure of CWP. Adiputra and Utsunomiya (2019) thus aimed to design commercial-scale OTEC CWP focusing on the effects of internal flow to the stability of the pipe. The design analysis was deliberated to select the pipe material, top joint configuration (fixed, flexible, pinned) and bottom supporting system (with and without clump weight). Separately, a fully coupled fluid-structure interaction analysis between the pipe and the ambient fluid was carried out using ANSYS interface. Adiputra and Utsunomiya (2021) further examined analytical and numerical analyses on self-induced vibration of OTEC CWP for a 100 MW-net OTEC power plant. The stability was assessed by discretizing the equations using Frobenius method and Galerkin method and then plotting its eigenfrequencies or its eigenvalues in an Argand diagram. Results indicated that the predicted critical velocity in the time domain was averagely 20% higher compared to the frequency domain. Also, the effect of the clump weight on the critical velocity was more significant for light material compared with relatively high-density material.

Hirao et al. (2021) presented the results of model tests and numerical simulations of a spar type floating OTEC with a single CWP in waves and currents with/without internal flow. The CWP model was made of material fitting the scaling law for a planned full scale OTEC. The effect of the internal flowing water was observed for the bending moment at the connecting point of the CWP and floater. On the other hand, the floater motions were not affected by the CWP internal flow. Hisamatsu and Utsunomiya (2021) aimed to formulate the coupled system of an OTEC floating plant and simplify the formula to clarify the characteristic of the coupled behavior.

They verified the formula for a 100 MW OTEC plantship and compared the results by OrcaFlex time domain simulation.

Bureau Veritas (2018) have issued tentative rules for classification and certification of Ocean Thermal Energy Converter (OTEC). General guidance for design and analysis of an Ocean Thermal Energy Conversion (OTEC) is also available as technical specification (IEC, 2019).

7. LIFE-CYCLE COST AND OPERATIONAL MANAGEMENT OF OFFSHORE RENEWABLE ENERGY

7.1 General aspects

Text

7.2 Current status and potential for cost reduction

Text

7.3 Cost models and analysis tools

Text

Offshore wind turbine

The most advanced ocean technology is offshore wind turbines (OWT) can be stand out: fixed on the seabed and floating platforms. The offshore wind industry is expected to experience a considerable increase in the coming future to meet the decarbonisation aim in 2050[1]. The total capacity of installed OWT was about 18 GW in Europe in 2018, and the United Kingdom made the most significant contribution with 42% of all installations in megawatts, followed by Germany (31%), Netherlands (6%), Denmark (7%)and Belgium (9%) [2]. The largest owners of offshore wind farms are including Ørsted (17%), RWE Renewables (10%), Vattenfall (6%), and Macquarie Capital (6%) [2]. The annual installed offshore wind energy capacity increased in 2019, and its estimation increases 30 GW by 2030 shown in Fig. 1, with a compound annual growth rate of 18.6% for the first half and 8.2% for the rest of the period. The motivation for offshore development can be a highly available area to harvest wind energy, stronger and more uniform wind speed with less turbulence, and limited visual and sound impact [3].

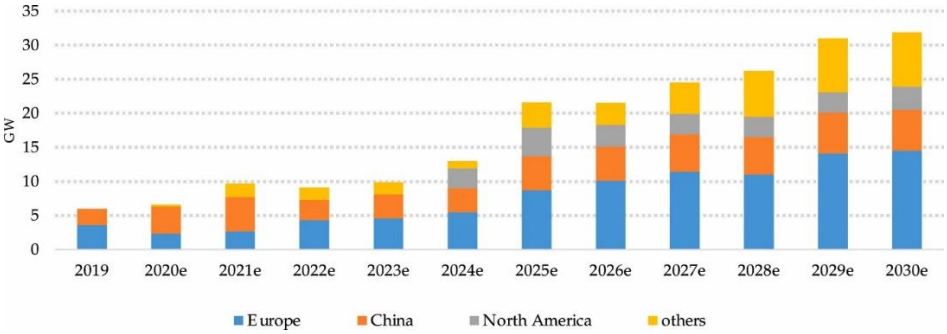

Fig. 1. New annual installation prediction until 2030[2]

According to the WindEurope report, Europe had a total installed offshore wind capacity of 25 GW until the end of 2020. It is involved 5,402 grid-connected wind turbines across 12 countries shown Fig. 2.

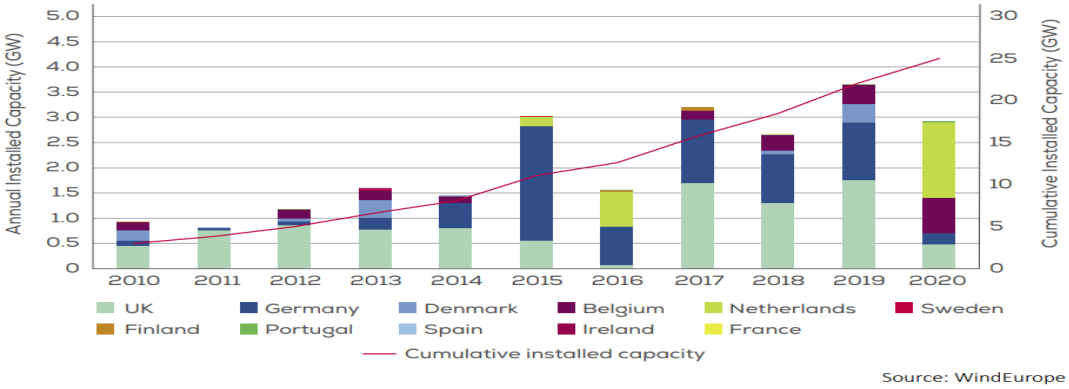

Fig. 2 Annual offshore wind installations by country and cumulative capacity

There is an increase in the average size of wind farms installed 788 MW in 2020 compared to 26% larger than last year. The average rated capacity of installed turbines in 2020 was 8.2 MW; the average size of wind farms was 788 MW, 26% larger than the previous year. The current OWT development situation can be restricted by the lack of uncertainty analysis for offshore wind economic studies and the challenges of accurately estimating levelized cost of energy. The life cycle cost regarding offshore wind projects' feasibility was studied based on various geographic locations[4]. A significant difference among LCOE values was observed in European countries (€ 100/MWh) concerning projects of Denmark and Sweden (€ 150/MWh to € 220/MWh) . This confirms the influence of national policy frameworks on offshore wind energy. The return of offshore wind farms investment in the United Kingdom is considered in[5]. It proposed the five different phases of the life cycle cost regarding offshore wind projects shown in fig. 3. The P&A and the O&M costs share 46% and 30%[5]. [6] proposed a techno-economic optimization scheme for OWFs based on LCA to support investment decisions, find the best investment solution, and increase confidence.

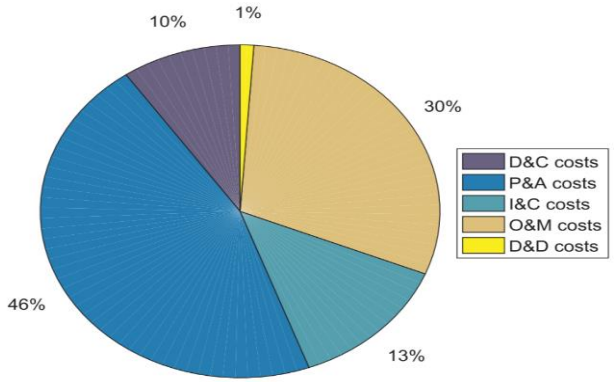

Fig. 3 five different phases of the life cycle cost regarding offshore wind projects

the cost evolution of offshore wind energy is proposed based on analyzing 46 operational offshore wind farms commissioned after 2000. The increasing CAPEX depends on these two parameters, including Water depth and distance to shore. It is necessary to provide proper research in the early stage of the project to minimize investment risk. In addition, Private investors need appropriate tools to evaluate their investment decisions.

The floating wind structures provide access to deeper waters. 11 floating offshore wind energy farm has been installed in the world with total 79 of capacity. The number of projects installed in Europe is 5 with 59 MW, and Asia is six with 20 MW.in addition, 15 projects represent approximately 293 MW that is currently under construction or have achieved either financial close or regulatory approval[6]–[8].

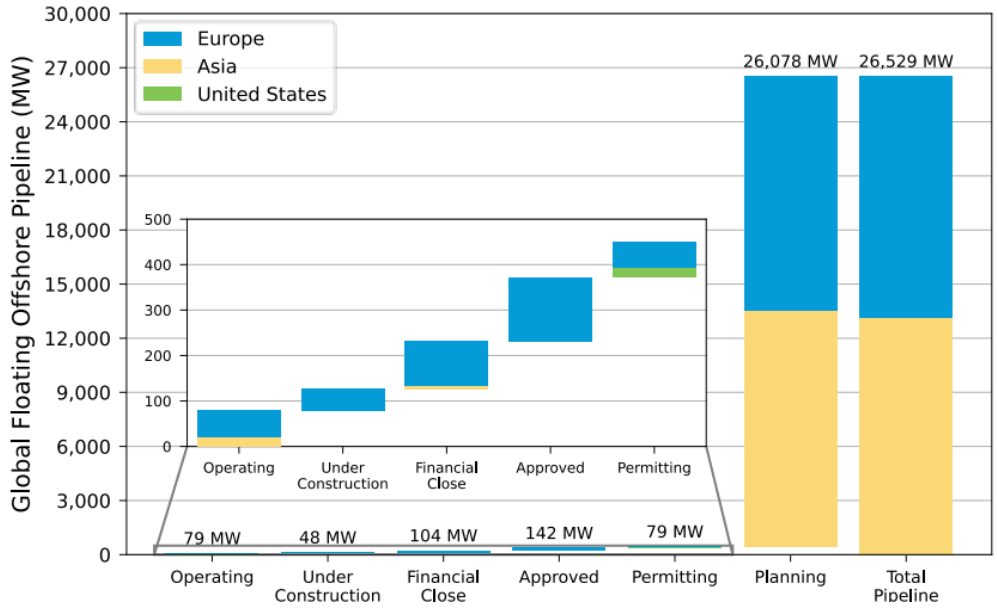

Fig. 4 Global floating offshore wind energy

floating offshore wind energy increased 18,866 MW globally in 2020 relative to the 2019 Offshore Wind Technology report, as shown in Fig. 4.

Floating offshore increased the variety of locations. Recently, there has been massive improvement regarding the technical aspects of floating offshore wind, which allows more accessibility to deep water. Technology development plays a crucial role regarding the cost reduction of energy production. However, It is essential to characterize the possible variables which could minimize the life-cycle costs of a floating offshore wind farm. Those groups include wind turbines, floating platforms, mooring, anchoring, seabed, electric system, installation, shipyard, and maintenance[7], [8]. The platform model selected, including TLP (Tensioned Leg Platform), spar, or semisubmersible, plays a crucial role in the installation method and the economic assessment. It is necessary to consider other aspects such as mooring material, mooring disposition, and anchor, which should be based on the geographic location (depth and distance to shore, mainly). Indeed, the floating offshore wind farm should be decommissioned when its lifespan is finished. Economic aspects of floating offshore wind farms have not been considered well because of a lack of experience regarding their operation at the moment. However, it is one of the most critical aspects for investors. The type of floating platform plays a vital role in optimizing the life-cycle cost. A case study in [9] determined the minimum and maximum value of floating offshore wind farm.The minimum value of the total life-cycle cost modified from 348 M€ to 949 M€ for the semisubmersible platform (Fig. 5a), from 444 M€ to 1071 M€ for the TLP platform (Fig. 5b) and from 370 M€ to 929 M€ for the spar platform (Fig. 5c) (Castro-Santos, 2013b).

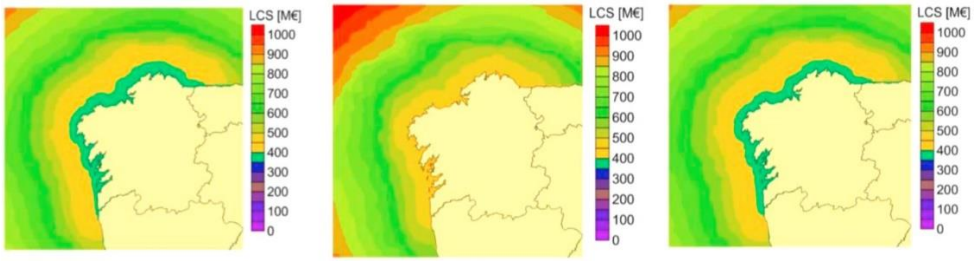

Fig. 5. Minimum life-cycle cost of a floating offshore wind farm using a semi-submersible platform (a), a TLP platform (b), and a spar platform (c).

The maximum value range of the life-cycle cost of a floating offshore wind farm changed from 606 M€ to 3967 M€ for the semisubmersible platform (Fig. 6a), from 612 M€ to 3894 M€ for the TLP platform (Fig. 6b), and from 605 M€ to 3811 M€ for the spar platform(Fig. 6c), [9]

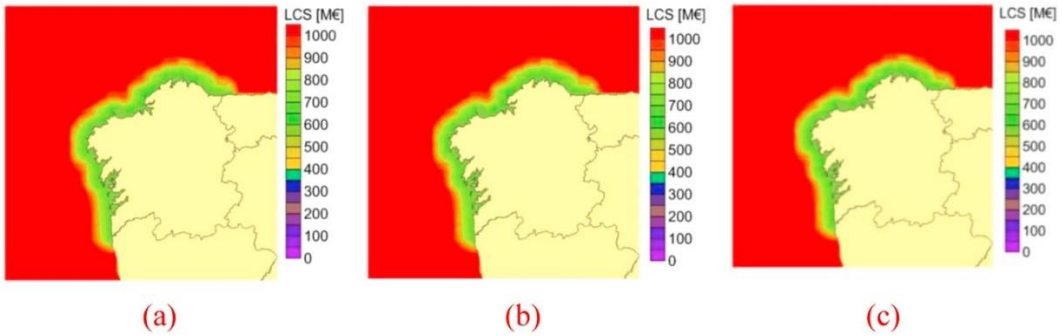

Fig. 6. Maximum life-cycle cost of a floating offshore wind farm using a semisubmersible platform (a), a TLP platform (b) and a spar platform (c).

Wave and tidal energy

There has been a massive deployment regarding Marine renewable energy, including wave and tidal, recently. However, the wave energy industry has not reached its technological maturity, and the cost is known as the main challenge. The harsh marine environment provides a high wave energy density; however, this environment needs novel engineering design and less expensive technologies. Selecting a location with higher energy production can justify the implementation of high technology; however, high installation cost and maintenance remaining the main boundary[10], [11]

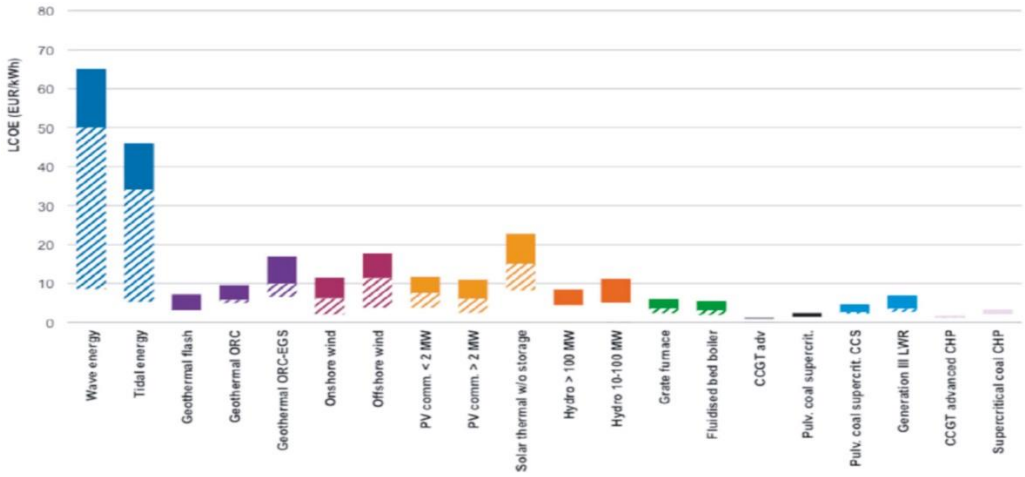

Fig. 7.LCOE for different energy technologies[10], [11]

LCOE for marine wave energy depending on various the location has been investigated in several studies. Current wave energy has much higher LCOE than the other more mature energy sources (e.g., coal, natural gas, and nuclear) or even the offshore floating wind projects. This confirms the need for research to reduce the LCOE of wave energy conversion projects to reach commercial viability [12]–[14].

Most of the existing waves and tidal strategies are at the low level of technology readiness stage in the EU, and providing a high-quality level of tidal and wave energy research is one challenge. The tidal barrage facilities are limited as another challenge by 2017; of the 529 MW of operating ocean energy capacity worldwide, only two barrage facilities provided over 90% [13]

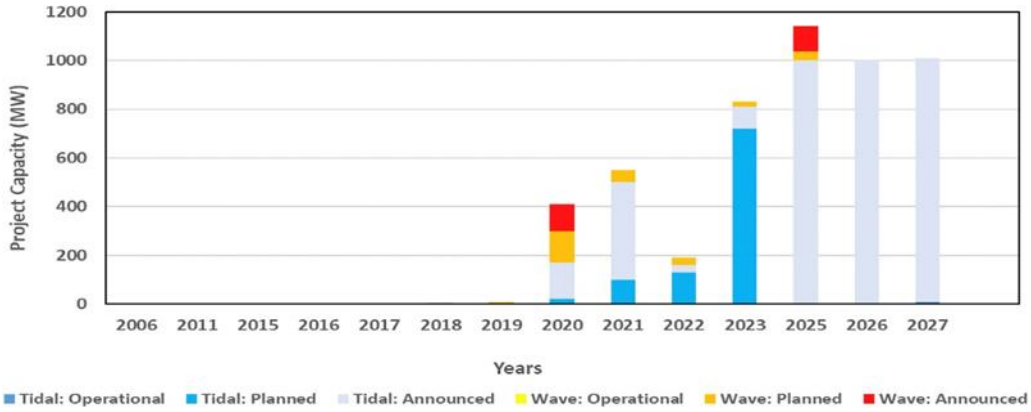

Fig. 8. Tidal and wave energy projects in the EU[12]

The estimation of LCoE for wave and tidal energy includes uncertainties such as the role of different technology types. The lowest value for wave energy is modified from 0.30 €/kWh, and the maximum level can increase by 1.20 €/kWh[12]. 40% of the Levelized cost is attributed to operation and maintenance (O&M), 35% to the initial investment, and 25% to replacement. The limited amount of available data regarding the component's reliability, failure, and downtime makes O&M cost involved the uncertainties and challenging to reduce costs [12]. Wave energy is not yet a competitive option for global energy . one of the solutions for the current situation is related to integrating synergetic technologies both through co-location or hybridization can increase the performance of Wave energy converters (WECs) and increment the expected revenue from the produced electricity, as well as provide cost-sharing opportunities. However, there is concern regarding the system's complexity based on the profitability of the energy production level. Wave energy converter devices can be categorized based on several aspects, including the location of operation, wave condition, and working principle.

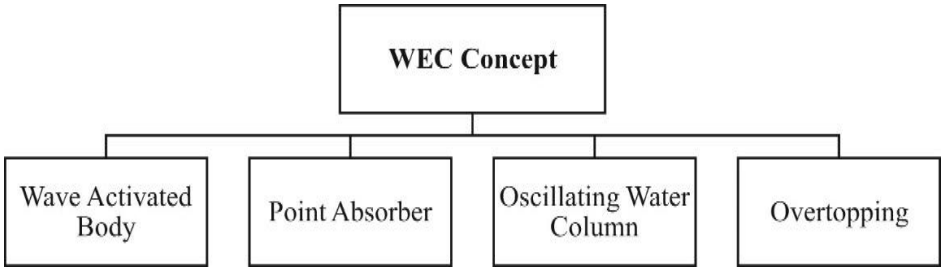

Fig. 9 shows the breakdown of the various WEC

Fig. 9 shows the breakdown of the various WEC being developed all over the world. The most popular device is based on the point absorber concept shown in Fig. 10 [14].

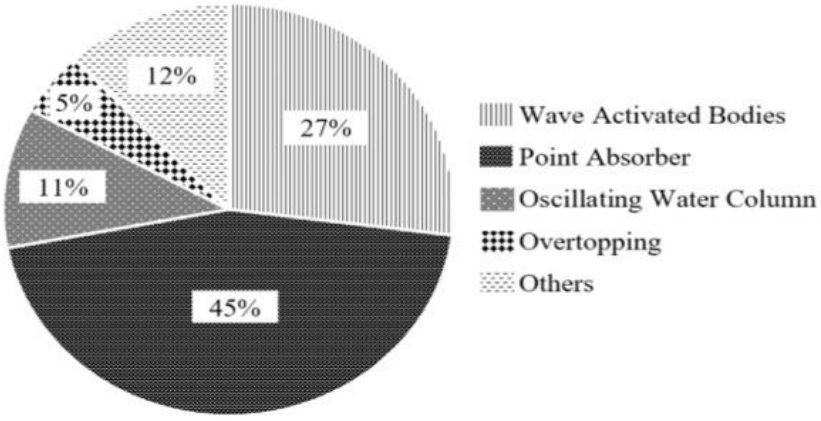

Fig. 10 The percentage of WEC development

There has been significant development regarding tidal energy technology. Tidal projects development in the UK achieved 10 GW installed capacity with an energy yield of around 15 TWh/year[15], [16].

One advantage of tidal energy is the high level of predictability. Since tides can be forecasted accurately, it is possible to calculate both levels and timings of tidal generation with high resolution for long timescales [17]. In addition, tidal power provides high-quality electrical output due to low levels of harmonics. The European Ocean Energy Association predicted 300 MW of tidal stream installed capacity in Europe by 2020, but the number achieved was 10 MW. Global future installation capacity of tidal energy involved uncertainty, and it is necessary to propose the structural plane to avoided missing aim. It is expected to achieve 101 GW tidal energy capacity by 2050[15]–[18].

First-generation tidal devices are based on bottom-mounted installation and classified into horizontal- and vertical-axis technologies. Tidal devices foundation can be classified based on the seabed mounted/gravity base, pile mounted, floating, hydrofoil inducing downforce, which evolves with increasing distance from the shore. There is considerable uncertainty in determining accurate whole life-cycle costs for tidal energy. The lowest and the highest estimated ranges on tidal stream CAPEX and LCOE include 2.25–4.0 £ m/MW and 150–320 £ m/MW [19]. Fig. 11 shows the cost breakdown per MW capacity for tidal stream.

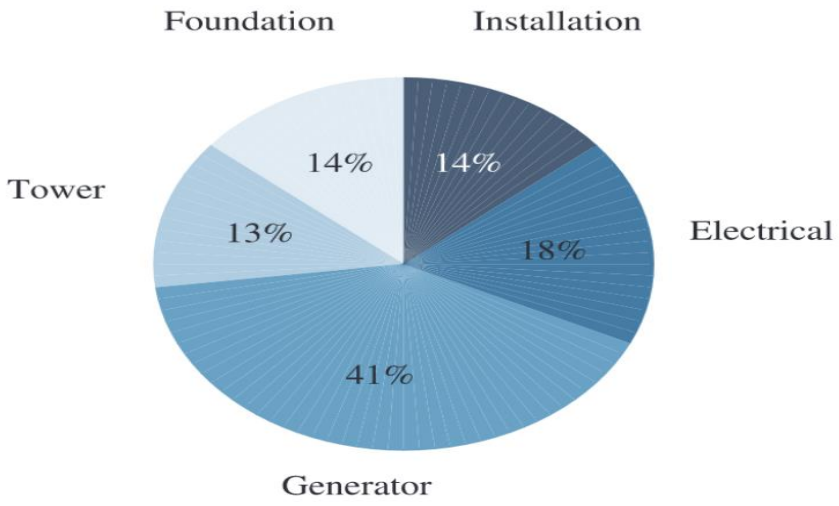

Fig. 11 Cost breakdown per MW capacity for tidal stream [19]

Reduction of $LCOE_{CAPEX}$ 10–12% from tidal stream sites by co-location of offshore wind turbines has been considered in [19]. The deployment of wind turbines mitigates the levelised capital cost of energy compared to a tidal alone; however, This combination increases the complexity of the platform,

This report generally considered the Life-cycle cost and operation of leading offshore renewable energy. The offshore wind turbine, floating types, has the primary role in achieving the decarbonization aim. This research selected those leading offshore renewable energy, including OWT, Wave, and tidal, due to European geographic locations. Lack of innovation and research regarding the combination of marine energy, especially with floating offshore wind turbines, is a critical current research challenge. Any proposal should justify the challenge of the maintenance cost in terms of system complexity and capacity of energy availability.

8. DESIGN FOR FLOATING WIND TURBINES: A BENCHMARK OF THE EXISTING DESIGN GUIDELINES

This benchmark was conceived with the objective of understanding the discrepancy among various classification societies when treating the safety of synthetic fiber mooring lines. Whereas the stated safety factors are in good agreement for chains and other steel-based mooring lines, Tables 1 and 2 list the differences in terms of safety factors for synthetic mooring lines, including both intact and redundant mooring systems. Appreciable differences can thus be found in both calculation procedures and safety margins proposed by classification societies regarding their use in station-keeping systems.

A noticeable example is the case of redundant polyester mooring lines for intact conditions, where the safety factors to be applied to the Minimum Breaking Strength (MBS) are found to vary between 1.05 and 2.5 (Tables 1 and 2). Furthermore, most classification societies are ambiguous when defining statistical fitting methods for retrieving the maximum expected tension when a time-domain analysis is performed, and only some introduce explicit safety factors in the mean, low frequency, and wave frequency load components of the design tension.

Table 1. Safety factors stated by classification societies for intact mooring systems.

Code issuing entity	Reference design code	Intact condition, non-redundant mooring system			
		Return period of environment	Safety factor		
			Steel	Polyester	Other fibres
ABS	Guide for Building and Classing Floating Offshore Wind Turbine Installations	50YRP	2.00	2.25	2.25
BV	NI572 Classification and Certification of Floating Offshore Wind Turbine	50YRP	2.00	2.20	2.40
DNV-GL	ST-0119 Floating wind turbine structures	50YRP	(1.5. Tmean + 2.2. Tdyn) / 0.95 / Tmax		
IEC	61400-3-2 Wind energy generation systems - Design requirements for floating offshore wind turbine	Refers to ABS, BV, DNV-GL			

Table 2. Safety factors stated by classification societies for redundant mooring systems.

Code issuing entity	Reference design code	Intact condition, redundant mooring system			
		Return period of environment	Safety factor		
			Steel	Polyester	Other fibres
ABS	Guide for Building and Classing Floating Offshore Wind Turbine Installations	50YRP	1.67	1.82	1.82
BV	NI572 Classification and Certification of Floating Offshore Wind Turbine	50YRP	1.67	1.84	2.00
Class NK	Guidelines for Offshore Floating Wind Turbines Structures	50YRP	1.67	2.50	2.50
DNV-GL	ST-0119 Floating wind turbine structures	50YRP	(1.3. Tmean + 1.75. Tdyn) / 0.95 / Tmax		
IEC	61400-3-2 Wind energy generation systems - Design requirements for floating offshore wind turbine	50YRP	1.67	1.67	1.67
LR	Guidance Notes for Offshore Wind Farm Project Certification	50YRP	1.67	1.67	2.00

The main function of station-keeping systems in FOWT's is to ensure that the substructure remains within the motion limits, imposed mainly by the dynamic power cable maximum excursion, while avoiding stiff restoring responses that can shift considerably the floating body natural frequencies; and proportionating stability, especially in the case of TLP's. These systems should be designed to withstand extreme, fatigue and accidental limit loads along with their service life, while respecting site-specific constraints such as mooring line footprint, anchor design requirements and so on. Moreover, due to the high coupling between the aerodynamic and hydrodynamic forces acting on a FOWT, time-domain analyses are commonly performed through the design stage, where the station keeping systems are usually modeled using quasi-static formulations, discrete lumped mass, and/or FEM approaches according to the desired accuracy [Life 50+, (Gomez, 2015)].

Aiming to reduce the costs of traditional station-keeping configurations (i.e., steel chain catenary systems), the interest and research on synthetic ropes have increased [Ridge, 2010;

Weller, 2015], while some FOWT's demonstrators have already implemented them [Windfloat, 2015; Floatgen, 2018]. Besides being cheaper, synthetic ropes are lighter, less prone to corrosion and have an outstanding fatigue resistance. However, due to their lower abrasion resistance, hybrid line configurations (i.e., chain-fiber-chain) are often designed to avoid the synthetic segments being in direct contact with any surface (i.e., seabed or floater connection). On the other hand, their mechanical analysis involves additional complexities because of their viscoelastic nature, such as non-linear stiffness, hysteretic behavior (load dependency) and creep.

In this work, a hybrid chain-polyester-chain mooring arrangement is used as a station-keeping system of the Olav Olsen Life 50+ benchmark floater [Life 50+]. Afterward, the utility factors obtained through different classification societies are retrieved and compared, for both intact redundant and non-redundant conditions, while discussing their influence on the system safety, platform motions and accelerations. All the simulations are conducted via the open-source platform OpenFast, adopting the code previously published within the project LIFE 50+ to the proposed hybrid chain-polyester-chain mooring system arrangement. The geometrical parameters of both chain and polyester mooring lines are listed in Table 3. Note that the intact system consists of 3 mooring lines, while the redundant mooring systems includes 6 mooring lines. Within the study, the environmental conditions correspond to an extreme scenario, whose wind, wave, and current parameters are stated in Table 4.

Table 3: Geometrical parameters of the studied mooring system.

Mooring radius	800 m
Chains: diameter	0.246 m
Chains: unstretched length (top; bottom)	50 m; 120m
Polyester lines: diameter	0.178 m
Polyester lines: unstretched length	566 m
Polyester lines: equivalent stiffness	34.5 MN
Polyester lines: maximum breaking load (kN)	8.83 MN
Pre-tension	500 kN

Table 4: Environmental conditions – extreme load design case.

Significant wave height	18 m
Peak-spectral period	13 s
Wind conditions	50 m/s at 100 m
Current conditions	1.5 m/s

The results of the benchmark analysis are showcased in Fig. 1, representing the mooring line tension over 3 hours, and considering 10 different random seeds. The limits imposed by classification societies and the corresponding most probable maximum tension (DNV, 2015) are also added into Fig.1, clearly reflecting the discrepancies among the examined safety standards. Whereas the tested intact mooring system does not comply with ABS and BV, DNV standards lead to a significant safety margin. Interestingly, the mooring system still does not comply with NK regulation, for the redundant studied mooring system, which consists of 6 mooring lines with the same properties and pretension as the intact case. The results verify the lack of agreement among the existing guidelines and demands for further investigations that will

hopefully lead to a consensus and perhaps less conservatisms, in terms of synthetic mooring lines safety considerations.

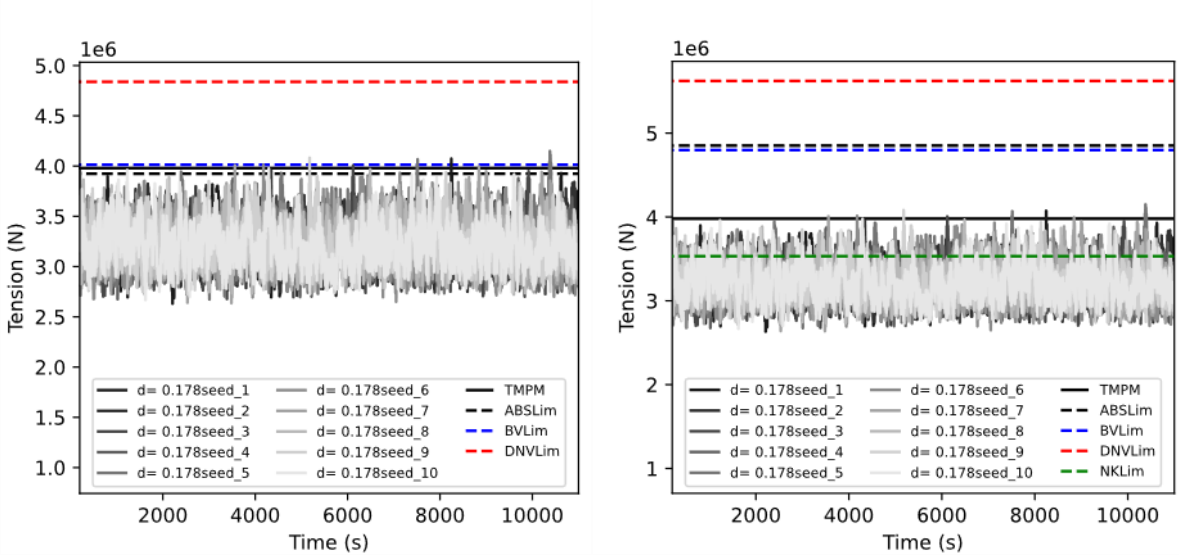

Figure 1: Time-domain OpenFast simulation for both intact (left) and redundant mooring (right) systems. The mooring line tension, from 10 random seeds, is represented over time. Safety limits imposed by various standards and the corresponding most probable maximum tension are also included in the figure as dashed and continuous lines, respectively.

9. MAIN CONCLUSIONS AND RECOMMENDATIONS FOR FUTURE WORK

To be added in the end.

10. REFERENCES

Det Norske Veritas (DNV), 2017. Energy Transition Outlook | DNV [WWW Document]. URL https://eto.dnv.com/2017/ (accessed 10.20.21).

International Renewable Energy Agency (IRENA), 2019. 2019a) Future of Wind: Deployment, investment, technology, grid integration and socio-economic aspects, International Renewable Energy Agency (IRENA).

Komusanac, I., Brindley, G., Fraile, D., Ramirez, L., 2021. Wind energy in Europe: 2020 Statistics and the outlook for 2021-2025 1–36.

Lee, J., Zhao, F., 2021. Global Wind Report 2021. Glob. Wind Energy Counc. 75.

Mathern, A., von der Haar, C., Marx, S., 2021. Concrete support structures for offshore wind turbines: Current status, challenges, and future trends. Energies. https://doi.org/10.3390/en14071995

WindEurope, 2021. Offshore wind in Europe – key trends and statistics 2020 | WindEurope [WWW Document]. URL https://windeurope.org/intelligence-platform/product/offshore-wind-in-europe-key-trends-and-statistics-2020/ (accessed 10.27.21).

4C Offshore, Global Offshore Wind Farms Database Database – Information & Intelligence, (2019). https://www.4coffshore.com/windfarms/.

JDN, JDN Annual Report, 2017. https://www.jandenul.com/sites/default/files/annual-report/attachments/Annual_Report_2017.pdf.

Nobelwind - DETAILS, (n.d.). http://www.nobelwind.eu/#details.

M. Vieira, B. Snyder, E. Henriques, L. Reis, European offshore wind capital cost trends up to 2020, Energy Policy. 129 (2019) 1364–1371. doi:10.1016/j.enpol.2019.03.036.

D. Kallehave, B.W. Byrne, C. LeBlanc Thilsted, K.K. Mikkelsen, Optimization of monopiles for offshore wind turbines, Philos. Trans. R. Soc. A Math. Phys. Eng. Sci. 373 (2015). doi:10.1098/rsta.2014.0100.

O.B. Leite, REVIEW OF DESIGN PROCEDURES FOR MONOPILE OFFSHORE WIND STRUCTURES, Thesis of Master in Science, University of Porto Department of Civil Engineering, 2015.

Gode Wind 1+2 - 97 XL offshore foundations, (2016). https://www.bladt.dk/UserFiles/05_Downloads/Foundations/Gode_Wind_12_Blaa_bjaelke_Low.pdf.

AMBAU produces 18 monopiles and transition pieces for the Nordergründe Wind Farm, (2015). http://ambau.com/uploads/media/AMBAU_PI_002-2015_Nordergruende_en_01.pdf.

A.G. Gonzalez-Rodriguez, Review of offshore wind farm cost components, Energy Sustain. Dev. 37 (2017) 10–19. doi:10.1016/j.esd.2016.12.001.

OFFSHORE WIND FARM SANDBANK, (2016). https://www.menck.com/news/11-news/179-offshore-wind-farm-sandbank.

EEW SPC produces 1st giant monopile for 402-MW Veja Mate wind park, SeeNews Renewables. (2016). https://www.emis.com/php/search/doc?dcid=521022710&ebsco=1?

Veja Mate Offshore Project GmbHAbout Us, (2019). http://www.vejamate.net/#aboutus.

P. Passon, K. Branner, S.E. Larsen, J. Hvenekær Rasmussen, Offshore Wind Turbine Foundation Design - Selected Topics from the Perspective of a Foundation Designer, Thesis in Doctor of Philosophy, Technical University of Denmark Department of Wind Energy, 2015.

S. Bhattacharya, Design of Foundations for Offshore Wind Turbines, Wiley, 2019.

Investor Presentation, (2015). http://northlandpower.com/cmsAssets/docs/pdfs/Investor Presentation/NorthlandInvestorPresentation_October.pdf.

DILLINGER, STEEL IS THE VITAL INGREDIENT - Solutions in Steel for Offshore Wind Energy Installations, (n.d.). https://www.dillinger.de/d/downloads/download/5995.

Dudgeon Offshore Wind Farm - Power Technology | Energy News and Market Analysis, (n.d.). https://www.power-technology.com/projects/dudgeon-offshore-wind-farm/#targetText=Each turbine has a rotor,weighing between 800t-1%2C200t.

Year ends on a high for Galloper as foundation construction starts, (2017). http://www.galloperwindfarm.com/year-ends-on-a-high-for-galloper-as-foundation-construction-starts/.

Facts & Figures, (n.d.). http://www.galloperwindfarm.com/about/#facts-figures.

Race Bank Offshore Wind Farm foundation T&I and scour protection, (n.d.). https://www.deme-group.com/geosea/references/race-bank-offshore-wind-farm-foundation-ti-and-scour-protection.

Steel monopile foundations | Rampion Offshore Wind, (n.d.). https://www.rampionoffshore.com/wind-farm/components/foundations/.

The south coast's first offshore wind farm | Rampion Offshore Wind, (n.d.). https://www.rampionoffshore.com/.

Rampion Wind Farm, (n.d.). https://www.4coffshore.com/windfarms/rampion-united-kingdom-uk36.html.

Van Oord's topduo Aeolus en Svanen klaren klus Walney Extension offshore windpark, (2017). https://www.linkmagazine.nl/oords-topduo-aeolus-en-svanen-klaren-klus-walney-extension-offshore-windpark/.

Walney Extension makes UK wind farm world's largest, (2018). https://www.theengineer.co.uk/walney-extension-worlds-largest/.

Walney Extension Wind Farm, (n.d.). https://www.4coffshore.com/windfarms/walney-extension-united-kingdom-uk63.html.

PROJECT PROFILE: WALNEY EXTENSION OFFSHORE WIND FARM, CUMBRIA, (n.d.). https://power.nridigital.com/power_technology_nov18_special/project_profile_walney_extension_offshore_wind_farm_cumbria.

First monopile was loaded at the quay of the Rostock foundation manufacturer EEW SPC for the offshore wind farm Arkona, (n.d.). https://eew-group.com/about/news/detail/eew-spc-loads-first-monopile-for-arkona/.

Ongoing project Arkona - 60 transition pieces and monopiles, 2017. https://www.bladt.dk/UserFiles/05_Downloads/Foundations/ONGOING_Arkona_Ongoing_verII.pdf.

[Arkona Wind Farm, (n.d.). https://www.4coffshore.com/windfarms/arkona-germany-de46.html.

Rentel Offshore Wind Farm | The Project, (n.d.). https://www.rentel.be/en.

J.G. Schepers, K. Boorsma, H.A Madsen, G.R. Pirrung, G. Bangga, G. Guma, T. Lutz, T. Potentier, C. Braud, E. Guilmineau, A. Croce, S. Cacciola, A. P. Schaffarczyk, B. A. Lobo, S. Ivanell, H. Asmuth, F. Bertagnolio, N.N. Sørensen, W. Z. Shen, … E. Cicirello. (2021). IEA Wind TCP Task 29, Phase IV: Detailed Aerodynamics of Wind Turbines. Zenodo. https://doi.org/10.5281/zenodo.4817875

Srinivas Guntur, Jason Jonkman, Ryan Sievers, Michael A. Sprague, Scott Schreck, and Qi Wang, A validation and code-to-code verification of FAST for a megawatt-scale wind turbine with aeroelastically tailored blades, Wind Energ. Sci., 2, 443–468, 2017, https://doi.org/10.5194/wes-2-443-2017

Stian Høegh Sørum, Jan-Tore H. Horn, Jørgen Amdahl, Comparison of numerical response predictions for a bottom-fixed offshore wind turbine, Energy Procedia, Volume 137, 2017, Pages 89-99, ISSN 1876-6102, https://doi.org/10.1016/j.egypro.2017.10.336.

Wojciech Popko, Amy Robertson, Jason Jonkman, Fabian Wendt, Philipp Thomas, Kolja Müller, Matthias Kretschmer, Torbjørn Ruud Hagen, Christos Galinos, Jean-Baptiste Le Dreff, Philippe Gilbert, Bertrand Auriac, Sho Oh, Jacob Qvist, Stian Høegh Sørum, Loup Suja-Thauvin, Hyunkyoung Shin, Climent Molins, Pau Trubat, Paul Bonnet, Roger Bergua, Kai Wang, Pengcheng Fu, Jifeng Cai, Zhisong Cai, Armando Alexandre, and Robert Harries, Validation of Numerical Models of the Offshore Wind Turbine from the Alpha Ventus Wind Farm Against Full-Scale Measurements Within OC5 Phase III, ASME 2019 38 th Annual Conference on Ocean, Offshore, and Arctic Engineering Glasgow, Scotland, June 9–14, 2019

Shilpa Thakur, Nilanjan Saha, LOAD REDUCTION ON OFFSHORE WIND TURBINES BY AERODYNAMIC FLAPS, Proceedings of the ASME 2017 36th International Conference on Ocean, Offshore and Arctic Engineering OMAE2017, June 25-30, 2017, Trondheim, Norway

Xiong Liu, Cheng Lu, Gangqiang Li, Ajit Godbole, Yan Chen, Effects of aerodynamic damping on the tower load of offshore horizontal axis wind turbines, Applied Energy 204 (2017) 1101–1114

Gerry Murphy , David Igoe, P. Doherty , K. Gavin, 3D FEM approach for laterally loaded monopile design, Computers and Geotechnics 100 (2018) 76–83

Burd H, Byrne B, McAdam R, Houlsby G, Martin C, Beuckelaers W, et al. Design aspects for monopile foundations. In: Proceeding 19th ICSMGE, Seoul; 2017.

Lars Einar S. Stieng, Michael Muskulus, Load case reduction for offshore wind turbine support structure fatigue assessment by importance sampling with two-stage filtering, Wind Energy, Volume22, Issue11 November 2019, Pages 1472-1486

Ingrid B. Løken, Amir M. Kaynia, Effect of foundation type and modelling on dynamic response and fatigue of offshore wind turbines, Wind Energy, Volume22, Issue12, December 2019, Pages 1667-1683

Yizhou Zhang, Chencong Liao, Jinjian Chen, Dagui Tong, Jianhua Wang, Numerical analysis of interaction between seabed and mono-pile subjected to dynamic wave loadings considering the pile rocking effect, Ocean Engineering 155 (2018) 173–188

Al-Hammadi, M., Simons, R.R., 2019. Local Scour Mechanism around Dynamically Active Marine Structures in Noncohesive Sediments and Unidirectional Current. Journal of Waterway, Port, Coastal, and Ocean Engineering 146, 04019026. https://doi.org/10.1061/(ASCE)WW.1943-5460.0000533

Bachynski, E., Thys, M., Delhaye, V., 2019. Dynamic response of a monopile wind turbine in waves: Experimental uncertainty analysis for validation of numerical tools. Applied Ocean Research 89, 96–114. https://doi.org/10.1016/J.APOR.2019.05.002

Bachynski, E.E., Thys, M., Dadmarzi, F.H., 2020. Observations from hydrodynamic testing of a flexible, large-diameter monopile in irregular waves. Journal of Physics: Conference Series 1669, 012028. https://doi.org/10.1088/1742-6596/1669/1/012028

Banfi, D., Raby, A., Simmonds, D., 2019. Dynamic loads arising from broken wave impacts on a cylindrical turbine substructure in shallow waters, in: 13th EWTEC 2019: European Wave and Tidal Energy Conference.

Bhattacharya, S., Lombardi, D., Amani, S., Aleem, M., Prakhya, G., Adhikari, S., Aliyu, A., Alexander, N., Wang, Y., Cui, L., Jalbi, S., Pakrashi, V., Li, W., Mendoza, J., Vimalan, N., 2021. Physical Modelling of Offshore Wind Turbine Foundations for TRL (Technology Readiness Level) Studies. Journal of Marine Science and Engineering 2021, Vol. 9, Page 589 9, 589. https://doi.org/10.3390/JMSE9060589

Chen, T., Zhang, C., Wang, X., Zhao, Q., Yuan, G., Chen, K., 2020. Hysteretic behavior of grouted connections in offshore wind turbine support structures. Journal of Constructional Steel Research 164, 105783. https://doi.org/10.1016/J.JCSR.2019.105783

H. Dadmarzi, F., Thys, M., Bachynski, E.E., 2019. Validation of Hydrodynamic Loads on a Large-Diameter Monopile in Regular Waves. Proceedings of the International Conference on Offshore Mechanics and Arctic Engineering - OMAE 7A-2019. https://doi.org/10.1115/OMAE2019-95929

Jeong, Y.-H., Kim, J.-H., Manandhar, S., Ha, J.-G., Park, H.-J., Kim, D.-S., 2020. Centrifuge modelling of drained pullout and compression cyclic behaviour of suction bucket. https://doi.org/10.1680/jphmg.18.00044 20, 59–70. https://doi.org/10.1680/JPHMG.18.00044

Lian, J., Zhao, Y., Dong, X., Lian, C., Wang, H., 2021. An experimental investigation on long-term performance of the wide-shallow bucket foundation model for offshore wind turbine in saturated sand. Ocean Engineering 228, 108921. https://doi.org/10.1016/J.OCEANENG.2021.108921

Tödter, S., el Sheshtawy, H., Neugebauer, J., el Moctar, O., Schellin, T.E., 2021. Deformation measurement of a monopile subject to vortex- induced vibration using digital image correlation. Ocean Engineering 221, 108548. https://doi.org/10.1016/J.OCEANENG.2020.108548

Wang, S., Larsen, T.J., Bredmose, H., 2020. Experimental and numerical investigation of a jacket structure subject to steep and breaking regular waves. Marine Structures 72, 102744. https://doi.org/10.1016/J.MARSTRUC.2020.102744

Wang, X., Zeng, X., Li, X., Li, J., 2020. Liquefaction characteristics of offshore wind turbine with hybrid monopile foundation via centrifuge modelling. Renewable Energy 145, 2358–2372. https://doi.org/10.1016/J.RENENE.2019.07.106

Wang, X., Zeng, X., Li, X., Li, J., 2018. Investigation on Offshore Wind Turbine with an Innovative Hybrid Monopile Foundation: An Experimental Based Study.

Zeng, X., Shi, W., Michailides, C., Zhang, S., Li, X., 2021. Numerical and experimental investigation of breaking wave forces on a monopile-type offshore wind turbine. Renewable Energy 175, 501–519. https://doi.org/10.1016/J.RENENE.2021.05.009

Morató, A., Sriramula, S., & Krishnan, N. (2019). Kriging models for aero-elastic simulations and reliability analysis of offshore wind turbine support structures. Ships and Offshore Structures, 14(6), 545-558.

Shittu, A. A., Mehmanparast, A., Wang, L., Salonitis, K., & Kolios, A. (2020). Comparative study of structural reliability assessment methods for offshore wind turbine jacket support structures. Applied Sciences, 10(3), 860.

Mai, Q. A., Weijtjens, W., Devriendt, C., Morato, P. G., Rigo, P., & Sørensen, J. D. (2019). Prediction of remaining fatigue life of welded joints in wind turbine support structures considering strain measurement and a joint distribution of oceanographic data. Marine Structures, 66, 307-322.

Hlaing, N., Morato, P. G., Rigo, P., Amirafshari, P., Kolios, A., & Nielsen, J. S. (2021). The effect of failure criteria on risk-based inspection planning of offshore wind support structures. In Life-Cycle Civil Engineering: Innovation, Theory and Practice (pp. 146-153). CRC Press.

Yeter, B., Garbatov, Y., & Soares, C. G. (2019). Uncertainty analysis of soil-pile interactions of monopile offshore wind turbine support structures. Applied Ocean Research, 82, 74-88.

Ren, Z., Verma, A. S., Li, Y., Teuwen, J. J., & Jiang, Z. (2021). Offshore wind turbine operations and maintenance: A state-of-the-art review. Renewable and Sustainable Energy Reviews, 144, 110886.

Yan, R., & Dunnett, S. (2021). Improving the Strategy of Maintaining Offshore Wind Turbines through Petri Net Modelling. Applied Sciences, 11(2), 574.

Rinaldi, G., Pillai, A. C., Thies, P. R., & Johanning, L. (2020). Multi-objective optimization of the operation and maintenance assets of an offshore wind farm using genetic algorithms. Wind Engineering, 44(4), 390-409.

Morato Dominguez, P. G. (2021). Optimal Inspection and Maintenance Planning for Deteriorating Structures via Markov Decision Processes and Deep Reinforcement Learning. Application to Offshore Wind Substructures (Doctoral dissertation, Université de Liège, Liège, Belgique).

Rinaldi, G., Thies, P. R., & Johanning, L. (2021). Current Status and Future Trends in the Operation and Maintenance of Offshore Wind Turbines: A Review. Energies, 14(9), 2484.

Dong, X., Lian, J., Wang, H., Yu, T., & Zhao, Y. (2018). Structural vibration monitoring and operational modal analysis of offshore wind turbine structure. Ocean Engineering, 150, 280-297.

Lian, J., Cai, O., Dong, X., Jiang, Q., & Zhao, Y. (2019). Health monitoring and safety evaluation of the offshore wind turbine structure: a review and discussion of future development. Sustainability, 11(2), 494.

Mai, Q. A., Weijtjens, W., Devriendt, C., Morato, P. G., Rigo, P., & Sørensen, J. D. (2019). Prediction of remaining fatigue life of welded joints in wind turbine support structures considering strain measurement and a joint distribution of oceanographic data. Marine Structures, 66, 307-322.

American Bureau of Shipping. Guide for Building and Classing Floating Turbines Installations. 2018

Azcona, J., Bouchotrouch, F., & Vittori, F. (2019). Low-frequency dynamics of a floating wind turbine in wave tank–scaled experiments with SiL hybrid method. Wind Energy, 22(10). https://doi.org/10.1002/we.2377

G. Bangga, P. Weihing, T. Lutz, E. Kramer, Effect of computational grid on accurate prediction of a wind turbine rotor using delayed detached-eddy simulations, J. Mech. Sci. Technol. 31 (5) (2017) 2359e2364.

Bayati, I., Facchinetti, A., Fontanella, A., Taruffi, F., & Belloli, M. (2020). Analysis of FOWT dynamics in 2-DOF hybrid HIL wind tunnel experiments. Ocean Engineering, 195. https://doi.org/10.1016/j.oceaneng.2019.106717

P. Benard, A. Vire, V. Moureau, G. Lartigue, L. Beaudet, P. Deglaire, L. Bricteux, Large-eddy simulation of wind turbines wakes including geometrical effects, Comput. Fluid 173 (2018) 133e139.

F. Blondel, G. Ferrer, M. Cathelain, D. Teixeira, Improving a BEM Yaw Model Based on NewMexico Experimental Data and Vortex/CFD Simulations, In: Congrès Français de Mecanique, 2017. Lille, France.

K. Boorsma, J.G. Schepers, et al., Final Report of IEA Task 29: Mexnext (Phase 3), ECN-E-18e1003, Energy Research Center of the Netherlands, January 2018.

K. Boorsma, L. Greco, G. Bedon, Rotor wake engineering models for aeroelastic applications, J. Phys. Conf. Ser 1037 (2018), 062013.

Bureau Veritas. NI572 Classification and Certification of Floating Wind Turbines. 2019

A. Calabretta, M. Molica Colella, L. Greco, M. Gennaretti, Assessment of a comprehensive aeroelastic tool for horizontal-axis wind turbine rotor analysis, Wind Energy 19 (12) (2016) 2301-2319.

Ping Cheng, Yang Huang, Decheng Wan, A numerical model for fully coupled aero-hydrodynamic analysis of floating offshore wind turbine, Ocean Engineering, Volume 173, 2019, Pages 183-196

Choisnet, T., Percher, Y., Dory, J.N., Adam, R., Favré, M., On the Correlation Between Floating Wind Turbine Accelerations, Rotor and Tower Loads, Proceedings of 39th OMAE conference, OMAE2020-18610

Coisnet, T., Rogier, E., Percher, Y., Courbois, A., Le Crom, I., Mariani, R., Performance and Mooring Qualification in Floatgen : the First French Offshore Wind Turbine Project, Nov. 2018, Proceedings of the 16th Journées de l'Hydrodynamique

DNV. ST-0119 Floating Wind Turbine Structures. 2021

DNV.SE-0422 Certification of Floating Wind Turbines. 2018

Paula Doubrawa , Matthew J. Churchfield , Marte Godvik , Senu Sirnivas, Load response of a floating wind turbine to turbulent atmospheric flow, Applied Energy 242 (2019) 1588–1599

Fontanella, A., Bayati, I., & Belloli, M. (2018). Control of Floating Offshore Wind Turbines: Reduced-Order Modeling and Real-Time Implementation for Wind Tunnel Tests. Proceedings of the International Conference on Offshore Mechanics and Arctic Engineering - OMAE, 10. https://doi.org/10.1115/OMAE2018-77840

Fontanella, A., Bayati, I., Taruffi, F., Mura, F. la, Facchinetti, A., & Belloli, M. (2019). A 6-DOFS hardware-in-the-loop system for wind tunnel tests of floating offshore wind turbines. Proceedings of the International Conference on Offshore Mechanics and Arctic Engineering - OMAE, 10. https://doi.org/10.1115/OMAE2019-95967

Luca Greco, Claudio Testa, Wind turbine unsteady aerodynamics and performance by a free-wake panel method, Renewable Energy, vol 164, 2021, pp. 444-459

Hall, M., & Goupee, A. J. (2018). Validation of a hybrid modeling approach to floating wind turbine basin testing. Wind Energy, 21(6). https://doi.org/10.1002/we.2168

Harrold, M. J., Thies, P. R., Newsam, D., Ferreira, C. B., & Johanning, L. (2020). Large-scale testing of a hydraulic non-linear mooring system for floating offshore wind turbines. Ocean Engineering, 206. https://doi.org/10.1016/j.oceaneng.2020.107386

John Marius Hegseth, Erin E. Bachynski, Joaquim R.R.A. Martins, Integrated design optimization of spar floating wind turbines, Marine Structures 72 (2020) 102771

International Electrotechnical Committee. IEC 61400-3-2 Design Requirements for floating offshore wind turbines. 2019

Kanner, S., Koukina, E., & Yeung, R. W. (2019). Power optimization of model- scale floating wind turbines using real-time hybrid testing with autonomous actuation and control. Journal of Offshore Mechanics and Arctic Engineering, 141(3). https://doi.org/10.1115/1.4041995

Ryan Kyle, Yeaw Chu Lee, Wolf-Gerrit Früh, Propeller and vortex ring state for floating offshore wind turbines during surge, Renewable Energy, Volume 155, 2020, Pages 645-657

Frank Lemmer, Wei Yu, Birger Luhmann, David Schlipf, Po Wen Cheng, Multibody modeling for concept-level floating offshore wind turbine design, Multibody Syst Dyn (2020) 49:203–236

Leroy, V, Gilloteaux, J-C, Lynch, M, Babarit, A, Ferrant, P. Impact of aerodynamic modeling on seakeeping performance of a floating horizontal axis wind turbine. Wind Energy. 2019; 22: 1019– 1033. https://doi.org/10.1002/we.2337

Lloyd's Register. Guidance on Offshore Wind Farm Certification. 2012

Lloyd's Register. Classification of Offshore Units. 2020

Madsen, F. J., Nielsen, T. R. L., Kim, T., Bredmose, H., Pegalajar-Jurado, A., Mikkelsen, R. F., Lomholt, A. K., Borg, M., Mirzaei, M., & Shin, P. (2020). Experimental analysis of the scaled DTU10MW TLP floating wind turbine with different control strategies. Renewable Energy, 155. https://doi.org/10.1016/j.renene.2020.03.145

Nakamura, A., Hayashi, Y., Icinose, H., Verification of Load Calculation Based on Site Measurements of a 7MW Offshore Wind Turbine on V-Shaped Semi-submersible Floating Structure, June 2018, Grand Renewable Energy 2018 Proceedings, O-We-10-4

B. Nelson, J.S. Kouh, The aerodynamic analysis of a rotating wind turbine by viscous-coupled 3D panel method, Appl. Sci. 7 (6) (2017) 1-15.

Stefan Netzband, Christian W. Schulz, Ulf Göttsche, Daniel Ferreira González & Moustafa Abdel-Maksoud, A panel method for floating offshore wind turbine simulations with fully integrated aero- and hydrodynamic modelling in time domain, Ship Technology Research, 65:3, 123-136, DOI: 10.1080/09377255.2018.1475710, 2018

Nippon Kaiji Kyokai. Guideline for Offshore Floating Wind Turbine Structures. 2012

F. Porcacchia, C. Testa, S. Zaghi, R. Muscari, M. Gennaretti, Assessment of permeable boundary integral formulations for rotating blades noise prediction, in: Proc. 24th International Congress on Sound and Vibration (ICSV 2017), 2017.

Néstor Ramos-García, Mads Mølholm Hejlese, Jens Nørkær Sørensen and Jens Honoré Walther, Hybrid vortex simulations of wind turbines using a three-dimensional viscous–inviscid panel method, Wind Energ. 2017; 20:1871–1889

A.N. Robertson, et al., OC5 project phase II: validation of global loads of the DeepCwind floating semisubmersible wind turbine, Energy Procedia 137 (2017) 38e57.

Robertson, A., Bachynski, E. E., Gueydon, S., Wendt, F., & Schünemann, P. (2020). Total experimental uncertainty in hydrodynamic testing of a semisubmersible wind turbine, considering numerical propagation of systematic uncertainty. Ocean Engineering, 195. https://doi.org/10.1016/j.oceaneng.2019.106605

J.G. Schepers, K. Boorsma, H.A Madsen, G.R. Pirrung, G. Bangga, G. Guma, T. Lutz, T. Potentier, C. Braud, E. Guilmineau, A. Croce, S. Cacciola, A. P. Schaffarczyk, B. A. Lobo, S. Ivanell, H. Asmuth, F. Bertagnolio, N.N. Sørensen, W. Z. Shen, … E. Cicirello. (2021). IEA Wind TCP Task 29, Phase IV: Detailed Aerodynamics of Wind Turbines. Zenodo. https://doi.org/10.5281/zenodo.4817875

N. Sedaghatizadeh, M. Arjomandi, R. Kelso, B. Cazzolato, M. Ghayesh, Modelling of wind turbine wake using large eddy simulation, Renew. Energy 115 (2018) 1166e1176.

Carlos Eduardo S. Souza, Erin E. Bachynski, Changes in surge and pitch decay periods of floating wind turbines for varying wind speed, Ocean Engineering 180 (2019) 223–237

Thys, M., Fontanella, A., Taruffi, F., Belloli, M., & Berthelsen, P. A. (2019). Hybrid model tests for floating offshore wind turbines. ASME 2019 2nd International Offshore Wind Technical Conference, IOWTC 2019. https://doi.org/10.1115/IOWTC2019-7575

Thys, M., Sauder, T., Chabaud, V., Eliassen, L., Sæther, L. O., & Magnussen, Ø. B. (2018). Real-time hybrid model testing of a semi-submersible 10MW floating wind turbine and advances in the test method. ASME 2018 1st International Offshore Wind Technical Conference, IOWTC 2018. https://doi.org/10.1115/IOWTC2018-1081

Tomasicchio, G. R., D'Alessandro, F., Avossa, A. M., Riefolo, L., Musci, E., Ricciardelli, F., & Vicinanza, D. (2018). Experimental modelling of the dynamic behaviour of a spar buoy wind turbine. Renewable Energy, 127. https://doi.org/10.1016/j.renene.2018.04.061

T. Tran, D. Kim, A CFD study of coupled aerodynamic-hydrodynamic loads on a semisubmersible floating offshore wind turbine, J Wind Energy, vol. 21, pp. 70-85, 2018

Urbán, A. M., & Guanche, R. (2019). Wind turbine aerodynamics scale-modeling for floating offshore wind platform testing. Journal of Wind Engineering and Industrial Aerodynamics, 186. https://doi.org/10.1016/j.jweia.2018.12.021

Utsunomiya T.,, Sato, I., Kobayashi, O., Shiraishi, T., Harada, T., Numerical Modeling and Spar Analysis of a Hybrid-Spar Floating Wind Turbine, Journal of Offshore Mechanics and Arctic Engineering, June 2019, Vol. 141 / 031903-1

Rajesh Vaithiyanathasamy, Hüseyin Özdemir, Gabriele Bedon, Arne van Garrel, A double wake model for interacting boundary layer methods, AIAA SciTech Forum 8–12 January 2018, Kissimmee, Florida, 2018 Wind Energy Symposium

B. Wiegard, M. König, J. Lund, L. Radtke, S. Netzband, M. Abdel-Maksoud, A. Düster, Fluid-structure interaction and stress analysis of a floating wind turbine, Marine Structures 78 (2021) 102970

Adam S. Wise, Erin E. Bachynski, Wake meandering effects on floating wind turbines, Wind Energy, Volume 23, Issue 5, May 2020, Pages 1266-1285

Wright, C., Yoshimoto, H., Wada, R., Takagi, K., Numerical Modelling of a Relatively Small Floating Body's Wave and Low Frequency Motion Response, Compared woth Observational Data, Proceedings of 38th OMAE conference, OMAE2019-96443

Yingguang Wang (2020) Efficient computational method for the dynamic responses of a floating wind turbine, Ships and Offshore Structures, 15:3, 269-279, DOI: 10.1080/17445302.2019.1614746

Mustapa M, Yaakob O, Ahmed YM, Rheem C-K, Koh K, and Adnan FA. 2017. Wave energy device and breakwater integration: A review. Renewable and Sustainable Energy Reviews 77:43-58.

Crowley S, Porter R, Taunton D, and Wilson PA. 2018. Modelling of the WITT wave energy converter. Renewable Energy 115:159-174.

de Almeida JL, Mujtaba B, and Fernandes AO. 2018. Preliminary laboratorial determination of the REEFS novel wave energy converter power output. Renewable Energy 122:654-664.

Ning D, Zhou Y, and Zhang C. 2018. Hydrodynamic modeling of a novel dual-chamber OWC wave energy converter. Applied Ocean Research 78:180-191.

Rezanejad K, and Guedes Soares C. 2019. Hydrodynamic investigation of a novel concept of OWC type wave energy converter device. Paper read at Proc. 38th International Conference on Ocean, Offshore and Arctic Engineering. ASME Paper No: OMAE2019-96510.

Rezanejad K, Gadelho J, Xu S, and Guedes Soares C. 2021. Experimental investigation on the hydrodynamic performance of a new type floating Oscillating Water Column device with dual-chambers. Ocean Engineering 234:109307.

Rezanejad K, and Guedes Soares C. 2021. Hydrodynamic Investigation of a Novel Concept of Oscillating Water Column Type Wave Energy Converter Device. Journal of Offshore Mechanics and Arctic Engineering 143 (4):042003.

Wang Y-J, and Lee C-K. 2019. Dynamics and power generation of wave energy converters mimicking biaxial hula-hoop motion for mooring-less buoys. Energy 183:547-560.

Siegel SG. 2019. Numerical benchmarking study of a cycloidal wave energy converter. Renewable Energy 134:390-405.

[Babarit A, Hals J, Muliawan MJ, Kurniawan A, Moan T, and Krokstad J. 2012. Numerical benchmarking study of a selection of wave energy converters. Renewable energy 41:44-63.

Moreno EC, and Stansby P. 2019. The 6-float wave energy converter m4: ocean basin tests giving capture width, response and energy yield for several sites. Renewable and Sustainable Energy Reviews 104:307-318.

Santo H, Taylor P, and Stansby P. 2020. The performance of the three-float M4 wave energy converter off Albany, on the south coast of western Australia, compared to Orkney (EMEC) in the UK. Renewable Energy 146:444-459.

Tongphong W, Kim B-H, Kim I-C, and Lee Y-H. 2021. A study on the design and performance of ModuleRaft wave energy converter. Renewable Energy 163:649-673.

Devolder B, Stratigaki V, Troch P, and Rauwoens P. 2018. CFD Simulations of Floating Point Absorber Wave Energy Converter Arrays Subjected to Regular Waves. Energies 11 (3).

Goteman M, Giassi M, Engstrom J, and Isberg J. 2020. Advances and Challenges in Wave Energy Park Optimization-A Review. Frontiers in Energy Research 8.

Windt C, Davidson J, and Ringwood JV. 2018. High-fidelity numerical modelling of ocean wave energy systems: A review of computational fluid dynamics-based numerical wave tanks. Renewable and Sustainable Energy Reviews 93:610-630.

McNatt JC, Porter A, and Ruehl K. 2020. Comparison of Numerical Methods for Modeling the Wave Field Effects Generated by Individual Wave Energy Converters and Multiple Converter Wave Farms. Journal of Marine Science and Engineering 8 (3):168.

Luczko E, Robertson B, Bailey H, Hiles C, and Buckham B. 2018. Representing non-linear wave energy converters in coastal wave models. Renewable Energy 118:376-385.

Atan R, Finnegan W, Nash S, and Goggins J. 2019. The effect of arrays of wave energy converters on the nearshore wave climate. Ocean Engineering 172:373-384.

O'Dea A, Haller MC, and Özkan-Haller HT. 2018. The impact of wave energy converter arrays on wave-induced forcing in the surf zone. Ocean Engineering 161:322-336.

Rollano FT, Tran TT, Yu YH, Garcia-Medina G, and Yang ZQ. 2020. Influence of Time and Frequency Domain Wave Forcing on the Power Estimation of a Wave Energy Converter Array. Journal of Marine Science and Engineering 8 (3).

Rodrigues JM. 2021. A Procedure to Calculate First-Order Wave-Structure Interaction Loads in Wave Farms and Other Multi-Body Structures Subjected to Inhomogeneous Waves. Energies 14 (6):1761.

Rijnsdorp DP, Hansen JE, and Lowe RJ. 2020. Understanding coastal impacts by nearshore wave farms using a phase-resolving wave model. Renewable Energy 150:637-648.

Oikonomou C, Gomes R, Gato L, and Falcão A. 2020. On the dynamics of an array of spar-buoy oscillating water column devices with inter-body mooring connections. Renewable Energy 148:309-325.

Yang S-H, Ringsberg JW, and Johnson E. 2020. Wave energy converters in array configurations—Influence of interaction effects on the power performance and fatigue of mooring lines. Ocean Engineering 211:107294.

Verao Fernandez G, Balitsky P, Stratigaki V, and Troch P. 2018. Coupling methodology for studying the far field effects of wave energy converter arrays over a varying bathymetry. Energies 11 (11):2899.

Stratigaki V, Troch P, and Forehand D. 2019. A fundamental coupling methodology for modeling near-field and far-field wave effects of floating structures and wave energy devices. Renewable Energy 143:1608-1627.

Belibassakis K, Bonovas M, and Rusu E. 2018. A novel method for estimating wave energy converter performance in variable bathymetry regions and applications. Energies 11 (8):2092.

Bonovas M, Belibassakis K, and Rusu E. 2019. Multi-DOF WEC performance in variable bathymetry regions using a hybrid 3D BEM and optimization. Energies 12 (11):2108.

Gaebele DT, Magana ME, Brekken TK, and Sawodny O. 2020. State space model of an array of oscillating water column wave energy converters with inter-body hydrodynamic coupling. Ocean Engineering 195:106668.

Faedo N, Peña-Sanchez Y, and Ringwood JV. 2020. Parametric representation of arrays of wave energy converters for motion simulation and unknown input estimation: a moment-based approach. Applied Ocean Research 98:102055.

Zou S, and Abdelkhalik O. 2020. Collective control in arrays of wave energy converters. Renewable Energy 156:361-369.

Liu Z, Wang Y, and Hua X. 2021. Proposal of a novel analytical wake model and array optimization of oscillating wave surge converter using differential evolution algorithm. Ocean Engineering 219:108380.

Wang Y, and Liu Z. 2021. Proposal of novel analytical wake model and GPU-accelerated array optimization method for oscillating wave surge energy converter. Renewable Energy 179:563-583.

Flavià FF, Mcnatt C, Rongère F, Babarit A, and Clément AH. 2018. A numerical tool for the frequency domain simulation of large arrays of identical floating bodies in waves. Ocean Engineering 148:299-311.

Yoshida K. 1990. A numerical method for huge semisubmersible responses in waves.

McNatt JC, Venugopal V, and Forehand D. 2015. A novel method for deriving the diffraction transfer matrix and its application to multi-body interactions in water waves. Ocean Engineering 94:173-185.

Kagemoto H, and Yue DK. 1986. Interactions among multiple three-dimensional bodies in water waves: an exact algebraic method. Journal of Fluid mechanics 166:189-209.

Tokić G, and Yue DK. 2019. Hydrodynamics of periodic wave energy converter arrays. Journal of Fluid Mechanics 862:34-74.

Tokić G, and Yue DK. 2021. Hydrodynamics of large wave energy converter arrays with random configuration variations. Journal of Fluid Mechanics 923.

Michele S, Renzi E, and Sammarco P. 2019. Weakly nonlinear theory for a gate-type curved array in waves. Journal of Fluid Mechanics 869:238-263.

Giassi M, and Göteman M. 2018. Layout design of wave energy parks by a genetic algorithm. Ocean Engineering 154:252-261.

Murai M, Li Q, and Funada J. 2021. Study on power generation of single Point Absorber Wave Energy Converters (PA-WECs) and arrays of PA-WECs. Renewable Energy 164:1121-1132.

Lyu J, Abdelkhalik O, and Gauchia L. 2019. Optimization of dimensions and layout of an array of wave energy converters. Ocean Engineering 192:106543.

Sharp C, and DuPont B. 2018. Wave energy converter array optimization: A genetic algorithm approach and minimum separation distance study. Ocean Engineering 163:148-156.

Giassi M, Castellucci V, and Göteman M. 2020. Economical layout optimization of wave energy parks clustered in electrical subsystems. Applied Ocean Research 101:102274.

Xu S, Wang S, and Guedes Soares C. 2019. Review of mooring design for floating wave energy converters. Renewable and Sustainable Energy Reviews 111:595-621.

Qiao D, Haider R, Yan J, Ning D, and Li B. 2020. Review of Wave Energy Converter and Design of Mooring System. Sustainability 12 (19):8251.

Davidson J, and Ringwood JV. 2017. Mathematical modelling of mooring systems for wave nergy converters—A review. Energies 10 (5):666.

Khalid F, Arini NR, and Johanning L. 2019. Recommendations for WEC mooring guidelines and standards. In OPERA - Open Sea Operating Experience to Reduce Wave Energy Costs.

Paredes GM, Thomsen JB, Ferri F, and Eskilsson C. 2019. Mooring system reliability analysis of an ORE device using general Polynomial Chaos. Paper read at 13th European Wave and Tidal Energy Conference.

Moura Paredes G, Eskilsson C, and P Engsig-Karup A. 2020. Uncertainty quantification in mooring cable dynamics using polynomial chaos expansions. Journal of Marine Science and Engineering 8 (3):162.

Johannesson P, Svensson T, and Gaviglio H. 2019. Reliability evaluation using variation mode and effect analysis: Application to CorPower's mooring pre-tension cylinder. Paper read at Proceedings of the Thirteenth European Wave and Tidal Energy Conference.

Palm J, and Eskilsson C. 2019. Influence of floater geometry on snap loads in mooring systems for wave energy converters. Paper read at European Wave and Tidal Energy Conference.

Parish D, Herduin M, Thies P, Gordelier T, and Johanning L. 2017. Reducing Peak & Fatigue Mooring Loads: A Validation Study for Elastomeric Moorings.

Hall M. 2017. Efficient modelling of seabed friction and multi-floater mooring systems in MoorDyn. Paper read at Proceedings of the 12th European Wave and Tidal Energy Conference, Cork, Ireland.

Oikonomou C, Gomes R, Gato L, and Falcão A. 2017. Analysis of a triangular array of floating oscillating water column devices with inter-body mooring connections in regular waves. Paper read at Proc. 12th European Wave and Tidal Energy Conference.

Thomsen JB, Ferri F, and Kofoed JP. 2017. Screening of available tools for dynamic mooring analysis of wave energy converters. Energies 10 (7):853.

Thomsen JB, Ferri F, Kofoed JP, and Black K. 2018. Cost optimization of mooring solutions for large floating wave energy converters. Energies 11 (1):159.

Luxcey N, Isorna R, Germain N, Nava V, Tunga I, and Noble D. 2020. Station Keeping Tools – alpha version. In DTOceanPLus - Advanced design tools for ocean energy systems innovation, development and deployment.

Barrera C, Guanche R, and Losada IJ. 2019. Experimental modelling of mooring systems for floating marine energy concepts. Marine Structures 63:153-180.

Xu S, Wang S, and Guedes Soares C. 2020. Experimental investigation on hybrid mooring systems for wave energy converters. Renewable Energy 158:130-153.

Xu S, and Guedes Soares C. 2020. Experimental investigation on short-term fatigue damage of slack and hybrid mooring for wave energy converters. Ocean Engineering 195:106618.

Xu S, Rezanejad K, Gadelho J, Wang S, and Guedes Soares C. 2020. Experimental investigation on a dual chamber floating oscillating water column moored by flexible mooring systems. Ocean Engineering 216:108083.

Gomes RP, Gato LM, Henriques JC, Portillo JC, Howey BD, Collins KM, Hann MR, and Greaves DM. 2020. Compact floating wave energy converters arrays: Mooring loads and survivability through scale physical modelling. Applied Energy 280:115982.

Fleming AN, and Macfarlane GJ. 2017. Experimental flow field comparison for a series of scale model oscillating water column wave energy converters. Marine Structures 52:108-125.

Yurchenko D, and Alevras P. 2018. Parametric pendulum based wave energy converter. Mechanical Systems and Signal Processing 99:504-515.

Sarmiento J, Iturrioz A, Ayllón V, Guanche R, and Losada I. 2019. Experimental modelling of a multi-use floating platform for wave and wind energy harvesting. Ocean Engineering 173:761-773.

Bacelli G, Spencer SJ, Patterson DC, and Coe RG. 2019. Wave tank and bench-top control testing of a wave energy converter. Applied Ocean Research 86:351-366.

Liu Z, Xu C, Qu N, Cui Y, and Kim K. 2020. Overall performance evaluation of a model-scale OWC wave energy converter. Renewable Energy 149:1325-1338.

He F, Leng J, and Zhao X. 2017. An experimental investigation into the wave power extraction of a floating box-type breakwater with dual pneumatic chambers. Applied Ocean Research 67:21-30.

Elhanafi A, Macfarlane G, Fleming A, and Leong Z. 2017. Experimental and numerical investigations on the hydrodynamic performance of a floating–moored oscillating water column wave energy converter. Applied energy 205:369-390.

Vyzikas T, Deshoulières S, Barton M, Giroux O, Greaves D, and Simmonds D. 2017. Experimental investigation of different geometries of fixed oscillating water column devices. Renewable Energy 104:248-258.

Ning D, Wang R-q, Chen L-f, and Sun K. 2019. Experimental investigation of a land-based dual-chamber OWC wave energy converter. Renewable and Sustainable Energy Reviews 105:48-60.

Zhao X, Ning D, and Liang D. 2019. Experimental investigation on hydrodynamic performance of a breakwater-integrated WEC system. Ocean Engineering 171:25-32.

Çelik A, and Altunkaynak A. 2019. Experimental investigations on the performance of a fixed-oscillating water column type wave energy converter. Energy 188:116071.

Martin D, Li X, Chen C-A, Thiagarajan K, Ngo K, Parker R, and Zuo L. 2020. Numerical analysis and wave tank validation on the optimal design of a two-body wave energy converter. Renewable Energy 145:632-641.

Zabala I, Henriques J, Gomez A, Falcão A, Amezaga A, Gomes RP, and Gato L. 2017. Assessment of a Spar Buoy Oscillating-Water-Column Wave Energy Converter Including a Fully Dynamic Model. Paper read at Proceedings of the 12th European Wave and Tidal Energy Conference, EWTEC.

Rezanejad K, and Guedes Soares C. 2018. Enhancing the primary efficiency of an oscillating water column wave energy converter based on a dual-mass system analogy. Renewable Energy 123:730-747.

Xu Q, Li Y, Yu Y-H, Ding B, Jiang Z, Lin Z, and Cazzolato B. 2019. Experimental and numerical investigations of a two-body floating-point absorber wave energy converter in regular waves. Journal of Fluids and Structures 91:102613.

Bingham HB, Yu Y-H, Nielsen K, Tran TT, Kim K-H, Park S, Hong K, Said HA, Kelly T, and Ringwood JV. 2021. Ocean energy systems wave energy modeling task 10.4: Numerical modeling of a fixed oscillating water column. Energies 14 (6):1718.

Ashlin SJ, Sundar V, and Sannasiraj S. 2017. Pressures and forces on an oscillating water column–type wave energy caisson breakwater. Journal of Waterway, Port, Coastal, and Ocean Engineering 143 (5):04017020.

Pawitan KA, Dimakopoulos AS, Vicinanza D, Allsop W, and Bruce T. 2019. A loading model for an OWC caisson based upon large-scale measurements. Coastal Engineering 145:1-20.

Nader J-R, Fleming A, Macfarlane G, Penesis I, and Manasseh R. 2017. Novel experimental modelling of the hydrodynamic interactions of arrays of wave energy converters. International journal of marine energy 20:109-124.

Zhao X, and Ning D. 2018. Experimental investigation of breakwater-type WEC composed of both stationary and floating pontoons. Energy 155:226-233.

Kamarlouei M, Gaspar J, Calvario M, Hallak T, Mendes MJ, Thiebaut F, and Guedes Soares C. 2020. Experimental analysis of wave energy converters concentrically attached on a floating offshore platform. Renewable Energy 152:1171-1185.

He F, Huang Z, and Law AW-K. 2013. An experimental study of a floating breakwater with asymmetric pneumatic chambers for wave energy extraction. Applied Energy 106:222-231.

WELLO LAUNCH PENGUIN WEC2 FOR H2020 CEFOW ARRAY. European Marine Energy Centre (EMEC) 2018 [cited. Available from https://www.emec.org.uk/press-release-wello-launch-penguin-wec2-for-h2020-cefow-array/.

Rosa-Santos P, Taveira-Pinto F, Rodríguez CA, Ramos V, and López M. 2019. The CECO wave energy converter: Recent developments. Renewable Energy 139:368-384.

Ahamed R, McKee K, and Howard I. 2020. Advancements of wave energy converters based on power take off (PTO) systems: A review. Ocean Engineering 204:107248.

Rusu E, and Onea F. 2018. A review of the technologies for wave energy extraction. Clean Energy 2 (1):10-19.

BioWAVE wave energy converter. 2020 [cited. Available from http://bps.energy/biowave.

Pelrine R, Kornbluh RD, Eckerle J, Jeuck P, Oh S, Pei Q, and Stanford S. 2001. Dielectric elastomers: generator mode fundamentals and applications. Paper read at Smart Structures and Materials 2001: Electroactive Polymer Actuators and Devices.

WaveRoller wave energy converter. 2020 [cited. Available from https://aw-energy.com/waveroller/.

Duck wave energy converter. 2020 [cited. Available from http://www.homepages.ed.ac.uk/v1ewaveg/.

Zhang Y, Zhao Y, Sun W, and Li J. 2021. Ocean wave energy converters: Technical principle, device realization, and performance evaluation. Renewable and Sustainable Energy Reviews 141:110764.

Weerakoon AS, Kim B-H, Cho Y-J, Prasad DD, Ahmed MR, and Lee Y-H. 2021. Design optimization of a novel vertical augmentation channel housing a cross-flow turbine and performance evaluation as a wave energy converter. Renewable Energy 180:1300-1314.

Wave energy device HAILONG 2. [cited. Available from http://www.xue63.com/toutiaojy/20180205G0K4J100.html.

Sheng SW, Wang KL, Lin HJ, Zhang YQ, You YG, and Wang ZP. 2019. Open sea tests of 100 kW wave energy convertor Sharp Eagle WANSHAN. Acta Energiae Solaris Sinica 40 (3):709-714.

WANG X, and YU YH X. 2019. Research on power characteristic field test analysis method of wave energy generation device. Chinese journal of scientific instrument 40 (1):71-76.

Sun P, Hu S, He H, Zheng S, Chen H, Yang S, and Ji Z. 2021. Structural optimization on the oscillating-array-buoys for energy-capturing enhancement of a novel floating wave energy converter system. Energy Conversion and Management 228:113693.

Wang SM, Yu T, Li ZY, Tian K, and Zhao YQ. 2020. Design of wave power generation device and monitoring system based on beidou system. Manufacturing Industry 42 (1):54-58.

Wang BT, He HZ, Zheng SG, and Zhang D. 2019. A review of wave power acquisition device. Energy and Environment 5:2-8.

Li YJ. 2018. Research on improvement of the buyo-rope-drum's power generation efficiency: Shandong University (Weihai).

Wang SM, Li ZY, Shen Y, Wang JZ, and Zhao YQ. 2019. Design and experimental study of a floating breakout based on wave power generation. Water Resources and Hydropower Engineering 50 (07):216-221.

Domenico P. Coiro, Giancarlo Troise, Nadia Bizzarrini and Guido Lazzerini (2019). Experimental and numerical analysis of GEMSTAR, a tethered tidal current energy harvester. In: Proceedings of the 13th European Wave and Tidal Energy Conference.

Alan Compelli, David Henry and Gareth P. Thomas (2019). Surface profile prediction from bottom pressure measurements with application to marine current generators. In: Proceedings of the 13th European Wave and Tidal Energy Conference.

Day et al (2014). Specialist Committee on Hydrodynamic Testing of Marine Renewable Energy Devices. Final Report and Recommendations to the 27th ITTC.

Robert Ellis, Joshua Bowman, Matthew Allmark, Shanti Bhushan, David Thompson, Allan Mason-Jones, Tim O'Doherty (2019). Comparison of numerical software for predicting the performance of a horizontal axis tidal turbine. In: Proceedings of the 13th European Wave and Tidal Energy Conference.

Job I. Encarnacion and Cameron Johnstone (2019). Investigation on the sea-state performance of a horizontal axis tidal turbine designed for less energetic flows. In: Proceedings of the 13th European Wave and Tidal Energy Conference.

Milo Feinberg, Pal Schmitt, James Donegan and Jarlath McEntee (2019). An efficient numerical framework for the assessment of free surface effects on crossflow tidal turbines. In: Proceedings of the 13th European Wave and Tidal Energy Conference.

Carwyn Frost, Ian Benson, Björn Elsäßer, Ralf Starzmann, Trevor Whittaker (2017). Mitigating Uncertainty in Tidal Turbine Performance Characteristics from Experimental Testing. In: Proceedings of the 12th European Wave and Tidal Energy Conference.

Benoît Gaurier, Grégory Germain, Jean-Valéry Facq (2017). Experimental study of the Marine Current Turbine behaviour submitted to macro-particle impacts. In: Proceedings of the 12th European Wave and Tidal Energy Conference.

Benoît Gaurier, Stéphanie Ordonez-Sanchez, Jean-Valéry Facq, Grégory Germain, Cameron Johnstone, Rodrigo Martinez, Ivan Santic and Francesco Salvatore (2019). First round of MaRINET 2 Tidal Energy Round Robin Tests: combined wave and current tests. In: Proceedings of the 13th European Wave and Tidal Energy Conference.

Grégory Germain, Antoine Chapeleau, Benoit Gaurier, Laura-Mae Macadré and Peter Scheijgrond (2017). Testing of marine energy technologies against international standards. Where do we stand? In: Proceedings of the 12th European Wave and Tidal Energy Conference.

Grondeau M., Mercier P., Guillou S., Poirier J.C., Poizot E. and Mear Y. (2017). Numerical simulation of a tidal turbine model in a turbulent flow with the Lattice Boltzmann Method. In: Proceedings of the 12th European Wave and Tidal Energy Conference.

Pragya Gupta, Malwattage Peiris, Jessica Walker, Sascha Kosleck and Irene Penesis (2019). Experimental investigation into the effects of waves on blade loading for a model scale horizontal axis tidal turbine. In: Proceedings of the 13th European Wave and Tidal Energy Conference.

Aleksandar Jakovljevic, Stéphane Paboeuf, Frédéric Dias (2017). Impact of wave-current interactions on tidal current turbine performance in storm conditions. In: Proceedings of the 12th European Wave and Tidal Energy Conference.

Yangjian Li, Wei Li, Hongwei Liu, Yonggang Lin, Yajing Gu, Bingling Xie (2020). Indirect load measurements for large floating horizontal-axis tidal current turbines. Ocean Engineering, Volume 198-106945

Catherine Lloyd, Matthew Allmark, Robert Ellis, Stephanie Ordonez, Allan Mason-Jones, Cameron Johnstone, Tim O'Doherty, Gregory Germain and Benoit Gaurier (2019). CFD surface effects on flow conditions and tidal stream turbine performance. In: Proceedings of the 13th European Wave and Tidal Energy Conference.

Guiomar Lopez, Anne-Claire Bennis, Yves Barbin, Laurent Benoit, Remi Cambra, Daniel C. Conley, Louis Marié, Alexei Sentchev, and Lucy R. Wyatt (2019). Surface hydrodynamics of the Alderney Race from HF radar measurements. In: Proceedings of the 13th European Wave and Tidal Energy Conference.

Rodrigo Martinez, Stephanie Ordonez-Sanchez, Matthew Allmark, Cameron Johnstone, Tim O'Doherty, Catherine Lloyd, Gregory Germain, Benoit Gaurier (2019). Effects on the loading of horizontal axis turbines when operating under wave and currents. In: Proceedings of the 13th European Wave and Tidal Energy Conference.

Grégory Pinon, Charifa El Hadi, Myriam Slama, José Nuño, Pablo Mansilla, Erwann Nicolas, Julie Marcille, Jean-Valéry Facq, Inès Belarbi, Benoît Gaurier, Grégory Germain, André Pacheco, and Michael Togneri (2019). Influence of turbulence and wave flow conditions on different scaled tidal turbines. In: Proceedings of the 13th European Wave and Tidal Energy Conference.

Mitchel Provan, Paul Knox, Andrew Cornett, Julien Cousineau (2019). Physical model study of the wake produced by multiple cross-flow turbines. In: Proceedings of the 13th European Wave and Tidal Energy Conference.

Anton Schaap, Nicholas Fyffe, Kimon Argyriadis, Peter Davies, Alan Henry, Budi Gunawan, Frederick Driscoll, Jeffrey Steynor and Peter Scheijgrond (2019). Development of the IEC TC114 Technical Specification for mechanical load measurements for Marine Energy Converters.

Peter Scheijgrond, Anna Southall, Claudio Bittencourt, Peter Davies, Pieter Mathys, Grégory Germain, Martijn Geertzen & al. (2019). Advancing IEC standardization and certification for tidal energy converters. In: Proceedings of the 13th European Wave and Tidal Energy Conference.

Alexei Sentchev, Maxime Thiébaut, Lucille Furgerot, Pascal Bailly du Bois, and Mehdi Morillon (2019). Advances in resource characterization in Alderney Race (English Channel). In: Proceedings of the 13th European Wave and Tidal Energy Conference.

Ralf Starzmann, Nicholas Kaufmann and Penny Jeffcoate (2019. Full-and model scale Testing of two different Rotor Diameters for Instream Power Generation. In: Proceedings of the 13th European Wave and Tidal Energy Conference.

Duncan R.J. Sutherland, Brian G. Sellar, Vengatesan Venugopal, Alistair G.L. Borthwick. Effects of Spatial Variation and Surface Waves on Tidal Site Characterisation (2017). In: Proceedings of the 12th European Wave and Tidal Energy Conference.

Vengatesan Venugopal, Brian Sellar, Duncan Sutherland, Alistair Borthwic, Gareth Wakelam (2017). Numerical Modelling of Combined Wave, Tidal Current and Turbulence Interaction at Tidal Energy Sites in the Fall of Warness, Scotland. In: Proceedings of the 12th European Wave and Tidal Energy Conference.

Stuart Walker, Lorenzo Cappietti, Irene Simonetti (2019). A laboratory study on the effects of waves on the performance and structural deflection of a tidal stream turbine. In: Proceedings of the 13th European Wave and Tidal Energy Conference.

Faisal Wani, Henk Polinder (2017). A Review of Tidal Current Turbine Technology: Present and Future. In: Proceedings of the 12th European Wave and Tidal Energy Conference.

Dodo, Y., Nagaya, S., Okada, T., Toyoda, M., Ito, A. (2021) Development and Design of a Floating Type Ocean Current Turbine System. In: Okada, T., Suzuki, K., Kawamura, Y. (eds) Practical Design of Ships and Other Floating Structures. PRADS 2019. Lecture Notes in Civil Engineering, vol 65. Springer, Singapore. https://doi.org/10.1007/978-981-15-4680-8_49.

IHI, NEDO (2017) "IHI and NEDO Completes World's First 100kW Class Demonstration Test of Ocean Current Power Generation – Acquiring data such as power output and attitude stability in the waters for practical applications –," press release https://www.ihi.co.jp/en/all_news/2017/technology/1191898_2070.html.

Imamura, J. T., Takagi, K., Waseda, T., Kodaira, T. (2018) Comparison of Numerical Simulations and Field Measurements of Current Flow in The Tokara Strait, OCEANS 2018 MTS/IEEE Charleston, 2018, pp. 1-5.

Imamura, J., Takagi, K., Nagaya, S. (2019) Engineering analysis of turbulent flow measurements near Kuchinoshima Island, J Mar Sci Technol 24, 329-337.

Sato, A., Kanoh, H., Takagi, K. (2021) Control of a Twin-Turbine Submerged Floating System in turbulent flow, Ocean Engineering 225, 108769.

Yahagi, K., Takagi, K. (2019) Moment loads acting on a blade of an ocean current turbine in shear flow, Ocean Engineering 172, 446-455.

Adiputra, R., Utsunomiya, T., 2019. Stability based approach to design cold-water pipe (CWP) for ocean thermal energy conversion (OTEC). Applied Ocean Research 92, 101921.

Adiputra, R., Utsunomiya, T., 2021. Linear vs non-linear analysis on self-induced vibration of OTEC cold water pipe due to internal flow, Applied Ocean Research 110, 102610.

Adiputra, R., Utsunomiya, T., Koto, J., Yasunaga, T., Ikegami, Y., 2020. Preliminary design of a 100 MW-net ocean thermal energy conversion (OTEC) power plant study case: Mentawai island, Indonesia. Journal of Marine Science and Technology 25 (1), 48-68.

Bureau Veritas, 2018. Classification and Certification of Ocean Thermal Energy Converter (OTEC) - Tentative Rules -. Guidance Note NI 637 DT R00 E, January 2018.

Cazzaniga, R., Cicu, M., Rosa-Clot, M., Rosa-Clot, P., Tina, G.M., Ventura, C., 2018. Floating photovoltaic plants: Performance analysis and design solutions. Renewable and Sustainable Energy 81, Part 2, 1730-1741.

Cheng, Z., Wen, T.R., Ong, M.C., Wang, K., 2019. Power performance and dynamic responses of a combined floating vertical axis wind turbine and wave energy converter concept. Energy 171, 190-204.

DNV GL, 2021. Design, development and operation of floating solar photovoltaic systems. DNVGL-RP-0584, Edition March 2021.

Elginoz, N., Bas, B., 2017. Life Cycle Assessment of a multi-use offshore platform: Combining wind and wave energy production. Ocean Engineering 145, 430-443.

Halkyard, J., Sheikh, R., Marinho, T., Shi, S., Ascari, M., 2014. Current developments in the validation of numerical methods for predicting the responses of an ocean thermal energy conversion (OTEC) system cold water pipe. OMAE2014-24636.

Hirao, S.C., Umeda, J., Kokubun, K., Fujiwara, T., 2021. Tank test and numerical simulation of spar type floating OTEC, OMAE2021-62107.

Hisamatsu, R., Utsunomiya, T., 2021. Simplified formulation of coupled system between moored ship and elastic pipe for OTEC plantship, OMAE2021-62122.

Howe, D., Nader, J.-R., Macfarlane, G., 2020a. Experimental investigation of multiple oscillating water column wave energy converters integrated in a floating breakwater: energy extraction performance. Applied Ocean Research 97, 102086.

Howe, D., Nader, J.-R., Macfarlane, G., 2020b. Performance analysis of a floating breakwater integrated with multiple oscillating water column wave energy converters in regular and irregular seas. Applied Ocean Research 99, 102147.

IEC, 2019. Marine energy - Wave, tidal, and other water current converters - Part 20: Design and analysis of an Ocean Thermal Energy Conversion (OTEC) plant - General guidance. IEC TS 62600-20, Edition 1.0, 2019-06.

Jahangir, M.H., Shahsavari, A., Rad, M.A.V., 2020. Feasibility study of a zero emission PV/Wind turbine/Wave energy converter hybrid system for stand-alone power supply: A case study. Journal of Cleaner Production 262, 121250.

Kibee, S., 2013. Ocean thermal energy conversion at SBM. Proceedings of the 18th Offshore Symposium, February 7, 2013, Houston, Texas.

Li, L., Gao, Y., Yuan, Z., Day, S., Hu, Z., 2018. Dynamic response and power production of a floating integrated wind, wave and tidal energy system. Renewable Energy 116, 412-422.

O'Kelly-Lynch, P., Long, C., McAuliffe, F.D., Murphy, J., Pakrashi, V., 2020. Structural design implications of combining a point absorber with a wind turbine monopile for the east and west coast of Ireland. Renewable and sustainable energy reviews 119, 109583.

OES, 2021. White paper on ocean thermal energy conversion (OTEC). IEA Technology Programme for Ocean Energy Systems (OES), www.ocean-energy-systems.org.

Oliveira-Pinto, S., Stokkermans, J., 2020. Assessment of the potential of different floating solar technologies - Overview and analysis of different case studies. Energy Conversion and Management 211, 112747.

Perez-Collazo, C., Greaves, D., Iglesias, G., 2018a. Hydrodynamic response of the WEC sub-system of a novel hybrid wind-wave energy converter. Energy conversion and management 171, 307-325.

Perez-Collazo, C., Greaves, D., Iglesias, G., 2018b. A novel hybrid wind-wave energy converter for jacket-frame substructures. Energies 11 (3), 637.

Perez-Collazo, C., Pemberton, R., Greaves, D., Iglesias, G., 2019. Monopile-mounted wave energy converter for a hybrid wind-wave system. Energy conversion and management 199, 111971.

Ranjbaran, P., Yousefi, H. Gharehpetian, G.B., Astaraei, F.R., 2019. A review on floating photovoltaic (FPV) power generation units. Renewable and Sustainable Energy Reviews 110, 332-347.

Ren, N., Ma, Z., Fan, T., Zhai, G., Ou, J., 2018. Experimental and numerical study of hydrodynamic responses of a new combined monopile wind turbine and a heave-type wave energy converter under typical operational conditions. Ocean Engineering 159, 1-8.

Ren, N., Ma, Z., Shan, B., Ning, D., Ou, J., 2020. Experimental and numerical study of dynamic responses of a new combined TLP type floating wind turbine and a wave energy converter under operational conditions. Renewable Energy 151, 966-974.

Rezanejad, K., Guedes Soares, C., 2021. Hydrodynamic Investigation of a Novel Concept of Oscillating Water Column Type Wave Energy Converter Device. Journal of Offshore Mechanics and Arctic Engineering 143 (4), 042003.

Sarmiento, J., Iturrioz, A., Ayllón, V., Guanche, R., Losada, I., 2019. Experimental modelling of a multi-use floating platform for wave and wind energy harvesting. Ocean Engineering 173, 761-773.

Seo, J., Kim, H.-J., 2019. Performance comparison of 1MW OTEC plant using numerical analysis and test. The 3rd China-Korea Ocean Energy Workshop, Qingdao, China, October 9-12, 2019.

Song, Y., 2019. A study of OTEC application on deep-sea FPSOs. Journal of Marine Science and Technology 24 (2), 466-478.

Talaat, M., Farahat, M., Elkholy, M., 2019. Renewable power integration: experimental and simulation study to investigate the ability of integrating wave, solar and wind energies. Energy 170, 668-682.

Wan, L., Greco, M., Lugni, C., Gao, Z., Moan, T., 2017. A combined wind and wave energy-converter concept in survival mode: Numerical and experimental study in regular waves with a focus on water entry and exit. Applied Ocean Research 63, 200-216.

N. Elginoz and B. Bas, "Life Cycle Assessment of a multi-use offshore platform: Combining wind and wave energy production," Ocean Eng., vol. 145, pp. 430–443, Nov. 2017, doi: 10.1016/J.OCEANENG.2017.09.005.

I. Dincer, V. Cozzani, and A. Crivellari, "Offshore renewable energy options," Hybrid Energy Syst. Offshore Appl., pp. 7–18, Jan. 2021, doi: 10.1016/B978-0-323-89823-2.00002-6.

K. A. Shah et al., "A synthesis of feasible control methods for floating offshore wind turbine system dynamics," Renew. Sustain. Energy Rev., vol. 151, p. 111525, Nov. 2021, doi: 10.1016/J.RSER.2021.111525.

M. Lerch, M. De-Prada-Gil, C. Molins, and G. Benveniste, "Sensitivity analysis on the levelized cost of energy for floating offshore wind farms," Sustain. Energy Technol. Assessments, vol. 30, pp. 77–90, Dec. 2018, doi: 10.1016/J.SETA.2018.09.005.

A. Ioannou, A. Angus, and F. Brennan, "A lifecycle techno-economic model of offshore wind energy for different entry and exit instances," Appl. Energy, vol. 221, pp. 406–424, Jul. 2018, doi: 10.1016/j.apenergy.2018.03.143.

W. Musial et al., "Offshore Wind Market Report: 2021 Edition," 2015.

B. Johnston, A. Foley, J. Doran, and T. Littler, "Levelised cost of energy, A challenge for offshore wind," Renew. Energy, vol. 160, pp. 876–885, Nov. 2020, doi: 10.1016/J.RENENE.2020.06.030.

A. Martinez and G. Iglesias, "Multi-parameter analysis and mapping of the levelised cost of energy from floating offshore wind in the Mediterranean Sea," Energy Convers. Manag., vol. 243, p. 114416, Sep. 2021, doi: 10.1016/J.ENCONMAN.2021.114416.

L. Castro-Santos, "Decision variables for floating offshore wind farms based on life-cycle cost: The case study of Galicia (North-West of Spain)," Ocean Eng., vol. 127, pp. 114–123, Nov. 2016, doi: 10.1016/J.OCEANENG.2016.10.010.

E. Segura, R. Morales, J. A. Somolinos, and A. López, "Techno-economic challenges of tidal energy conversion systems: Current status and trends," Renew. Sustain. Energy Rev., vol. 77, pp. 536–550, Sep. 2017, doi: 10.1016/J.RSER.2017.04.054.

D. Magagna and A. Uihlein, "Ocean energy development in Europe: Current status and future perspectives," Int. J. Mar. Energy, vol. 11, pp. 84–104, Sep. 2015, doi: 10.1016/J.IJOME.2015.05.001.

"European Commission: The EU Blue Economy Report 2019 - Google Scholar." https://scholar.google.com/scholar_lookup?title=The EU blue economy report 2019&publication_year=2019&author=European Comission (accessed Oct. 03, 2021).

D. Clemente, P. Rosa-Santos, and F. Taveira-Pinto, "On the potential synergies and applications of wave energy converters: A review," Renew. Sustain. Energy Rev., vol. 135, Jan. 2021, doi: 10.1016/J.RSER.2020.110162.

M. A. Mustapa, O. B. Yaakob, Y. M. Ahmed, C. K. Rheem, K. K. Koh, and F. A. Adnan, "Wave energy device and breakwater integration: A review," Renew. Sustain. Energy Rev., vol. 77, pp. 43–58, Sep. 2017, doi: 10.1016/J.RSER.2017.03.110.

"Tidal Range Alliance - British Hydro Association." https://www.british-hydro.org/tidal-range-alliance/ (accessed Oct. 04, 2021).

"Medium-term variability of the UK's combined tidal energy resource for a net-zero carbon grid | Elsevier Enhanced Reader." https://reader.elsevier.com/reader/sd/pii/S0360544221022386?token=44E35433ED72945B2385A51968FBB7D010A7583A3DF862A8D165AA5C2BF914C39AEB73D1DECB23804A7259723DAEE474&originRegion=eu-west-1&originCreation=20211004002359 (accessed Oct. 04, 2021).

M. Lewis et al., "Power variability of tidal-stream energy and implications for electricity supply," Energy, vol. 183, pp. 1061–1074, Sep. 2019, doi: 10.1016/J.ENERGY.2019.06.181.

"Future Energy Scenarios | National Grid ESO." https://www.nationalgrideso.com/future-energy/future-energy-scenarios (accessed Oct. 04, 2021).

"Co-located deployment of offshore wind turbines with tidal stream turbine arrays for improved cost of electricity generation | Elsevier Enhanced Reader." https://reader.elsevier.com/reader/sd/pii/S1364032119300450?token=934FE4C19851821CEC4B47E434F53F48EB1389F17E6008F51D00608F69BFBB0B90482AB40FA45B907D74EE3CFBA79199&originRegion=eu-west-1&originCreation=20211004014915 (accessed Oct. 04, 2021).

Gómez, P., Sánchez, G., Llana, A., & Gonzalez, G. (2015). LIFE50+ D2. 2: LCOE tool description, technical and environmental impact evaluation procedure. Technical report.

Ridge, I. M. L., Banfield, S. J., & Mackay, J. (2010, September). Nylon fibre rope moorings for wave energy converters. In OCEANS 2010 MTS/IEEE SEATTLE (pp. 1-10). IEEE.

Weller, S. D., Johanning, L., Davies, P., & Banfield, S. J. (2015). Synthetic mooring ropes for marine renewable energy applications. Renewable energy, 83, 1268-1278.

Choisnet, T., Rogier, E., Percher, Y., Courbois, A., Le Crom, I., & Mariani, R. (2018). Performance and mooring qualification in Floatgen: the first French offshore wind turbine project. 16ième Journées de l'Hydrodynamique, 1, 1-10.

DNV, G. (2015). DNVGL-OS-E301 Position Mooring. DNV GL, Oslo.